The role of endosomal phosphatidylinositol 3-phosphate in neurotransmission and synaptic vesicle recycling

Inaugural-Dissertation

to obtain the academic degree

Doctor rerum naturalium (Dr. rer. Nat.)

Submitted to the Department of Biology, Chemistry, Pharmacy

of Freie Universität Berlin

by

Guan-Ting Liu

from Changhua City, Taiwan

2020

Period of doctorate studies: June 2016 to October 2020

Supervisor: Prof. Dr. Volker Haucke

conducted at:
Leibniz Forschungsinstitut für Molekulare Pharmakologie (FMP), Berlin-Buch
(from June 2016)

1st Reviewer: Prof. Dr. Volker Haucke

2nd Reviewer: Prof. Dr. Stephan Sigrist

Date of defense: 20.11.2020

Acknowledgement

First of all, I would like to express my deepest gratitude to my supervisor Prof. Dr. Volker Haucke for his supervision and great support during the time of my PhD training in his lab. Also, I would like to thank Dr. Tolga Soykan for his mentorship and support. Their patient guidance and clear thoughts equipped me with research capabilities and scientific thinking, and their optimism and enthusiasm inspired me a lot when I felt depressed.

Secondly, I would like to thank all the people who were involved in my project: Dr. Gaga Kochlamazashvili, Dr. Dmytro Puchkov, Albert I. Mackintosh, Dennis Vollweiter, our subgroup members: Irving, Svenja and Kristine, I could not have finished my PhD study without your input and great help. Also, I would like to thank all the members of AG Haucke. I had very wonderful and happy time in the lab, and it was my pleasure to work with all of you.

Lastly, I would like to express my gratitude to my parents, my brother and my friends for supporting me all the time and your great accompany. I really had a great time in Berlin, and I definitely will miss the time I had here.

I. Table of Contents

II. Summary

The function of neural network is based on the regulated release of neurotransmitters by exocytosis and the subsequent recycling of synaptic vesicles (SV) membranes and proteins by endocytosis. The nascent SVs can be generated from plasma membrane or endosome-like vacuoles, however, the exact mechanism of SV recycling and the role of endosomes in this process are controversial. Furthermore, an essential element for maintaining neural networks is the regulation of neurotransmission through mechanisms of pre- and postsynaptic plasticity as well as homeostatic scaling, a process in which the activity-dependent changes of postsynaptic receptors lead to adaptive adjustment of the presynaptic neurotransmitter release. Whether and how the presynaptic neurotransmitter release is controlled intrinsically in an activity-dependent manner has not yet been fully understood. In my work, I examined the physiological function of the endosomal signal lipid phosphatidylinositol 3-phosphate [PI(3)P], a putative factor for regulation of SV recycling and control of presynaptic neurotransmission. By combining acute pharmacological and chemical-genetic approaches, I was able to show that excitatory neurotransmission and synaptic vesicle cycle are controlled by PI(3)P levels. Neuronal activity or pharmacological inhibition of PI 3-Kinase VPS34 lead to a drastic reduction in PI(3)P synthesis. PI(3)P reduction further inhibits excitatory neurotransmission and affects SV exo-/endocytosis. Conversely, silencing of neural network activity leads to increased PI(3)P levels. I was also able to show that the inhibition of exocytosis and endocytosis SV due to reduced PI(3)P levels is based on the Rab5-mediated hyperactivation of calcium-dependent protease calpain. Calpain-mediated cleavage and activation of the regulatory p35 subunit of the cyclin-dependent kinase 5 (Cdk5) is in turn responsible for the inhibition of exo- and endocytosis SV. As part of my doctorate, I was able to decipher an unexpected and novel function of the endosomal lipid PI(3)P in the control and scaling of the excitatory

neurotransmission and thus neural network activity. This mechanism could explain the essential role of VPS34 in the development of the central nervous system as well as in neurological diseases and in neurodegeneration.

III. Zusammenfassung

Die Funktion neuronaler Netzwerke basiert auf der regulierten Freisetzung von Neurotransmittern durch Exozytose und nachfolgendes Recycling Botenstoff enthaltender Synaptischer Vesikel (SV) durch Endoztyose und Budding naszenter SV aus endosomenartigen Vakuolen. Der genaue Mechanismus des Recyclings SV und die Rolle von Endosomen in diesem Prozess sind umstritten. Ein wesentliches Element der Funktion neuronaler Netzwerke ist die Regulation der Neurotransmission durch Mechanismen der prä- und postsynaptischen Plastizität sowie durch homeostatisches Scaling, ein Prozess bei der die Änderungen in der Aktivität postsynaptischer Rezeptoren zu adaptiven Anpassungen der präsynaptischen Neurotransmitterfreisetzung führen. Ob und wie die präsynaptische Neurotransmitterausschüttung intrinsisch aktivitätsabhängig kontrolliert wird, ist bislang unvollständig verstanden. In meiner Arbeit habe ich die physiologische Funktion des endosomalen Signallipids Phosphatodylinositol 3-Phosphat [PI(3)P], eines putativen Faktors im Recycling SV Membranen, in der SV Exo- und Endoztyose sowie der Kontrolle der präsynaptischen Neurotransmission untersucht. Ich konnte durch Kombination akuter pharmakologischer und chemisch-genetischer Ansätze zeigen, dass die exzitatorische Neurotransmission und der synaptische Vesikelzyklus durch PI(3)P kontrolliert werden. Neuronale Aktivität oder pharmakologische Hemmung der PI 3-Kinase VPS34 führen zu einer drastischen Reduktion der PI(3)P Synthese und inhibieren die exzitatorische Neurotransmission sowie die SV Exo-/Endozytose. Silencing der neuronalen Netzwerkaktivität führt umgekehrt zu erhöhten PI(3)P Levels. Ich konnte ferner zeigen, dass die Inhibition der Exo- und Endozytose SV infolge reduzierter PI(3)P Levels auf der Rab5-vermittelten Hyperaktivierung der Protease Calpain beruht. Calpain-vermittelte Spaltung und Aktivierung der regulatorischen p35 Untereinheit der Cyclin-abhängigen Kinase 5 (Cdk5) ist wiederum für die Inhibition der Ex- und Endozytose SV verantwortlich.

Damit ist es mir gelungen, im Rahmen meiner Promotion eine unerwartete und neuartige Funktion des endosomalen Lipids PI(3)P in der Kontrolle und Skalierung der exzitatorischen Neurotransmission und damit der neuronalen Netzwerkaktivität zu entschlüsseln. Dieser Mechanismus könnte die essentielle Rolle von VPS34 in der Entwicklung des Zentralnervensystems sowie bei neurologischen Erkrankungen und in der Neurodegeneration erklären.

1. Introduction

1.1 Neurotransmission and synaptic vesicle recycling

The mammalian brain is a complex network of specialized cells, such as glial cells and neurons. While glial cells support neuronal function, neurons are the main cell type that processes, stores and transmits information in the brain. Neurons are composed of four morphologically defined regions: The soma, dendrites, the axon, and synaptic terminals. Each region has its distinct role in signaling and communicating with other neurons. To maintain the neural network, neurotransmission is a fundamental process that drives information transfer between neurons. It requires the physical coupling and coordinated activity of pre- and post-synaptic compartments (Thomas Biederer, Pascal S. Kaeser, 2017). When an action potential (AP) arrives at the presynaptic terminal, signaling molecules called neurotransmitters that are stored in synaptic vesicles (SVs), are released by exocytosis into the synaptic cleft (Südhof and Rizo, 2011). Depending on the nature of the neurotransmitter and the type of postsynaptic receptors that they bind to, neurotransmitter release can regulate the activity of brain circuits by either facilitating or hindering action potential propagation. (Fon and Edwards, 2001).

SVs are small and complex organelles with an uniform diameter of approximately 40 nm. They contain numerous proteins which are required for membrane trafficking, fusion and neurotransmisster uptake (Takamori et al., 2006). SV recycling is a key process for sustained neurotransmission. Readily releasable synaptic vesicles are clustered at a specialized region of presynaptic membrane called active zone (AZ) (Südhof, 2012). Due to its small size, presynaptic terminals contain a limited number of SVs. Therefore, sustained neurotransmission may very rapidly deplete SVs in the absence of an efficient SV reformation mechanism. SVs have a well-defined protein composition and homogenous size, suggesting that a rigorous SV reformation mechanism is required to maintain the releasable

pool of SVs (Heuser and Reese, 1973; Milosevic, 2018). During presynaptic activity, voltage-gated calcium channels open and allow Ca^{2+} to enter presynaptic terminals. The rising Ca^{2+} concentration at the AZ triggers SV fusion with plasma membrane to release the neurotransmitters. After SV fusion, SV endocytosis retrieves the excess plasma membrane and synaptic proteins to maintain membrane surface area and to locally generate new SVs in the presynaptic compartment (Figure 1.1; Soykan et al., 2016). Depending on the type of synapses and firing pattern, different modes of SV endocytosis with different time constants have been proposed: classical clathrin-mediated endocytosis (CME), an alternative clathrin-independent endocytosis (CIE) pathway, rapid kiss-and-run exo-endocytosis, and activity-dependent bulk endocytosis. However, the exact nature and mechanism of various modes of SV recycling require more studies (Kokotos and Cousin, 2015; Soykan et al., 2016; Watanabe and Boucrot, 2017).
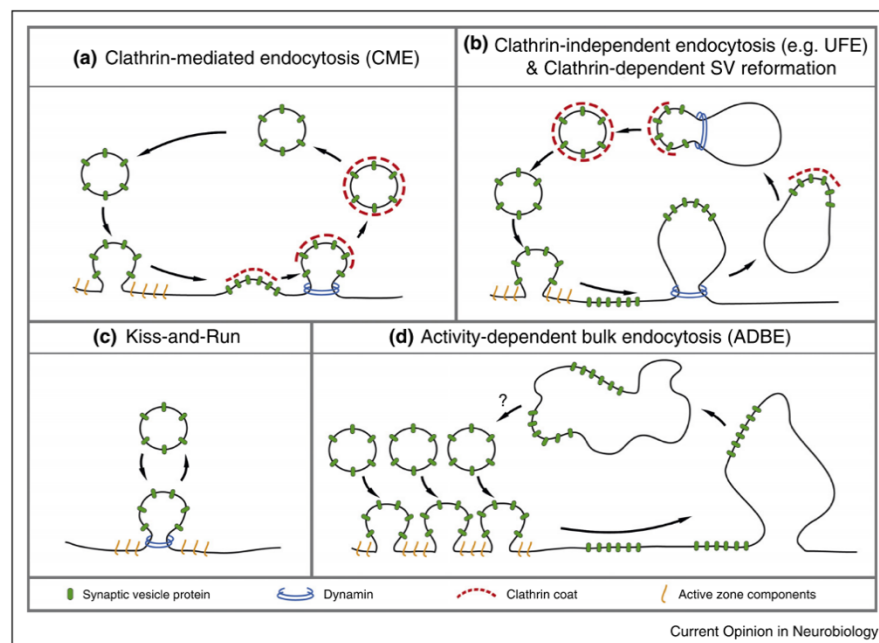
Figure 1.1. Proposed modes of SV endocytosis.
(a) Full fusion of SV and followed by clathrin-coated vesicle reform from the plasma membrane. **(b)** After SV exocytosis followed by a large invagination reformation on the membrane, and further recruit clathrin and other SV proteins to reform SVs. **(c)** Opening and closure of SV fusion pore directly occur on the AZ. **(d)** Bulk membrane internalize at the AZ. (Soykan et al., 2016)

1.1.1 Clathrin-mediated endocytosis

Clathrin-mediated endocytosis (CME) is a well-studied and classical pathway for SV cycling. After SV fusion, the membrane and synaptic proteins are integrated into plasma membrane, and subsequently followed by clathrin-dependent endocytosis to maintain membrane integrity. The process starts with the recruitment of clathrin adaptors onto phosphatidylinositol (4,5)-biphsophate [PI(4,5)P$_2$]-positive plasma membrane. Adaptor proteins initiate recruitment of clathrin triskelia around a budding vesicle, resulting in the clathrin-coated pit formation. The fission event is triggered by the GTPase dynamin at the neck of pit. After fission, the coated vesicle is internalized into the synapse and rapidly loses its coat via the action of Auxilin, the ATPase Hsc70 and Synaptojanin-1, a phosphatase that hydrolyzes PI(4,5)P$_2$ to promote the dissociation of adaptors. Synaptic proteins and lipid molecules are involved in the regulation of CME, for instance, Bin/Amphiphysin/RVS (BAR) domain-containing proteins that bind to phosphoinositides (PIPs) and are involved in curvature generation and stabilization (Figure 1.2). However, in contrast to the very rapid response of SVs to physiological action potential stimulation, CME is a relatively slow process that may be too slow to internalize proteins from the plasma membrane and support the recovery of vesicle pools. Besides, several studies showed that SV recycling was not fully impaired in clathrin-depleted neurons (Kononenko et al., 2014; Soykan et al., 2017), suggesting there is another pathway may involve in SV recycling (Watanabe and Boucrot, 2017).
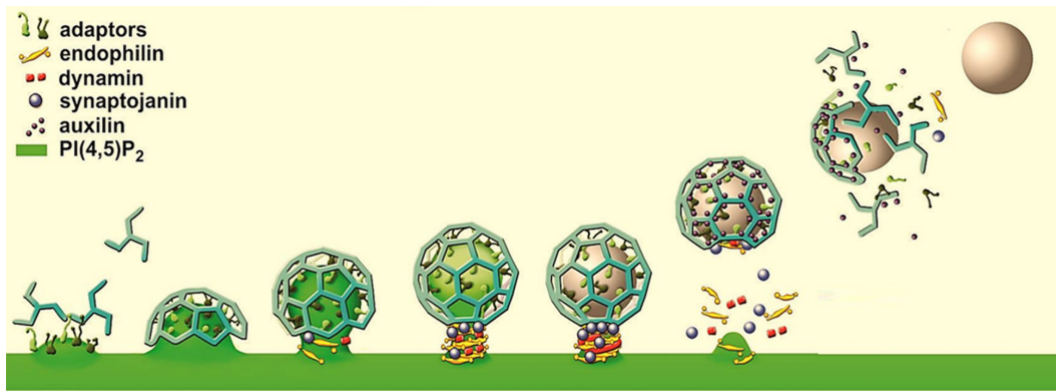
Figure 1.2. Mode of Clathrin-mediated endocytosis.
Clathrin and adaptor proteins are recruited to the endocytic vesicles. (Milosevic, 2018)

1.1.2 Clathrin-independent fast endocytosis

This pathway was first identified in the *Caenorhabditis elegans* neuromuscular junction (Watanabe et al., 2013a) and in cultured mammalian hippocampal neurons (Watanabe et al., 2013b). After SV fusion, a large invagination is generated from the plasma membrane by clathrin-independent endocytosis (CIE), and clathrin and its adaptors are subsequently recruited to endosome-like structures to reform new SVs (Kononenko et al 2014) (Figure 1.1b). The CIE pathway highly depends on the fission activity of dynamin and, possibly, physiological temperature, and can be completed in less than a second. Thus, it was considered as a faster endocytic mechanism for excessive membrane and SV proteins retrieval (Watanabe et al., 2013b). This endocytic pathway does not require clathrin. The amount of membrane exocytosed equals the amount of internalized membrane, indicating that this pathway is compensatory and likely a major mechanism for SV endocytosis (Watanabe et al., 2013b). However, it was later shown that SVs are endocytosed over many seconds in response to AP trains, while only minor portion of SV proteins are rapidly internalized in millisecond timescale at physiological temperature. It is further suggested that CIE has a limited capacity and is capable of compensating for small number of SVs fused upon a single or few APs in mammalian hippocampal neurons (Soykan et al., 2017). Given that this mode of endocytosis is triggered very rapidly after SV fusion, it may serve crucial

roles in removing the excess membrane from the surface of the synaptic terminal for maintaining membrane homeostasis and allow for further vesicle fusion. How this pathway is kinetically controlled needs to be addressed further.

1.1.3 Kiss-and-run

Kiss-and-run has been observed in neuroendocrine cells as an alternative clathrin-independent rapid mechanism to retrieve membrane and proteins without full collapse of SVs at the active zone (Figure 1.1c). In this mechanism, a vesicle transiently contacts the plasma membrane followed by opening and closing of a fusion pore at the same site. The vesicle is quickly recycled to the cytoplasm after closure of fusion pore (Wen et al., 2017). Even though hormone or peptide secreting large dense core vesicles favor this mode of membrane recycling, it remains to be proven whether SVs dominantly or partly use the kiss and run route.

1.1.4 Activity-dependent bulk endocytosis

To prevent complete breakdown of synaptic architecture and neurotransmission upon sustained and strong stimulation, neurons utilize activity-dependent bulk endocytosis (ADBE) to eliminate excessive membrane. This pathway can serve as an emergency response to high intensity stimulation. Strong stimulus drives Ca^{2+} influx into synapse and activates ADBE sensor Calcineurin, a phosphatase for dephosphorylation of SV proteins, that dephosphorylates Dynamin, and further trigger membrane curvature and tabulation for generating bulk membrane invaginations from the plasma membrane (Figure 1.1d). ADBE retrieves large regions of plasma membrane at the periactive zone, and then invaginations are transformed into bulk endosomes, which recruit clathrin and its adaptors for SV generation (Cousin, 2015).

Despite many studies on identifying the precise mechanism of SV recycling, many

key questions remain controversial. It is possible that the dominant mode of SV recycling and membrane retrieval depends on the neuron or synapse type and its activity pattern. In general, SVs are endocytosed via CME and CIE during moderate activity levels, whereas ADBE operates only during high activity. At physiological temperature, CIE is the predominant mechanism for SV cycling after brief neuronal activity (Watanabe et al., 2014) or high frequency stimulation (Soykan et al., 2017). Regardless of different modes of SV entry, endocytic vesicles at the presynaptic terminal are usually delivered to the endosome-like structures.

1.2 Synaptic vesicle reformation from endosome-like structures

After stimulation, a dynamic population of endosome-like structures are generated either by strong and sustained stimulation through ADBE, or following weak and brief stimulation by CIE. It remains to be fully investigated whether these endosome-like structures have the true characteristics of a classical early endosomes. Conventionally, classical endosomes are considered as stable organelles that serve as sorting platforms for endocytic proteins and lipids (Huotari and Helenius, 2011). Cargo sorting on endosomes requires numerous protein and lipid machineries which are involved in fission of endosomal intermediates, fusion with other endosomes or with autophagosomes and lysosomes for degradation. The phospholipid phosphatidylinositol 3-phosphate [PI(3)P], the major phosphoinositide residing on endosomes, the PI(3)P-binding protein EEA1 and Rab family protein Rab5 are important factors for endosome maturation, cargo trafficking and cellular signaling (Gautreau et al., 2014). Classical Rab5-positive, PI(3)P-containing endosomes have been observed at presynaptic terminals of *Drosophila*. These endosomes have been found to have important roles in determining neurotransmitter release probability and maintaining SV pool size (Wucherpfennig et al., 2003)

In contrast to classical endosomes, endosome-like structures that are formed at the synapse soon after SV fusion appear to be more transient in nature. Although these endosome-like structures disappear rapidly, they may play a crucial role in SV recycling and degradation of membrane proteins (Saheki and De Camilli, 2012). Despite years of research on endosomal membrane trafficking, little is known regarding the function of *bona fide* endosomes or endosome-like structures at the synapse and how they precisely contribute to SV recycling. A key question is whether these endosome-like structures contain classical endosomal PI(3)P or whether they maintain plasma membrane properties (e.g., PI(4,5)P$_2$) for a short time frame and participate in SV reformation. To date, synaptic endosomes are seen either as stable organelles, or as short-lived intermediates formed by homotyptic fusion of vesicles or intermediates of SV recycling. It is also known that neuronal synapses contain several endosomal proteins, for example Rab5, Rab7, Rab11 and APP-like protein (Rodal et al., 2011; Takamori, 2016; Wucherpfennig et al., 2003). Thus, many questions about the role of synaptic endosomal compartment and its role in SV recycling require further investigation.

1.3 Endosomal phosphatidylinositol 3-phosphate and VPS34

Phosphoinositides (PI) are short-lived membrane phospholipids which are involved in several cellular signaling pathways, development, cytoskeleton regulation as well as intracellular membrane trafficking (Di Paolo and De Camilli, 2006). Phosphorylation of the inositol ring of phosphatidylinositol at the 3-position generates phosphatidylinositol 3-phosphate [PI(3)P], a key component of endosomal membrane. PI(3)P is mainly synthesized by Class III PI3 kinase VPS34, and several studies have shown that PI(3)P is important for endocytic trafficking (Figure 1.3).
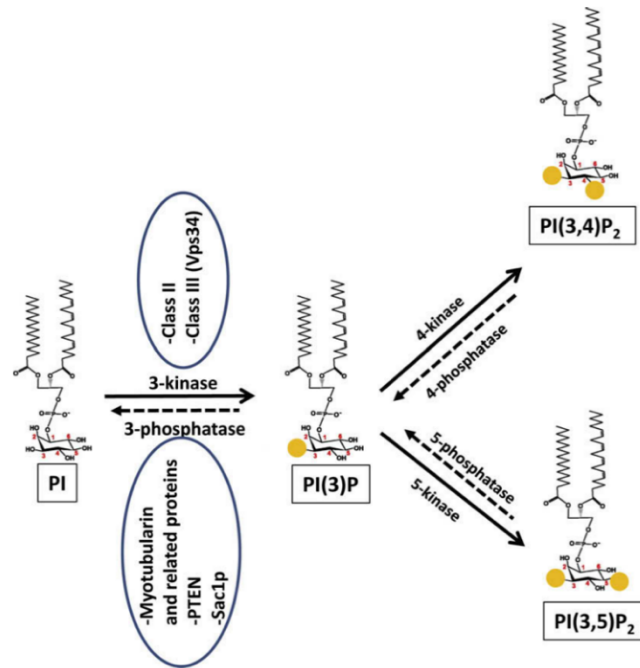
Figure 1.3. Mechanism of PI(3)P synthesis.
PI(3)P is produced by Class II and Class III PI3-kinase. 3-Phosphatase can hydrolysis PI(3)P back into PI. PI(3)P can further convert to PI(3,4)P$_2$ or PI(3,5)P$_2$ by different kinases (Burman and Ktistakis, 2010).

Two major groups of PI(3)P-binding domains have been reported: FYVE domains, and Phox homology (PX) domains. Proteins containing these domains bind to PI(3)P with high affinity and are involved in various steps of intracellular trafficking. For example, FYVE-containing EEA1, an early endosomal protein, interacts with endosomal SNARE proteins and regulates endocytic membrane fusion through its recruitment by Rab5 and PI(3)P (Burman and Ktistakis, 2010).

VPS34 functions as two tetrameric complexes that consist of the catalytic subunit VPS34, regulatory subunit VPS15, the adaptor protein Beclin-1 and either ATG14L to form complex I, or UV irradiation resistance-associated gene (UVRAG) to form complex II. The distinct complexes have a multitude of functions in intracellular trafficking. For instance, complex I plays a role in autophagy, while complex II is involved in endosomal fusion and sorting, endosomal trafficking towards the lysosome as well as multivesicular body (MVB) formation (Backer, 2016; Marat and Haucke, 2016).

17

1.3.1 VPS34 complex and its regulatory subunits

The lipid kinases VPS34 subunit of complex I and II consists of a N-terminal C2 domain, a helical domain and a C-terminal kinase domain (Figure 1.4). The C2 domain is essential for complex assembly, and it can be phosphorylated by AMP-activated protein kinase (AMPK) (at T163) (Kim et al., 2013) or Cdk5 (at T159) (Furuya et al., 2010). These phosphorylations interrupt the interaction between subunits and thereby reduce VPS34 activity. Another essential subunit VPS15, a common component of both complexes, is a regulator for VPS34 activity. VPS15 contains a N-terminal pseudokinase domain, a helical repeated HEAT domain and C-terminal WD40 domain which interacts with C2 domain of VPS34 and Rab5 on endosomes (Figure 1.4) (Murray et al., 2002). VPS15 mutations cause the instability of VPS34 complex which in turn perturbs the neuronal migration in mice (Gstrein et al., 2018). The other shared subunit of complex I and II is Beclin1, which is composed of a BH3 domain, two coil-coil domains and a membrane-binding BARA domain (Figure 1.4). The numerous posttranslational modifications of Beclin1 play crucial roles in mediating the specific function of different complexes, their localizations, binding partners and complex stabilities. For instance, the autophagy-promoting modifications are found in the BH3 domain (Abrahamsen et al., 2012; Kehrl, John and Shi, 2019; Russell et al., 2014), whereas autophagy-inhibiting modifications are mostly found in the coil-coil domain or the BARA domain (Munson et al., 2015). The autophagy-specific subunit ATG14L is the defining component for complex I. It consists of a ER-targeting N-terminal domain, three coil-coil domains, a C-terminal Backor/ATG14L autophagosome targeting sequence (BATS) domain (Figure 1.4). Phosphorylation of the BATS domain by mTOR inhibits autophagy (Xu et al., 2016). One the other hand, UVRAG is a component of the VPS34 complex II. It contains a proline-rich domain, a lipid-binding C2 domain, two coil-coil domains, a BARA2 domain and a C-terminal domain (Figure 1.4). The UVRAG localizes on Rab5-positive endosomes as a part of complex II, and it can be phosphorylated by mTOR to inhibit

autophagosome maturation (Munson et al., 2015) (Ohashi et al., 2019).

Structural and biochemical studies have identified many posttranslational modification sites in VPS34 complex I and II. The phosphorylation, ubiquitination and other modification of VPS34 complexes strongly affect their kinase activity and subcellular membrane binding ability. Also, several accessory proteins, including NRBF2, PAQR3, AMBRA1 and Rubicon, are associated with complex I or II to control their activity and localization (Backer, 2008, 2016).
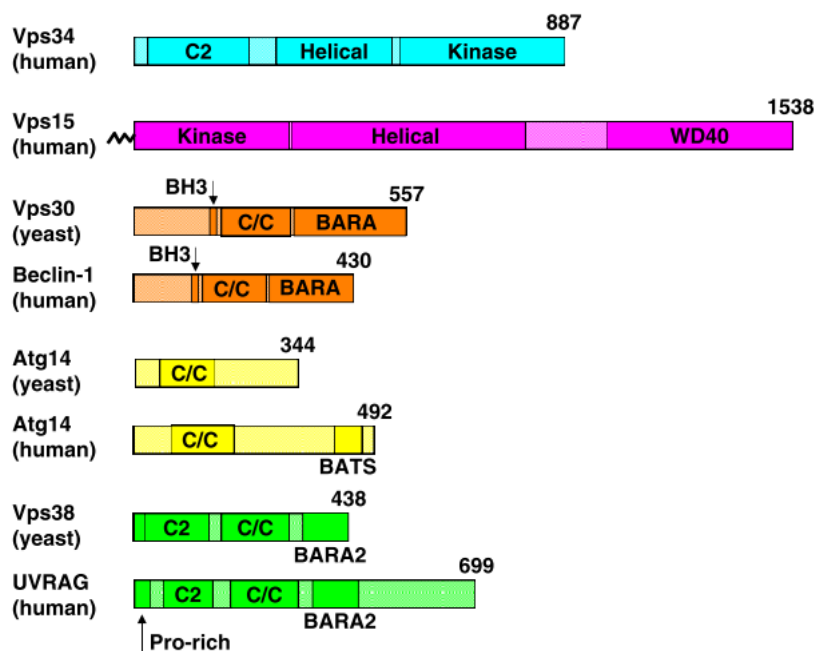
Figure 1.4. Domain organization of VPS34 complexes.
The domain structure of different subunits in VPS34 complex I and II. VPS, vacuolar protein sorting; WD40, approx. 40 amino acids that often ends with tryptophan (W) and aspartic acid (D); BECLIN, Bcl-2 interacting protein; C2, protein kinase C conserved region 2; ATG, Autophagy-related gene; BARA, beta-alpha repeated; BARKOR, Beclin 1-associated autophagy-related key regulator; C/C, coiled coil; UVRAG, UV radiation resistance-associated gene (Backer, 2016).

1.3.2 VPS34 complex I and autophagy

VPS34 is essential for autophagy, a degradation mechanism triggered by nutrient insufficiency, which removes unnecessary and dysfunctional cellular components. PI(3)P that is produced by VPS34 serves as a platform for autophagosome biogenesis (Backer,

2016). During autophagy, damaged or aged molecules are initially sequestered and surrounded by a flat membrane, which is followed by elongation and sealing of the membrane and leads to the formation of autophagosomes that are delivered to lysosomes for degradation. Autophagy cargo proteins are then digested by lysosomes to fuel new biosynthesis (Figure 1.5).

The induction of autophagy is triggered by starvation, hypoxia or low energy, and is related to the regulation of mammalian target of rapamycin (mTOR) complex I (mTORC1) signaling. The interplay between three key kinases; mTOR itself, (AMPK) and ULK1 is important for autophagy induction (Alers et al., 2012). mTORC1 is activated when nutrients are available and promotes growth through increased protein translation (Sabatini, 2006). On the other hand, in starved cells, AMPK and ULK1 not only phosphorylate downstream proteins to induce autophagy, but also phosphorylate Beclin1 for VPS34 activation and autophagosomal PI(3)P synthesis (Figure 1.5). The ATG14 subunit of VPS34 complex I is required for targeting the complex to ER and pre-autophagosomal structure, and involved in autophagosome initiation (Lamb et al., 2013)
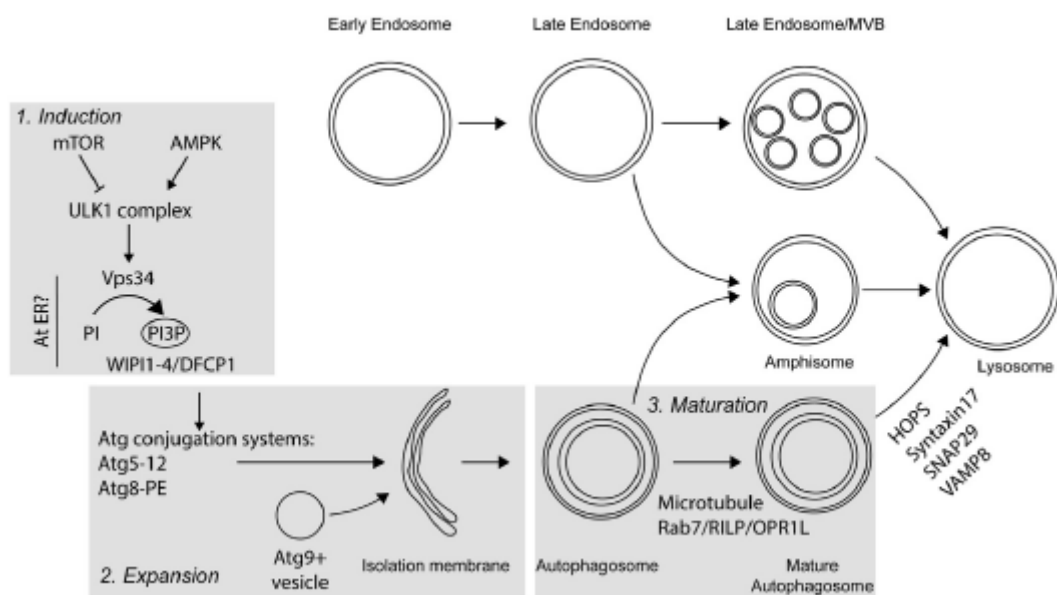
Figure 1.5. Schematic of autophagy mechanism.
Autophagy is triggered by mTOR and AMPK, subsequcent PI(3)P production recruits PI(3)P binding protein to the membrane. Autophagic substrates are packaged into autophagosome, which were then fused with lysosome for degradation (Lieberman andSulzer, 2020).

Maintaining protein and organelle quality and preventing misfolded protein accumulation in neurons are essential for neuronal function and preventing various forms of neurodegeneration. In neurons autophagosomes originate in the distal end of axons and undergo retrograde transport towards the proximal end of axons and soma where most lysosomes are located for degradation. On the other hands, autophagosomes in the soma are trafficked from the axon or generated locally in response to enhanced synaptic activity. These functions depend on the type and age of neurons, although the complexity of autophagic activity in the brain requires further study (Kulkarni et al., 2018).

Recent works has shown that autophagy has roles in pre- and postsynaptic functions during normal development and in disease. In *Drosophila*, overexpression of Atg1, a homolog of ULK1, causes an increased number of synaptic sites, whereas loss of autophagy decreases size of neuromuscular junction (Shen and Ganetzky, 2009). More studies suggested that autophagy shapes neurotransmission. Ultrastructural analysis of autophagy-deficient dopaminergic neurons showed enlarged presynaptic terminals and changes in morphology and number of synapses (Hernandez et al., 2012). suggesting that autophagy has roles in homeostasis of SVs and neurotransmitter release (Figure 1.6). Autophagy is also implicated in the clearance of damaged SV proteins. It has been proposed that a highly regulated clearance system is required for neurons to maintain the synapse integrity and synaptic function (Hoffmann et al., 2019).
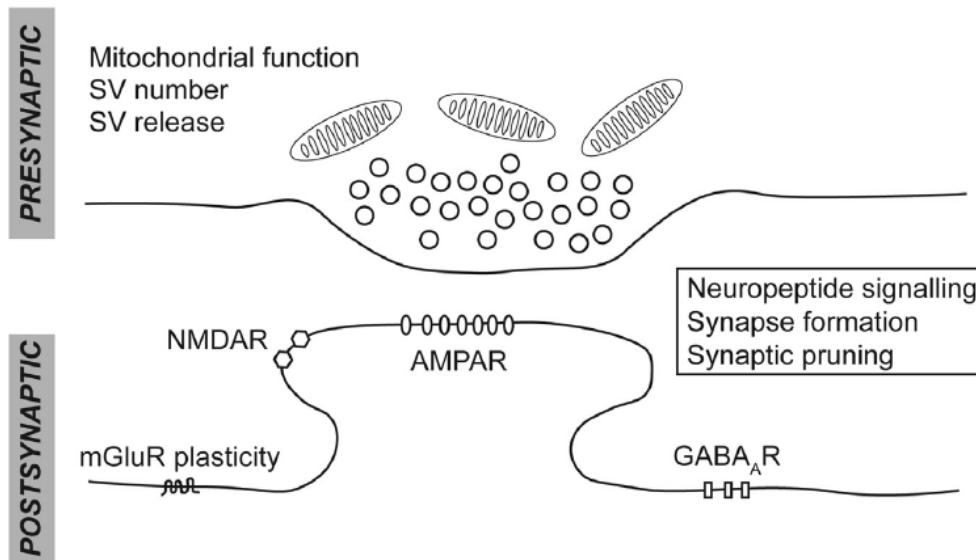
Figure 1.6. The roles of autophagy in pre- and postsynaptic functions.
Autophagy can control neurotransmission at both pre- and postsynapses. The presynaptic, autophagy controls SV homeostasis and release as well as mitochondrial function. The postsynaptic autophagy regulates excitatory neurotransmission by degrading AMPA and GABA$_A$ receptors. Autophagy modulates synaptic plasticity, neuropeptide signaling, synapse formation, and synaptic pruning (Lieberman andSulzer, 2020).

1.3.3 The role of VPS34 complex II in the endosomal system

VPS34 complex II is recruited to early endosome through early endosomal GTPase Rab5 and VPS15 interactions, and it locally generates more PI(3)P on endosomal membrane. Rab proteins, such as Rabenosyn-5 and Rabankyrin-5, and EEA1 interact with Rab5 and PI(3)P via FYVE domains. The assembly of early endosomal proteins are involved in the regulation of endosomal docking and fusion. The conversion of PI(3)P into other phosphoinositides are involved in endosomal maturation along the early endosome/late endosome/lysosome pathway. The transition between early and late endosomes is mediated by Rab5 to Rab7 conversion, and interaction between VPS34-VPS15 and Rab7 is crucial for endosome maturaton (Poteryaev et al., 2010). Additionally, EEA1 interacts with SNARE proteins (soluble NSF-attachment protein receptor) Syntaxin-6 and Syntaxin-13 to regulate

vesicle docking and priming during early endosomal fusion (McBride et al., 1999; Simonsen et al., 1999).

Besides, Retromer complex is localized at endosomal compartment, and VPS34 complex II is required for the function of the Retromer complex that is involved in retrograde trafficking of endocytic cargos to the Golgi compartment (Figure 1.7). Retromer regulates the homeostasis of many endosome-related transmembrane proteins. Mutations in Retromer complex cause defects in protein turnover that are implicated in neurodegenerative diseases (Vilariño-Güell et al., 2011). Retromer complex is composed of three core proteins, VPS35, VPS29 and VPS26, and membrane-associated sorting nexin dimer (SNX1, SNX2, SNX5 and SNX6) that mediates endosomal membrane targeting through a PI(3)P binding PX domain The association of Retromer with endosomes also requires Rab7, which plays a central role in the retrieval of different cargo proteins from endosome to trans-Golgi network (Seaman et al., 1997; Wang et al., 2018)

In addition to Retromer complex, VPS34 complex II is also involved in the assembly of ESCRT (endosomal sorting complexes required for transport) machinery, that plays a vital role in multivesicular body (MVB) biogenesis, cytokinetic abscission and viral budding (Wollert et al., 2009). In this pathway, VPS34 produces PI(3)P which then recruits the ESCRT-0 protein Hrs to the endosome through a FYVE binding domain. Hrs is the initial factor for assembly of ESCRT subcomplexes (ESCRT-I, -II, -III and VPS4) that drives internalization of ubiquitinated membrane proteins into intraluminal vesicles (ILVs) of MVBs, and finally leads to lysosomal degradation. ESCRT dysfunction is associated with numerous diseases, such as cancer and neurodegeneration (Henne et al., 2011)

In summary, generation of PI(3)P by VPS34 plays important roles in cellular mTOR signaling, endocytic protein trafficking as well as autophagy (Figure 1.7). VPS34 knockdown or conditional knockout mice have shown that VPS34 plays critical roles in different tissues or organs, which are highly linked to human disease, especially

neurodegeneration and autism (Inaguma et al., 2016; Miranda et al., 2018). However, only few studies have addressed the role of VPS34 in neurons and its contribution to neuronal function.
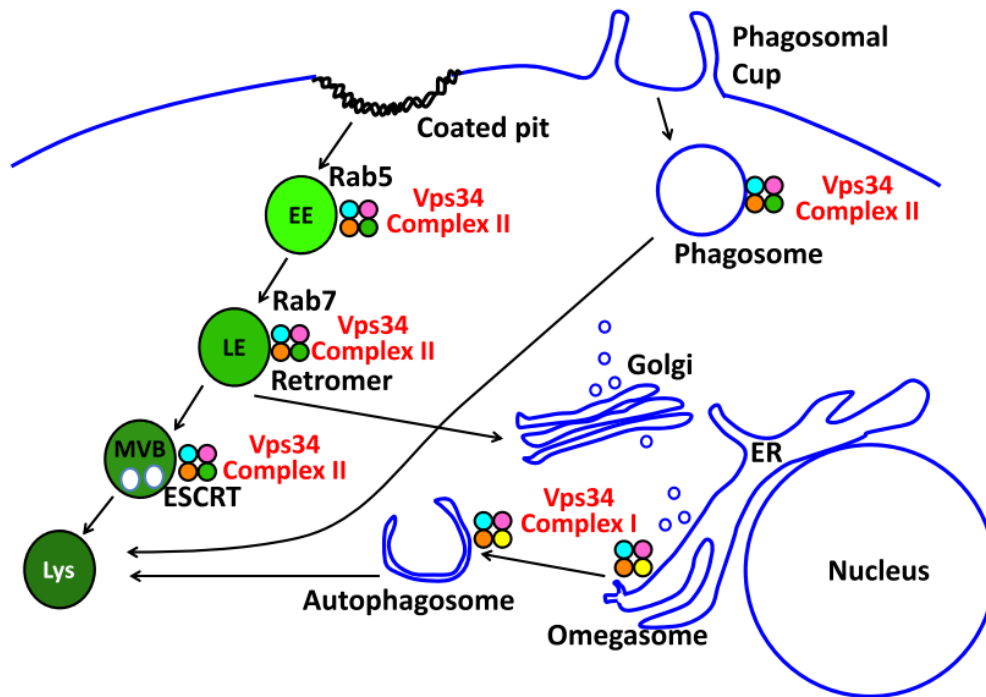
Figure 1.7. Classical functions of VPS34.
PI(3)P is synthesized by VPS34 in intracellular membrane. VPS34 complex I is involved in autophagosome formation, while VPS34 complex II regulates fusion and maturation of Rab5-positive early endosome, mediates endosome to Golgi retrograde transport, and ESCRT complex (Backer, 2016).

1.3.4 Dysregulation of PI(3)P levels in the nervous system

Neurons are susceptible to any disruption of endocytic or autophagic pathways. Several studies have demonstrated that genetic mutations in ubiquitous proteins which regulate endocytic or autophagic events result in various forms of neurodegeneration. Phosphoinositides are crucial for diverse membrane trafficking mechanisms. For example, mutation of the PI 3-phosphatase myotubularin-1 (MTM1) causes X-linked centronuclear myopathy, whereas its homologs MTMR-2, MTMR-13 and FIG4 which drive dephosphorylation of $PI(3,5)P_2$ into PI(3)P, or PI(3)P into PI, are implicated in

Charcot-Marie-Tooth peripheral neuropathies, suggesting that an imbalanced PI(3)P-PI(3,5)P$_2$ or PI-PI(3)P conversion may lead to neuromuscular disorders (Nicot and Laporte, 2008).

In addition, PI(3)P has been reported to be localized at dendrites, axons and synapses in hippocampal neurons. A study has showed that additional application of membrane permeable PI(3)P-AM in cultured hippocampal neurons promoted the formation of gephyrin clusters, a scaffold protein of inhibitory postsynapses, and accompanied with an increase in postsynaptic GABA receptors. This study suggested that endosomal PI(3)P is required for clustering of GABA receptors and the regulation of the synaptic strength at inhibitory postsynapses of hippocampal neurons (Papadopoulos et al., 2017). Some patients with learning disorder have been showed to carry genetic microdeletion of VPS34, suggesting that VPS34 is essential for brain development (Inaguma et al., 2016). Also, the polymorphisms in the VPS34 promoter region were reported to associate with schizophrenia and bipolar diseases (Stopkova et al., 2004).

Furthermore, several studies based on conditional VPS34 deficient mice have shown that VPS34 deletion in sensory and pyramidal neurons lead to loss of dendritic spines, decreased number of synapses, gliosis and neurodegeneration, which were linked to defects in the endosomal system but not in autophagy (Wang et al., 2011; Zhou et al., 2010). Besides, recent studies have shown that selective depletion of PI(3)P can be found in the brains of human patients or mouse models of Alzheimer's disease. Disruption of neuronal VPS34 impairs autophagy, lysosomal degradation and causes endolysosomal membrane damage. PI(3)P deficiency due to loss of VPS34 activity also affects APP processing, which is associated with Alzheimer's disease (Miranda et al., 2018; Morel et al., 2013). Intriguingly, the hallmarks of Alzheimer's disease include presence of neuronal plaques composed of amyloid beta, intracellular neurofibrillary tangles containing hyperphosphorylation of tau protein, and these phenotypes are accompanied with abnormal activity of Calpain in

pathological conditions (Zheng et al., 2002)

1.4 Abnormal Calpain activity in neurodegeneration

In addition to the role of VPS34 and PI(3)P in neurodegeneration, a number of pathological conditions have been associated with abnormal Calpain activity, including Parkinson's disease, Alzheimer's disease, ischemia, stroke and brain trauma (Zatz and Starling, 2005). Calpains are calcium-dependent cysteine proteases that regulate cellular functions via a unique posttranslational proteolytic modification. Two well-studied ubiquitous Calpains, Calpain1 and Calpain2, are highly expressed in the central nervous system, and are crucial for neuronal function. More than 200 Calpain substrates have been identified in neurons, such as membrane receptors, cytoskeleton, postsynaptic density proteins, kinases and phosphatases which are localized at nerve terminals (Wu and Lynch, 2006). Calpain-mediated synaptic protein cleavage plays important roles in the regulation of synaptic processes, not only in physiological states but also in pathological conditions.

1.4.1 The regulation of Calpain activity

Calpain1 and Calpain2 (also called μ-Calpain and m-Calpain, respectively) are two major Calpains expressed in neurons. Calpain activity is triggered by calcium binding: Calpain1 requires 3-50 μM calcium, whereas Calpain2 requires 0.4-0.8 mM calcium *in vitro*. Calpain has been identified as a phosphoinositide binding protein. The interaction between Calpain and charged membrane phospholipids such as phosphoinositides lowers the calcium requirement for Calpain activation (Shao et al., 2006). In the absence of an external stimulus, Calpains are diffusely distributed in the cytoplasm, while they change their localization and bind to the plasma membrane or organelle membranes upon sensing elevated intracellular calcium concentration (Hood et al., 2004; Mendoza et al., 2018; Michetti et al., 1996). To tightly regulate the activity of Calpain, Calpastatin is an endogenous inhibitor of Calpain,

which can bind to the substrate binding site of Calpain for activity inhibition (Goto et al., 1994). The Calpastatin/Calpain ratio varies in different brain regions. Imbalanced Calpastatin/Calpain ratio has been found in mice with Alzheimer's disease, suggesting that Calpastatin is an important regulator for Calpain activation in the brain (Vaisid et al., 2007).
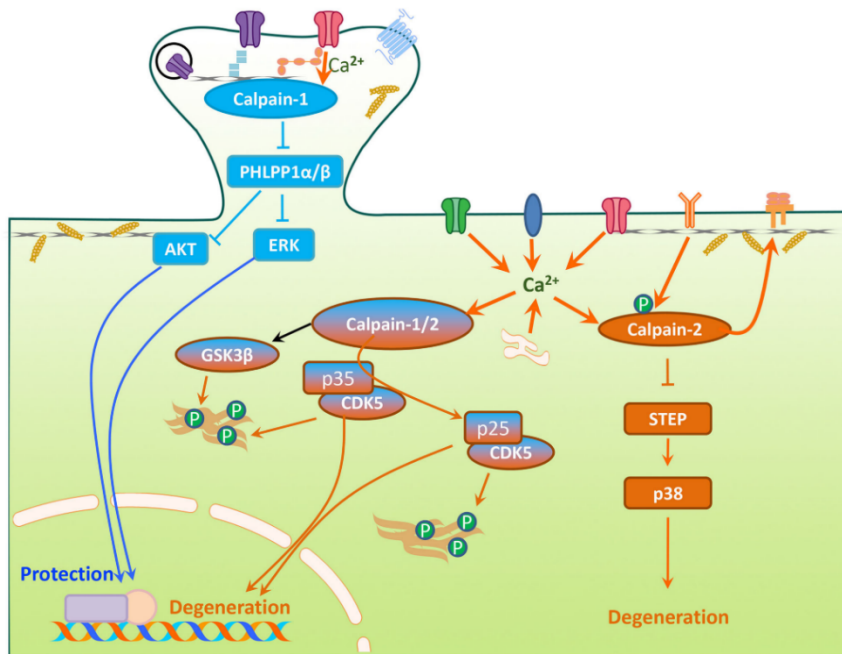
Figure 1.8. Opposite function of Calpain1 and Calpain2 in neurodegeneration
Calcium influx activates Calpian1, which cleaves PHLPP1, resulting in activation of ERK and Akt for neuron protection. Activation of Calpain2 leads to p35 cleavage and hyperaction of cdk5, and finally lead to neurodegeneration (Huo et al., 2017).

Additionally, Calpain1 and Calpain2 are believed to play opposite roles in neurodegeneration (Figure 1.8). After calcium triggered Calpain activation, Calpain1 cleaves PHLPP1 (PH domain and Leucine rich repeat Protein Phosphatase 1) which is a negative regulator of ERK and Akt, resulting in activation of ERK and Akt pathways and neuroprotection (Bickler and Fahlman, 2004). On the other hand, activation of Calpain2 results in cleavage of STEP, leading to neurotoxicity (Xu et al., 2009). In particular, the Cdk5 activator p35 is cleaved by Calpain2 into p25, such that hyperactived cdk5/p25 induces tau hyperphosphorylation, that is a hallmark of Alzheimer's disease (Huo et al., 2017;

Kimura et al., 2014)

1.4.2 The Calpain2/p35-p25/Cdk5 pathway

As mentioned above, calcium influx through NMDA receptors activates Calpain2, resulting in conversion of the Cdk5-activator p35 to p25. p35 is a membrane-bound protein that consists of two parts, N-terminal p10 and C-terminal p25. The p10 region is myristoylated which is important for membrane targeting of p35, and p10 also contains a signal for p35 turnover (Figure 1.9). Cdk5 is autoinhibited via phosphorylation of p35, which leads to shorter half-life of p35, since this phosphorylation not only prevents the intramolecular cleavages of p35 into p25 and p10, but increases its proteasomal degradation (Kamei et al., 2007). However, when p35 is cleaved by Calpain2 to form p25 in certain pathological conditions, such as exposure to amyloid β peptide (Aβ) and excitotoxicity, the degradation signal is lost and mistargeted p25/cdk5 becomes hyperactivate. p25/Cdk5 has an extended half-life thereby substantially extending the activation period of Cdk5. Under neurotoxic conditions, p25/Cdk5 induces tau hyperphosphorylation, which aggregates to form neurofibrillary tangles during the pathogenesis of Alzheimer's disease (Kimura et al., 2014; Shah and Lahiri, 2014).
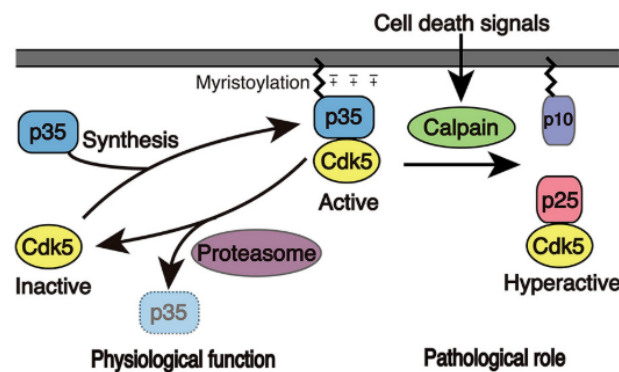

Figure 1.9. Calpain/p35-p25/Cdk5 pathway.
Cdk5 along is inactive, it needs to be activated by p35. Myristoylated p35 targets the whole complex to the membrane. P35-p25 conversion by Calpain leads to hyperactivation of Cdk5 which is involved in several pathological condition (Kimura et al., 2014).

1.5 The role of Cdk5 in neuronal function

Cyclin-dependent kinase 5 (Cdk5) is a serine threonine kinase that functions in neuronal migration, neurite extension, pre- and postsynaptic synaptic transmission and synaptic plasticity. Cdk5 activity is limited in post mitotic neurons due to the absolute requirement of its regulatory factor p35. The association between Cdk5 and p35 induces a conformational change in the catalytic subunit of Cdk5 and results in induction of kinase activity (Tarricone et al., 2001). Dysregulation of Cdk5 is associated with neurodegenerative diseases such as Alzheimer's disease, Parkinson's disease, Huntington's disease and some other brain disorders (McLinden et al., 2012).

1.5.1 The role of Cdk5 in synaptic vesicle recycling

Cdk5 is a key factor to control synaptic vesicle exo- and endocytosis. Cdk5/p35 interacts with multiple synaptic proteins to modulate exocytosis. For example, phosphorylation of Munc18 by Cdk5 disrupts its interaction with Syntaxin1A, which then affects their association with vesicular SNAREs, and facilitates exocytosis and neurotransmitter release (Fletcher et al., 1999). In addition, Cdk5 acts as a negative regulator of vesicle release: Inhibition of Cdk5 unlocks access to the resting vesicle pool, which normally stays stationary during neuronal activity, and causes a profound potentiation of presynaptic function. The balance between Cdk5 and Calcineurin, a calcium-dependent phosphatase that has an opposing function to Cdk5, is important for controlling the size of the recycling vesicle pool, and thus the release of neurotransmitter (Kim and Ryan, 2010).

In spite of the role in exocytosis, Cdk5 also participates in regulation of vesicle endocytosis (Figure 1.10). Cdk5 constitutively phosphorylates dephosphins such as Amphiphysin-1, Synaptojanin-1 and Dynamin-1 at rest. Amphiphysin-1 is a scaffold protein for Dynamin-1 recruitment, whereas Synatojanin-1 is required for vesicle uncoating. Upon presynaptic Ca^{2+} influx and neurotransmitter release, dephospin proteins are

29

dephosphorylated by the calcium-dependent phosphatase Calcineurin to trigger SV endocytosis. When synaptic activity stops the dephosphins are phosphorylated again by Cdk5. This phosphorylation/dephosphorylation cycle is mediated by the balance between Cdk5 and Calcineurin, and is essential for SV endocytosis (Samuels and Tsai, 2003).
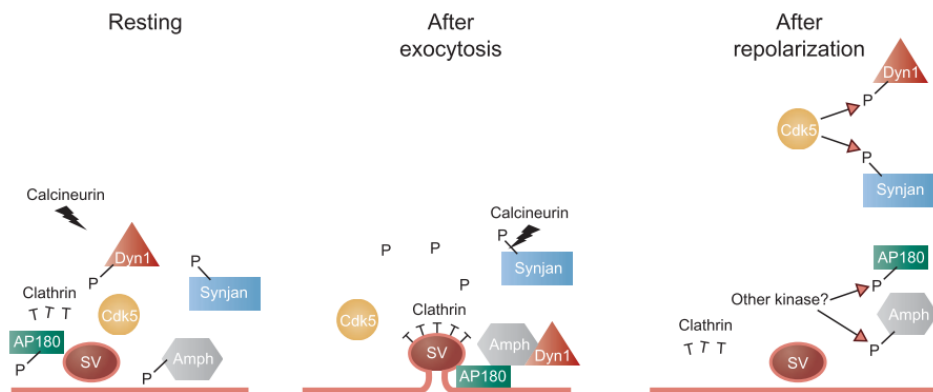
Figure 1.10. The phosphorylation cycle in SV endocytosis.
In the resting state, dephosphin proteins are phosphorylated (left), and SV are stored at synaptic terminals. After exocytosis, Calcineurin rapidly dephosphorylates dephosphin proteins and triggers SV endocytosis (middle). After repolarization, Cdk5 rephosphorylates dephosphins makes neuron back to resting state (Samuels and Tsai, 2003).

1.5.2 The role of Cdk5 in neurotransmission

Apart from its cricital role in regulating neurotransmitter release and SV recycling, Cdk5 also controls the postsynaptic receptor function in different types of neurotransmission. For example, Cdk5 activation is required for acetylcholine (Ach) receptor clustering and signaling in neuromuscular junction and motor axons (Fu et al., 2005). In the glutamatergic postsynapse, Cdk5 phosphorylates NR2A, a subunit of NMDA-type glutamate receptors, to increase channel activity which is important for induction of long-term potentiation (LTP) in the hippocampal CA1 region. Conversely, Cdk5 inhibition facilitates NMDA-mediated glutamatergic neurotransmission in the striatum. Additionally, Cdk5 also phosphorylates PSD-95, a postsynaptic scaffold protein, to regulate the clustering and density of ionotropic glutamate receptors. Inhibition of Cdk5 also decreases NMDA receptor endocytosis

(Bianchetta et al., 2011). This up and down regulation of NMDA receptor trafficking to the surface by Cdk5 is important for dynamic synaptic changes and synaptic plasticity (McLinden et al., 2012).

1.6 Homeostatic synaptic scaling and synaptic plasticity

Synaptic plasticity is a way how neurons adapt their behavior to a changing environment through changes in synaptic number and strength, and therefore store information and contribute to learning. When hippocampal neurons were induced to fire more than normal, over firing returns to baseline level, and contrarily, if neuron firing rate is reduced over time, neurons compensate and restore firing via synaptic scaling and plasticity (Figure 1.11). The coordination and balance between excitatory and inhibitory neurotransmission modulates network activity (Turrigiano, 2012; Turrigiano and Nelson, 2004). It is not surprising that varied homeostatic mechanisms are operated by neurons to adapt external perturbation and maintain stable firing rate.

1.6.1 Synaptic scaling is tightly regulated in different type of synapses

Synaptic scaling is a form of synaptic plasticity in the central nervous system. Manipulation of neuronal activity induces bidirectional compensatory changes in the synaptic strength of glutamatergic neurons and this process is best understood for postsynapses. When hippocampal neurons are induced to fire more intensely, after a period of time neuronal firing returns to basal levels, and conversely, when neuronal firing rate is reduced over time, neurons compensate and restore the firing to normal levels (Turrigiano et al., 1998) (Figure 1.11). The activity-dependent up- or downscaling of synaptic strength regulates the number of the N-methyl-D-aspartate (NMDA) and α-amino-3-hydroxy-5-methyl-4-isoxazole-propionic acid (AMPA) receptors on the postsynaptic plasma membrane (Watt et al., 2000). This mechanism is highly dependent on calcium influx and operates via

CaMK (Calcium/Calmodulin-dependent protein kinase) or Polo-like kinase 2 (Plk2)-Cdk5 pathway. Specifically, in the Plk2-Cdk5 pathway, calcium influx activates Plk2 and Cdk5 and affects the phosphorylation and degradation of its downstream target SPAR, a postsynaptic RapGAP and scaffolding protein which is involved in growth of dendritic spines and of the postsynaptic compartment (Seeburg et al., 2008). The detailed cellular and molecular mechanisms require further studies in different type of neurons.

Neural circuits are composed of different types of excitatory and inhibitory neurons. It is not surprising that the homeostatic plasticity rules are specific for particular types of synapses. In cortical neurons it has been reported that excitatory synapses that connect to excitatory pyramidal neurons are scaled up by activity blockade, whereas the same mechanism does not operate for excitatory synapses that provide input to inhibitory neurons. On the other hand, enhanced network activity increases excitatory transmission onto GABAergic interneurons and induces additional inhibition (Rutherford et al., 1998; Turrigiano et al., 1998). Although excitatory and inhibitory synapses have their distinct plasticity rules, an overall consistent homeostatic shift applies to balance between excitation and inhibition. This mechanism is crucial for stabilizing firing rates, maintaining the neuronal network and preventing excitotoxicity in response to changes in stimulation (Turrigiano and Nelson, 2004).
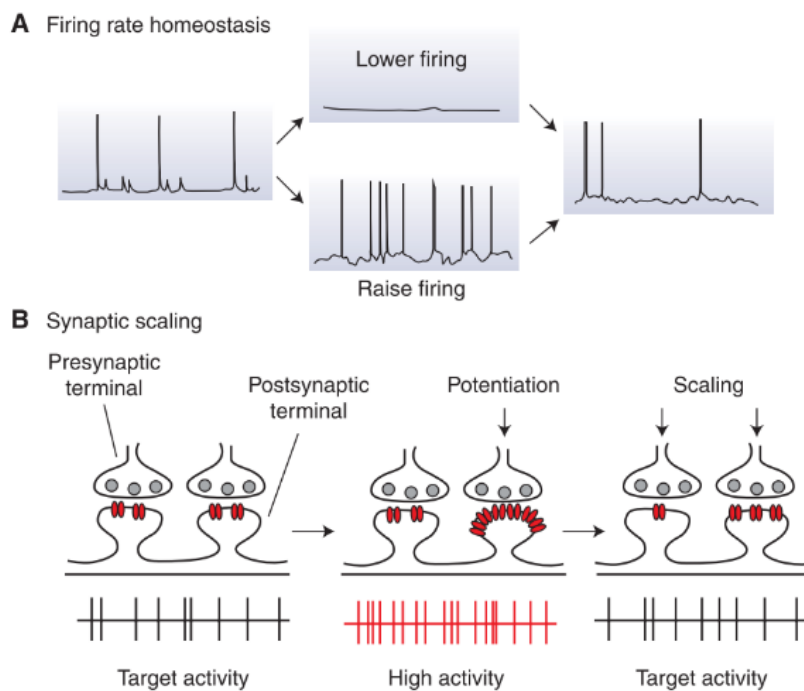
Figure 1.11. Controlling of neuronal firing through homeostasis synaptic plasticity.
(A) Demonstration of firing rate is homeostatic regulated by neuronal networks. **(B)** Synaptic scaling contributes to firing rate homeostasis. Perturbed neuron activity triggers synaptic scaling, which reduce the strength at all synapses with high activity to return to baseline level (Turrigiano, 2012).

1.6.2 Presynaptic homeostatic plasticity

Homeostatic plasticity is not only confined to the postsynaptic site, but can also affect the presynaptic machinery in a similar fashion. At the *Drosophila* neuromuscular junction, activity blockade by tetrodotoxin TTX or the AMPA receptor blocker NBQX leads to a 50% decrease of the readily releasable pool (RRP) and SV release probability, whereas elevation of synaptic activity causes a decrease in RRP size. This suggests that an activity-dependent bidirectional plastic regulation of neurotransmitter release is important for maintaining neuronal firing rates within certain boundaries (Moulder et al., 2006; Murthy et al., 2001). Besides, multiple studies have suggested that different SV pools are regulated by homeostatic adaption to the overall neuron activity (Figure 1.12). As discussed above, Cdk5 is a key player for controlling the recycling pool size during homeostatic plasticity.

The protein phosphatase Calcineurin antagonizes Cdk5 in the regulation of the total recycling pool size. Additionally, Cdk5 can phosphorylate voltage-gated Ca^{2+} channel to control homeostatic changes in evoked Ca^{2+} influx and basal neurotransmission (Jeans et al., 2017; Tomizawa et al., 2002). Presynaptic homeostatic adaption is important for preventing the runaway excitation or excitotoxicity during physiological or pathological conditions such as seizures.
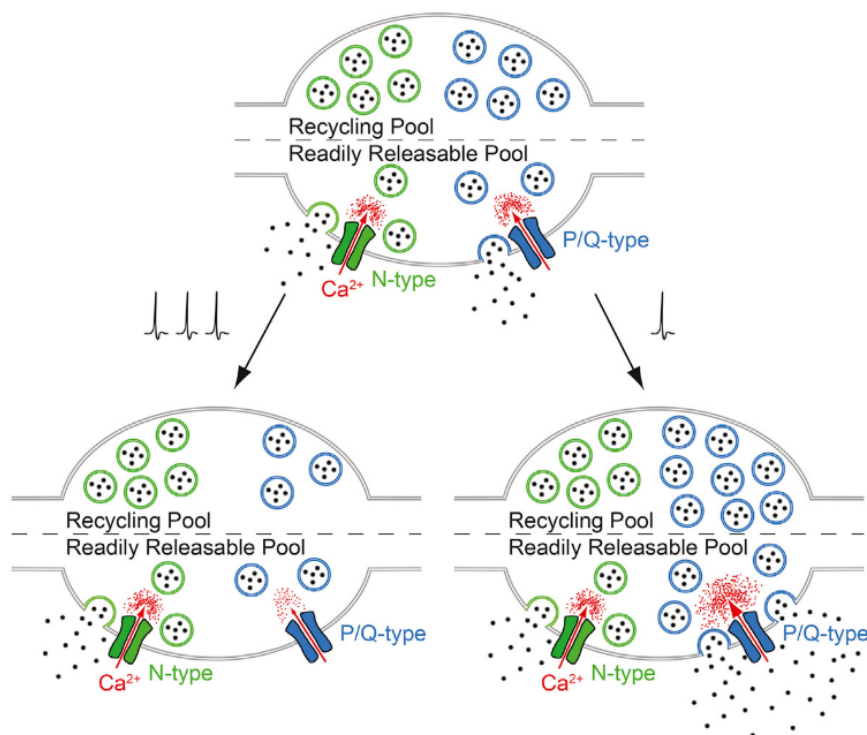
Figure 1.12. Homeostatic changes of SV pool at presynapse.
Neuron excitation reduce Ca^{2+} influx via P/Q type calcium channel and SV recycling pool, whereas silence led to increased ca^{2+} influx and elevated recycling pool at the presynaptic site (Jeans et al., 2017).

Defective homeostatic plasticity has been found in variety of animal models with neurological, neurodevelopmental and neuropsychiatric diseases. Especially, impaired homeostatic synaptic plasticity has been proposed to be a key factor for pathogenesis of Alzheimer's disease. Additionally, the neuropsychiatric disorder Schizophrenia is also linked to dysfunction of synaptic plasticity. Impairment of certain neurotransmitter systems (e.g.

hyperdopaminergic and hypofunction of glutamatergic transmission) can be observed in patient or mouse models of schizophrenia, and manipulation of synaptic plasticity is considered as the treatment for mental disorders (Kavalali and Monteggia, 2020). Synaptic plasticity is important for reorganization of the structure, function and connection between neurons in response to stimulation, and it is necessary for brain development, homeostasis, memory and learning (Davis and Müller, 2015; Dhuriya and Sharma, 2020; Frere and Slutsky, 2018). Given that the importance of homeostatic synaptic plasticity, the detailed mechanisms and how signal cascade is triggered need to be answered.

1.7 Aims of the study

Exo- and endocytic recycling of SVs is a key process for neurotransmission. Even though it is widely accepted that an endosome-like vesicle is commonly found in synaptic terminals and act as an intermediate recycling platform in many different modes of SV endocytosis, a clear picture on the exact function and the precise lipid composition of this structure is still missing. Given that endosomal PI(3)P serves as a hub for regulating different intracellular signaling pathway, it is possible that presynaptic endosomal PI(3)P has a role in controlling of neuronal activity.

The aims of this study were: 1) to identify synaptic PI(3)P in hippocampal neurons; 2) to investigate the role of PI(3)P-positive endosomes at the presynaptic terminals; 3) to understand the role of PI(3)P in SV recycling and how the levels of PI(3)P-positive endosomes correlate with neuronal activity. Based on our findings on the crucial role of PI(3)P in the maintenance of SV recycling and the regulation of PI(3)P levels by electrical activity, 4) we further investigated the molecular mechanism underlying PI(3)P-mediated synaptic homeostatic scaling and how PI(3)P functions in control of excitatory neurotransmission.

2. Materials and Methods

2.1 Preparation of primary hippocampal and cerebellar neuron cultures

Primary hippocampal neurons were used for transfection, live-imaging, immunocytochemistry, and electron microscopy. The detection of synaptic protein levels by immunoblotting after pharmacological treatments were carried out using cerebellar neurons. To prepare neuronal cultures, hippocampus or cerebellum were surgically removed from postnatal mice at p1-3 or p6, respectively. The tissues were cut into small pieces, and were digested in trypsin and DNAase containing buffer for 15 min at 37℃ (137 mM NaCl, 5 mM KCl, 7 mM Na_2HPO_4, 25 mM Hepes and pH 7.2). After digestion, the neurons were washed twice with HBSS with and without 20% FCS, and then followed by pipetting up and down in DNase containing dissociation buffer (25 mM $MgSO_4 \cdot 7H2O$ in HBSS) into single neurons. Primary neurons were plated onto PLL-coated coverslips for 6-well plates and cultured in MEM medium (Thermo Fisher) containing 2% B27 and 5% FCS. The medium for cerebellar cultures additionally contained 25 mM KCl. All neuronal cultures were treated with 2 μM AraC to avoid astrocyte growth, and cultured at 37°C, 5% CO_2.

2.2 Calcium phosphate transfection

Calcium phosphate method (Promega) were used for neuron transfection at DIV 7-9. Briefly, 2X HEPES buffer and 6 μg plasmid DNA were mixed with 250 mM $CaCl_2$ and incubated for 20 min to have precipitate formation. In parallel, neurons were starved in osmolarity-adjusted by D-mannitol (Sigma-Aldrich), serum-free NBA medium (Gibco) at 37°C, 5% CO_2. Precipitates were added to the neurons and incubated for 30 min at 37°C, 5% CO_2. Finally, the coverslips were washed twice with osmolarity-adjusted HBSS (Gibco) and returned to the original medium.

2.3 Live imaging of synaptic vesicle exo- and endocytosis via pHluorins

pHluorin-based assays (e.g. Synaptophysin-pHluorin, vGlut1-pHluorin or Synaptotagmin-pHluorin) were used for tracking kinetics of SV exo-/ endocytosis. Cultured hippocampal neurons at DIV12-14 were pre-incubated with different inhibitors for 1 h and placed into an RC-47FSLP stimulation chamber (Warmer instruments) for electrical field stimulation and imaged at 37°C in basic imaging buffer (3.5 mM KCl, 170 mM NaCl, 20 mM N-Tris[hydroxyl-methyl]-methyl-2-aminoethane-sulphonic acid (TES), 5 mM glucose, 0.4 mM KH_2PO_4, 5 mM $NaHCO_3$, 1.2 mM Na_2SO_4, 1.2 mM $MgCl_2$, 1.3 mM $CaCl_2$ (or 4 mM $CaCl_2$ for 2AP stimulation), 50 mM AP5 and 10 mM CNQX, pH 7.4). To distinguish whether increased surface retention of pHluorin-tagged SV proteins is due to defective endocytosis or impaired re-acidification of endocytic vesicles, acid quench assays were performed by locally perfused neurons with acidic imaging buffer (where TES was replaced by 2-(N-morpholino) ethane-sulfonic acid, adjusted to pH 5.5) for 20 s before and after electrical stimulation. All images were obtained by epifluorescence microscopy (Nikon Eclipse Ti) using an eGFP filter set F36-526, 40X oil-immersion objective and a sCMOS camera (Neo, Andor), and analyzed by imageJ using custom-written macros. At least 10-20 responded boutons were randomly selected for analysis. The surface normalized curve was obtained by normalization of the fluorescent changes to the average signal of the first 10 s before electrical stimulation, and the peak normalized traces were calculated by normalization of the signal to the first peak as 1. SV exocytosis was quantified by measuring the fold-change in fluorescence upon stimulation. SV endocytosis was quantified by two complementary methods: For brief stimulations (e.g. 2 APs) endocytic time constants were determined by fitting the kinetic data points to monoexponential [y0 - A*exp(-x/t)] with zero offset using Prism 5 (Graphpad) software. For stimulations with multiple trains (e.g. 4 x 200 APs or 4 x 50APs) the surface levels of SynaptopHluorin at 90 seconds after each stimulation was plotted. Surface retention was assessed by normalizing the surface pHluorin

levels to baseline fluorescence. For the acidic quench experiment, the acidic buffer-treated fluorescence was subtracted by the initial signals which were taken in neutral imaging buffer to obtain ΔF1, and the ΔF2 were calculated by subtraction of acidic buffer-treated fluorescence to the average signal of 10 s after 4 x 200 APs stimulation.

2.4 Rescue of defective SV endpcytosis by membrane-permeant PI(3)P

Hippocampal neurons were transfected with Synaptohpysin-pHluorin at DIV7. Synthesized PI(3)P-AM (Subramanian et al., 2010) was dissolved in dry DMSO to a stock concentration of 40 mM and mixed with same volume of 10% pluronic F127 to enhance solubility. PI(3)P-AM is directly supplied together with 10 μM VPS34IN1 in growth medium and incubated with Synaptophysin-pHluorin-expressing neurons for 1 h prior to imaging by epifluorescence microscopy (Nikon Eclipse Ti).

2.5 Immunocytochemistry of hippocampal neurons in culture

For PI(3)P labeling, DIV 14 neurons were fixed with 2% PFA for 15min at room temperature, washed 3 times for 5 minutes with PBS containing 50 mM NH_4Cl and permeabilized for 5 min by 20 μM Digitonin in buffer A (20 mM Pipes, 137 mM NaCl and 2.7 mM KCl, pH 6.8). Excess Digitonin was removed by washing neurons in buffer A. To block the antibody epitopes and to label PI(3)P, neurons were treated with buffer A containing 5% normal goat serum and 0.05 mg/mL GFP-2XFYVE probe for 45 minutes. To remove the unbound probe, neurons were washed for 5 min with buffer A, followed by 1 h incubation with primary antibodies against GFP, MAP2 and Synaptophysin and a 45 min incubation with corresponding secondary antibodies coupled to Alexa Flour 488, 568 and 647 (ThermoFisher) at room temperature. Unbound antibodies were removed by washing with buffer A after each steps. Stained neurons were post-fixed with 2% PFA for 5 min and mounted on glass slides using Immun-Mount (ThermoFisher). For Calpain2 and Rab5

staining, DIV14 neurons were fixed with ice-cold methanol for 3 min and with 2% PFA for 15 min at room temperature. Neurons were then permeabilized for 5 minutes with 20 μM Digitonin in PBS and were blocked for 30 minutes by PBS containing 5% normal goat serum at room temperature, followed by overnight incubation with primary antibodies against Rab5, Calpain2, MAP2 and vGLUT1 at 4 °C, and then followed by 45 min incubation with Alexa Flour 488, 568 and 647-coupled secondary antibodies at room temperature. Neurons were washed twice with PBS after each steps, and mounted using Immu-Mount (ThermoFisher). Finally, all the neurons were imaged by spinning disk confocal microscopy (Ultraview ERS, Perkin Elmer) with Volocity software (Improvision, Perkin Elmer), and analyzed by ImageJ. For PI(3)P quantification, the cumulative intensity of fluorescence was obtained from mean intensity of selected region multiplied by thresholded positive area. To eliminate the difference of each experiments, the treated condition was normalized to control group. For Calpain and Rab5 quantification, the mean intensity was measured in MAP2-positive soma or vGlut1-positive synapses.

2.6 Immunoblotting and quantification of protein content

DIV7 cerebellar granule neurons were treated with different inhibitors for 1 h, and washed 2x with ice-cold PBS. Neuron lysates were harvested in sample lysis buffer (20 mM Tris pH 7.4, 1% SDS, 5% glycerol, 5mM β-mercaptoethanol, 0.01% bromophenol blue, 0.3% protease inhibitor cocktail (Sigma-Aldrich) and phosphatase inhibitors (cocktails 2 and 3, Sigma-Aldrich). Equal protein amounts of lysates were analyzed by SDS-PAGE and immunoblotting. Primary antibodies against various synaptic proteins were used in immunoblotting, followed by LI-COR 800CW and 680RD as secondary antibodies. Immunoblots were imaged by LI-COR system. The antibodies used in immunoblotting were listed in session 2.8.

2.7 Somatic and synaptic calcium measurement

For somatic basal calcium, hippocampal neurons at DIV14 were treated with DMSO or 10μM VPS34IN1 for 1 h. 3μM Fluo4-AM (ThermoFisher) and 1% pluronic F-127 were applied in growth medium for 15 min. Coverslips were washed three times with growth medium, and imaged by epifluorescence microscopy (Nikon Eclipse Ti) using an eGFP filter set F36-526, 40X oil-immersion objective and a sCMOS camera (Neo, Andor), and analyzed by imageJ. The mean intensity was measured in each condition. To detect synaptic calcium, hippocampal neurons were transfected with sypHy-RGECO plasmid at DIV7, and imaged by epifluorescence microscopy. The mean intensity of RGECO-expressing synapses was measured in control and inhibitor-treated neurons.

2.8 Quantification and statistics

All data are presented as mean ± SEM, and are obtained from ≥ 3 independent experiments, with total sample number provided in figure legend. In the experiments that involve light or electron microscopy the statistical significance between two groups for all normally distributed data (e.g. effects of chemical inhibitors or genetic knockdowns on endocytic time constants, pHluorin surface retention levels, relative PI(3)P intensity) was evaluated with a two-tailed paired Student's t-test. The statistical significance between more than two groups for all normally distributed data (e.g., percentage of pHluorin surface retention where inhibitor-treatment, protein overexpression and gene knockdown constructs are combined) was determined by two-way ANOVA using GraphPad6 (Prism). SigmaPlot (Systat Software Inc.) and IGOR Pro (WaveMetrics, Inc.) were used for electrophysiological data analyses and presentation. For PPF measurements significance was evaluated using Two Way RM ANOVA. For PS and polyspike amplitude and area measurements significance was evaluated using One Way ANOVA or student's t-test. Significant differences were marked as *= $p<0.05$, **= $p<0.01$, ***= $p< 0.001$, ****= $p< 0.0001$.

2.9 Reagents for the study

Reagent	Source	Identifier
Plasmids		
Synaptophysin-pHluorin	(Granseth et al., 2006)	
vGlut1-pHluorin	(Voglmaier et al., 2006)	
Synaptotagmin-pHluorin	(Wienisch andKlingauf, 2006)	
mRFP-FKBP-hMTM1	Addgene	Cat#: 51614
FRB*-iRFP-Rab5	This thesis	
mCherry-Rab5 S34N (DN)	Addgene	Cat#: 35139
hSyn1-sypHy-RGECO	Addgene	Cat#: 84078
Antibodies		
GFP (rabbit polyclonal, used at 1:500 in IF)	Abcam	Cat#: ab6556
DeRed (rabbit polyclonal, used at 1:300 in IF)	Takara Bio Clontech	Cat#: 632496
MAP2 (guinea pig polyclonal, used at 1:500 in IF)	Synaptic system	Cat#: 188004
Synaptophysin (mouse monoclonal, used at 1:500 in IF)	Synaptic system	Cat#: 101011
Rab5 (mouse monoclonal, used at 1:100 in IF)	Synaptic system	Cat#: 108011
CAPN1 (mouse monoclonal, used at 1:100 in IF)	Thermo-FIsher	Cat#: MA3-940
CAPN2 (rabbit polyclonal, used at 1:100 in IF)	Cell signaling	Cat#: 2539
CAPN2 (mouse polyclonal, used at 1:50 in IF)	Santa cruz	Cat#: SC-373966
vGlut1 (guinea pig polyclonal, used at 1:500 in IF)	Synaptic system	Cat#: 135304
vGAT (guinea pig polyclonal, used at 1:100 in IF)	Synaptic system	Cat#: 131011
Goat anti mouse IgG Alexa Fluor 488 (used in 1:400)	Thermo-FIsher	Cat#: A11001
Goat anti rabbit IgG Alexa Fluor 488 (used in 1:400)	Thermo-FIsher	Cat#: A11008
Goat anti mouse IgG Alexa Fluor 568 (used in 1:400)	Thermo-FIsher	Cat#: A11004
Goat anti rabbit IgG Alexa Fluor 568 (used in 1:400)	Thermo-FIsher	Cat#: A11011
Goat anti mouse IgG Alexa Fluor 647 (used in 1:400)	Thermo-FIsher	Cat#: A21235
Goat anti guinea pig IgG Alexa Fluor 568 (used in 1:400)	Thermo-FIsher	Cat#: A11075
VPS34 (rabbit monoclonal, used at 1:250 in IB)	Cell signaling	Cat#: 4263S
Synaptophysin (mouse monoclonal, used at 1:500 in IB)	Synaptic system	Cat#: 101011
Synaptotagmin1 (mouse monoclonal, used at 1:500 in IB)	Synaptic system	Cat#: 105011
Clathrin heavy chain (mouse, used at 1:10 in IB)	Volker Haucke Lab	Custom-made
Syntaxin 1A (mouse monoclonal, used at 1:500 in IB)	Synaptic system	Cat#: 110001
SNAP25 (mouse monoclonal, used at 1:500 in IB)	Synaptic system	Cat#: 111011
Dynamin (rabbit polyclonal, used at 1:500 in IB)	Synaptic system	Cat#: 115002
HSP70 (mouse monoclonal, used at 1:1000 in IB)	Thermo-FIsher	Cat#: MA3006
PI3K c2α (rabbit polyclonal, used at 1:100 in IB)	Abcam	Cat#: ab154583
PI3K c2β (mouse monoclonal, used at 1:100 in IB)	BD transduction	Cat#: 611342
Rab5 (mouse monoclonal, used at 1:200 in IB)	BD transduction	Cat#: 610724

GM130 (mouse monoclonal, used at 1:5000 in IB)	Sigma-Aldrich	Cat#: G8795
cdk5 (mouse monoclonal, used at 1:250 in IB)	Santa Cruz	Cat#: sc6247
p35/p25 (rabbit monoclonal, used at 1:250 in IB)	Cell Signaling	Cat#: 2680
active capase3 (rabbit polyclonal, used at 1:100 in IB)	Cell Signaling	Cat#: 9661T
β3-tubulin (rabbit polyclonal, used at 1:10000 in IB)	Synaptic system	Cat#: 302302
GAPDH (mouse monoclonal, used at 1:5000 in IB)	Sigma-Aldrich	Cat#: G8795

shRNA

Non-target shRNA control	Sigma-Aldrich	SHC002
shVPS34	Sigma-Aldrich	TRCN000025373
shVPS15	Sigma-Aldrich	TRCN000027018
shCAPN1	Sigma-Aldrich	TRCN0000030664
shCAPN2	Sigma-Aldrich	TRCN0000030672

Chemicals

VPS34IN1 (used at 3-10 μM)	MRC PPU Reagents	Provided by J. Hastie
SAR405 (used at 20-30 μM)	MRC PPU Reagents	Provided by J. Hastie
ALLN (used at 100 μM)	Sigma-Aldrich	Cat#: A6185
Calpeptin (used at 10 μM)	Sigma-Aldrich	Cat#: C8999
Roscovitine (used at 10 μM)	Sigma-Aldrich	Cat#: R7772
Cyclosporin A (used at 10 μM)	Sigma-Aldrich	Cat#: C3662
Dynasore (used at 20 μM)	Sigma-Aldrich	Cat#: D7693
Fluo4-AM (used at 3 μM)	Thermo-FIsher	Cat#: F14201
Rapalog (used at 2 μM)	Takara Bio	Car#: 635056
PI(3)P-AM (used at 20 μM)	Carsten Schulz Lab	Custom-made
Xestospongin C (used at 1 μM)	Sigma-Aldrich	Cat#: X2628
EGTA (used at 2 mM)	Sigma-Aldrich	Cat#: E3889
EGTA-AM (used at 50 μM)	Sigma-Aldrich	Cat#: 324628
AP5 (Used at (used at 20 μM)	Abcam	Cat#: ab120003
CNQX (used at (used at 10 μM)	Sigma-Aldrich	Cat#: C127
MK801 (used at 1 μM)	Sigma-Aldrich	Cat#: M108

3. Results

3.1 Regulation of excitatory neurotransmission and SV cycling by endosomal PI(3)P

The exocytic fusion and endocytic reformation of synaptic vesicles from endosome-like vacuoles are important for sustained neurotransmission. To investigate the relationship between neuronal activity and endosomal trafficking in hippocampal neurons, we used a recombinant GFP-2x FYVE domain of EEA1 to detect PI(3)P positive endosomes in neuronal somata and presynaptic terminals marked by dendritic microtubules MAP2 or SV protein Synaptophysin, respectively. Here, we were able to detect the presence of PI(3)P at Synaptophysin-positive synapses which were indicated by the white arrow, and this is consistent with the previous finding showing the existence of PI(3)P in purified synaptosomes (Hoopmann et al., 2010). Interestingly, We found PI(3)P levels to be reduced in both somata and synapses upon sustained stimulation with trains of action potentials (Figure 3.1A-B). Conversely, blockage of neuronal network activity by the NMDA receptor antagonist AP5 or the AMPA receptor blocker CNQX induced a noticeable increase in PI(3)P level in somata and synapses (Figure 3.1C-D), suggesting that PI(3)P levels can be modulated by neuronal activity. Moreover, we tested whether PI(3)P levels are differentially regulated at excitatory or inhibitory synapses. Profound depletion of PI(3)P at vGlut1-positive excitatory synapses was observed upon train stimulation, whereas PI(3)P levels at vGAT-positive inhibitory synapses stayed unchanged (Figure 3.2). These data suggest that somatic and synaptic PI(3)P levels in excitatory neurons are inversely correlated with neuronal activity.
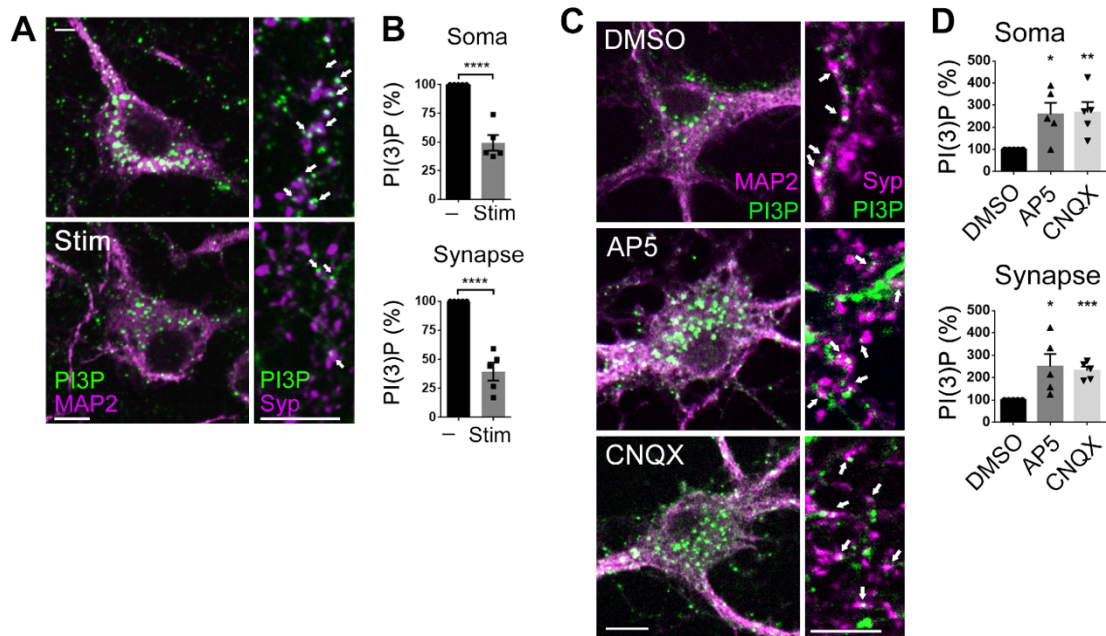
Figure 3.1. Neuronal activity regulates endosomal PI(3)P levels.
(A) Cultured hippocampal neurons were electrical stimulated with trains of 200APs (Stim) or without stimulation (-), and stained for MAP2 as somatic marker, Synatophysin (Syp) as synaptic marker and PI(3)P. Scale bar, 10 µm. **(B)** Activity induced PI(3)P reduction. Relative intensity of PI(3)P were quantified in somata (MAP2-positive) or synapses (Synaptophysin-positive) in unstimulated and stimulated neurons. Quantification were obtained from ≥ 60 images per condition, 5 independent experiments. **(C)** Cultured hippocampal neurons were incubated with glutamate receptor blockers, AP5 (20µM) or CNQX (10µM) for 24 h, and stained for MAP2, Synaptophysin and PI(3)P. Scale bar, 10 µm. **(D)** Increased PI(3)P level was in silenced neurons. Quantification were obtained from ≥ 75 images per condition, 5 independent experiments.
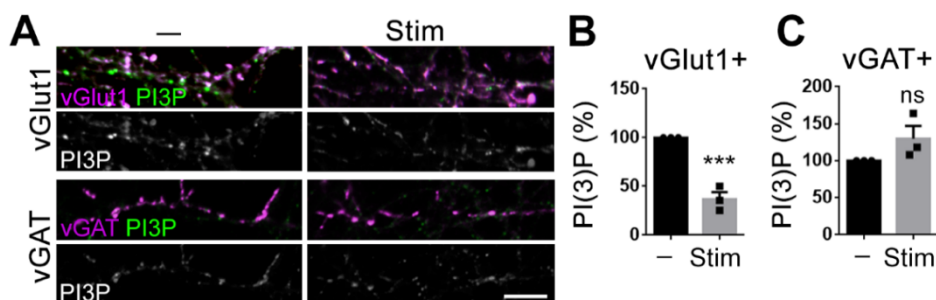

Figure 3.2. Synaptic PI(3)P levels are reduced in excitatory neurons upon stimulation.
(A) Cultured hippocampal neurons were stimulated with 200APs and stained for PI(3)P, vesicular glutamate transporter 1 (vGlut1) as a marker for excitatory neuron or co-stained with vesicular GABA transporter (vGAT) for inhibitory neurons, Scale bar, 10 µm. **(B-C)** Relative intensity of PI(3)P in vGlut1- or vGAT-positive presynaptic terminals in unstimulated vs. stimulated condition. Field stimulation reduces PI(3)P levels in vGlut1- but not vGAT-positive synapses. A total of 60 images per condition from 3 independent experiments.

Endosomal PI(3)P is mainly generated by class III PI3-kinase VPS34, which is an essential factor for neuronal development, spine formation, neuronal survival as well as preventing neurodegeneration. To study the role of PI(3)P in neurotransmission, we first investigated the localization of VPS34. My colleague Albert Mackintosh performed brain fractionation to examine the presence of Class II and Class III PI3Ks in the brain tissue. Here, the VPS34 was found to be co-fractionated with presynaptic proteins, Synaptotagmin and Synaptophysin, in crude SV fractions (Figure 3.3A). Besides, a small portion of PI(3)P can be synthesized by class II PI3-kinases, PI3K-C2α and PI3K-C2β, which are also found in SV-enriched brain fractions (Fig3.3A). Next, to manipulate PI(3)P levels in neurons, a selective VPS34 inhibitor, VPS34IN1 (Bago et al., 2014), was applied to hippocampal neurons in culture. VPS34IN1 is a highly selective and potent inhibitor of VPS34, and it does not significantly affect the activity of other protein kinases or class I and class II PI3K. Using the GFP-2XFYVE probe to detect PI(3)P, we found that somatic and synaptic PI(3)P were effectively depleted to nearly undetectable levels upon VPS34IN1 treatment (Figure 3.3B-C), indicating Class III PI3-kinase VPS34 is the major enzyme that synthesizes PI(3)P in hippocampal neurons.
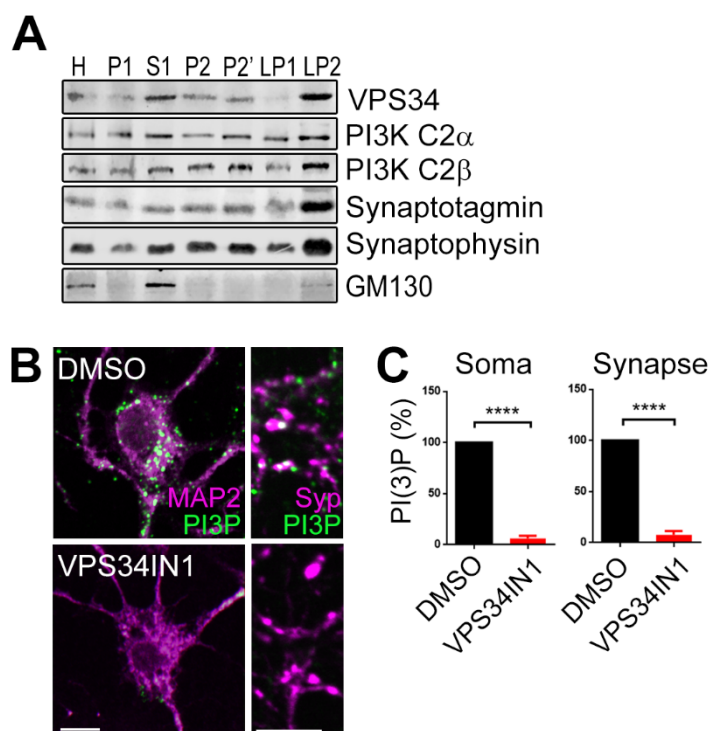
Figure 3.3. Presence of VPS34 in a synaptic vesicle-enriched fraction.
(A) Subcellular fractionation of mouse brains reveals the presence of Class II (PI3KC2a, PI3KC2b) and Class III (VPS34) PI3Ks in the synaptic vesicle enriched LP2 fraction. H: total homogenate fraction, P1: crude nuclei, S1: cytoplasmic fraction, P2: crude synaptosomal membrane, P2': purer synaptosomal fraction, LP1: postsynaptic membrane, LP2: crude presynaptic vesicles. The experiment was performed by Albert Mackintosh. **(B)** Cultured hippocampal neurons treated with VPS34IN1 (10 μM) were fixed and stained for MAP2, synaptophysin and PI(3)P. **(C)** Relative PI(3)P intensity in the MAP2-positive soma and in Synaptophysin-positive synaptic regions were quantified in control and VPS34IN1-treated neurons. A total of $\geq$ 35 images per condition from 3 independent experiments.

These findings help us to study the effects of reduced PI(3)P production on excitatory neurotransmission in hippocampal slices from wild-type mice. Dr. Gaga Kochlamazashvili performed the electrophysiological experiment. In control conditions, the field excitatory postsynaptic potential (fEPSP) amplitude showed normal basal neurotransmission, whereas pharmacological inhibition of VPS34-induced PI(3)P depletion by VPS34IN1 or SAR405, another selective VPS34 inhibitor (Pasquier, 2015), showed a rapid and progressive decline of fEPSP amplitudes (Figure 3.4A), suggesting that VPS34 inhibition causes a rundown of

basal excitatory neurotransmission in hippocampal neurons. A paired-pulse facilitation experiment was applied to test if reduced PI(3)P level affects the SV release probability. A facilitated second fEPSP curve means the lower initial release probability release, and it yields increased pair-pulse ratio when the second response is divided by the first one. Here, we observed that paired-pulse ratio is significantly increased in VPS34IN1-treated hippocampal slice (Figure 3.4C). These results indicate that VPS34 inhibition reduces the basal neurotransmission and the presynaptic release probability.
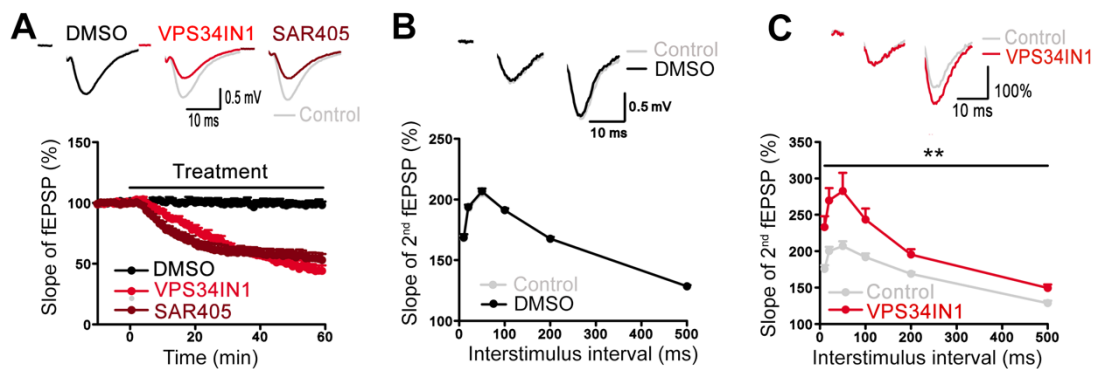

Figure 3.4. PI(3)P depletion reduces neurotransmission and release probability.
(A) Basal excitatory synaptic transmission of CA3-CA1 connections in acute hippocampal slices treated with DMSO (0.03%) or the VPS34 inhibitors, VPS34IN1 (3µM) or SAR405 (20µM). Representative fEPSP traces (above) and the relative slope of fEPSPs (below) are shown. VPS34 inhibition causes a rundown of excitatory synaptic transmission. **(B)** Measurements of paired-pulse facilitation (PPF) with different interstimulus intervals (10 to 500 ms) show no change in the slope of the second fEPSP following DMSO application (0.03%). **(C)** Increased paired-pulse facilitation (PPF) at hippocampal CA3-CA1 synapses after VPS34 inhibition. Representative traces of fEPSPs PPF at a 20 ms interpulse interval and quantification over a range of interstimulus intervals (10–500 ms), given as ratio of the second to the first response, show an increased facilitation of the second response in VPS34IN1-treated acute hippocampal slices. PI(3)P depletion causes a significant facilitation of the second fEPSP, indicative of reduced initial release probability. All the experiments shown in this figure were done by Dr. Gaga Kochlamazashvili.

To further understand the detailed mechanism underlying reduced neurotransmission and reduced release probability in PI(3)P-depleted hippocampal neurons, we challenged these results by directly probing SV exo-/ endocytosis using the reporter

Synaptophysin-pHluorin expressed in cultured hippocampal neurons. Synaptophysin-pHluorin is a pH sensitive GFP fused to the luminal domain of the SV protein Synaptophysin (Granseth et al., 2006). Upon action potential stimulation SVs containing Synaptophysin-pHluorin fuse with the presynaptic plasma membrane and get exposed to the neutral environment, the luminal pHluorin moiety becomes dequenched resulting in elevated fluorescence. This is followed by decay of the pHluorin signal as SVs are internalized via endocytosis and undergo vATPase-driven reacidification. Hippocampal neurons were transfected with a Synaptophysin-pHluorin expression plasmid at day 8 *in vitro* (DIV), and imaged at DIV14. In experiments conducted by Dr. Tolga Soykan we found reduced SV exocytosis in PI(3)P-depleted neurons upon 2 AP stimulation (Figure 3.5A-B). Reduced SV exocytosis was accompanied by a concomitant kinetic impairment of Synaptophysin-pHluorin endocytosis. To exclude the exocytic depression is because of defective SV endocytosis, we applied endocytosis inhibitor Dynasore and found that the SV endocytosis was not affected in response to same 2AP stimuli (Figure 3.5C). These results suggest that PI(3)P reduction limits excitatory neurotransmission via a signaling cascade that represses SV exocytosis and endocytosis by an unknown mechanism.
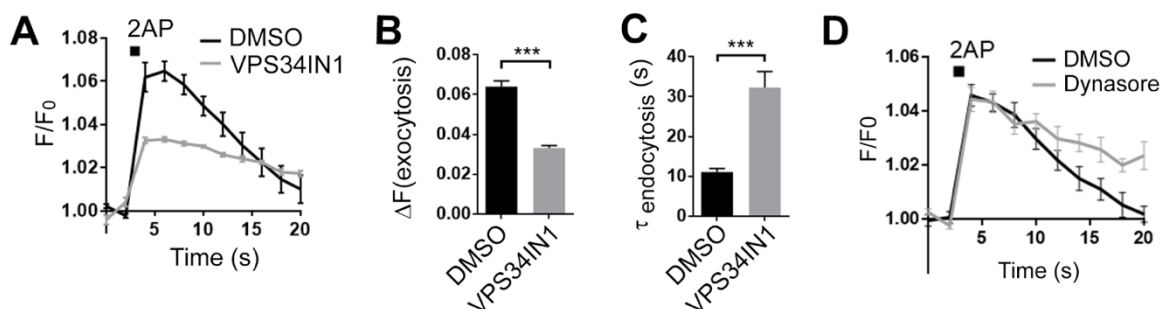

Figure 3.5. PI(3)P depletion reduces SV exocytosis and slows SV endocytosis
(A-C) Cultured hippocampal neuron was treated DMSO (0.1%) or VPS34IN1 (3μM) for 1h, and Synaptophsin-pHluorin assay was performed in imaging buffer containing 4mM Calcium. Surface normalized traces **(A)**, peak responses **(B)** and endocytic decay constants **(C)** of Synaptophysin-pHluorin signals in response to 2 AP (10 Hz, 0.2s) stimulation. A total of 20 images per condition from 4 independent cultures. **(D)** Average traces of

Synaptophysin-pHluorin signals in response to 2 AP (10 Hz, 0.2s) stimulation in DIV14 hippocampal neurons treated with Dynasore (20 µM). A total of 5 images per condition. The Experiments were performed by Dr. Tolga Soykan.

3.2 Activity-dependent kinetic block of SV endocytosis at PI(3)P-depleted excitatory synapses

To investigate the signaling pathway underlying the effect of PI(3)P depletion on excitatory synaptic transmission and SV recycling, I analyzed the partitioning the endogenous SV protein Synaptotagmin-1 (Syt-1), an essential calcium sensor for SV cycling, between internal SV compartments and the cell surface at excitatory or inhibitory synapses upon train stimulation. Using a specific Syt-1 antibody which only recognizes the luminal part of the protein, to stain the surface accumulated pool of Syt-1 before puncturing of plasma membrane, and followed by Digitonin membrane permeabilization, the same antibody was used to detect total pool of Syt-1. Non-endocytosed surface accumulated Synaptotagmin-1 was increased in vGlut1-positive excitatory synapses (Figure 3.6A-B), but not vGAT-positive inhibitory synapses in VPS34IN1-treated hippocampal neurons after repetitive stimulation (Figure 3.6C-D), indicating that the role of PI(3)P in controlling SV exocytosis and endocytosis is restricted to excitatory neurons. Taken together, endosomal PI(3)P has a crucial physiological function in activity-dependent control of excitatory synaptic transmission by feedback regulation of SV exocytosis and endocytosis. These findings open the possibility that sustained activity may lead to depletion of PI(3)P, which in turn can cause rundown of excitatory transmission by reducing SV release probability and delaying SV endocytosis driven vesicle replenishment.
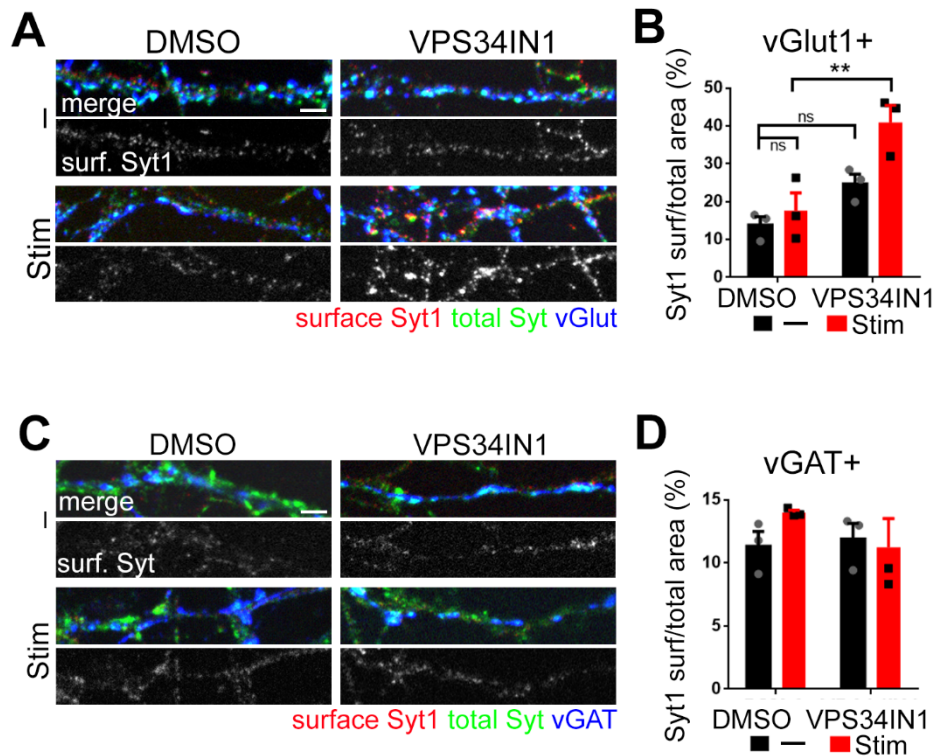
Figure 3.6. Activity induces surface accumulation of Synaptotagmin-1 in excitatory neurons.
(A) Cultured hippocampal neurons pre-treated with DMSO (0.1%) or VPS34IN1 (10 μM) were either field-stimulated with trains of 200 APs (Stim) or left unstimulated (-), fixed and stained for, total Synaptotagmin-1 (Syt), surface-stranded Synaptotagmin-1 and vGlut1. Scale bar, 10 μm. **(B)** VPS34-mediated PI(3)P synthesis is required for SV cycling at excitatory synapses **(C)** Cultured hippocampal neurons pre-treated with DMSO (0.1%) or VPS34IN1 (10μM) were either field-stimulated with trains of 200 APs (Stim) or left unstimulated (-), fixed and stained for surface-stranded Synaptotagmin-1, total Synaptotagmin-1, and vGAT. Scale bar, 10 μm. **(D)** VPS34-mediated PI(3)P synthesis is not involved in SV cycling at inhibitory synapses. A total of 40 images per condition from 3 independent experiments.

To further delineate this mechanism, we focused on the effects of PI(3)P depletion on SV endocytosis as a readout. Synaptophysin-pHluorin-expressing hippocampal neurons were stimulated with trains of 200 APs, a strong stimulation condition that can override the defects in release probability caused by loss of PI(3)P that was observed in brain slices and cultured neurons stimulated with 2 APs. Hippocampal neurons were pre-treated with VPS34IN1 for 1 h and stimulated with successive trains of 200 APs. The fluorescence of

Synaptophysin-pHluorin in individual boutons was normalized either to baseline fluorescence to eliminate the variations that arise from different levels of Synaptophysin-pHluorin expression, or to the maximum peak value during the first train to standardize the starting point of fluorescence decay during SV endocytosis. A progressive kinetic delay in SV endocytosis can be observed in PI(3)P-depleted neurons (Figure 3.7B), but without showing any exocytic defects (Figure 3.7A). Surface retention was plotted for each stimulus, displaying a profoundly increased surface accumulated pool of Synaptophysin-pHluorin upon VPS34IN1 treatment (Figure 3.7C), and surface accumulated fluorescence was built up after each stimulus. Washout of the drug (Figure 3.7D-F) by re-incubating neurons in inhibitor-free medium overnight or restoring PI(3)P levels by co-bath application of synthetic cell permeable PI(3)P (Subramanian et al., 2010) with VPS34IN1 reversed the defective phenotype (Figure 3.7G-I). The surface retention were plotted for both rescue conditions, and no surface accumulated pHluorin signal can be observed (Figure 3.7F and I), A similar kinetic block of SV endocytosis was further confirmed by another selective VPS34 inhibitor SAR405 (Figure 3.7J-L). Furthermore, we also used other pHluorin reporters to confirm this phenotype. Hippocampal neurons were transfected with either vGlut1-pHluorin (Figure 3.8D-F) or Synaptotagmin-pHluorin (Figure 3.8G-I), and stimulated with 200AP trains. These neurons displayed similar delays in SV endocytosis after VPS34IN1 treatment. Stimulation of neurons with trains of 50 APs also led to a similar SV endocytic defect after PI(3)P depletion (Figure 3.8A-C). These data suggest that defects in SV endocytosis after PI(3)P depletion are independent of the stimulation strength and the reporters used for tracking endocytosis.
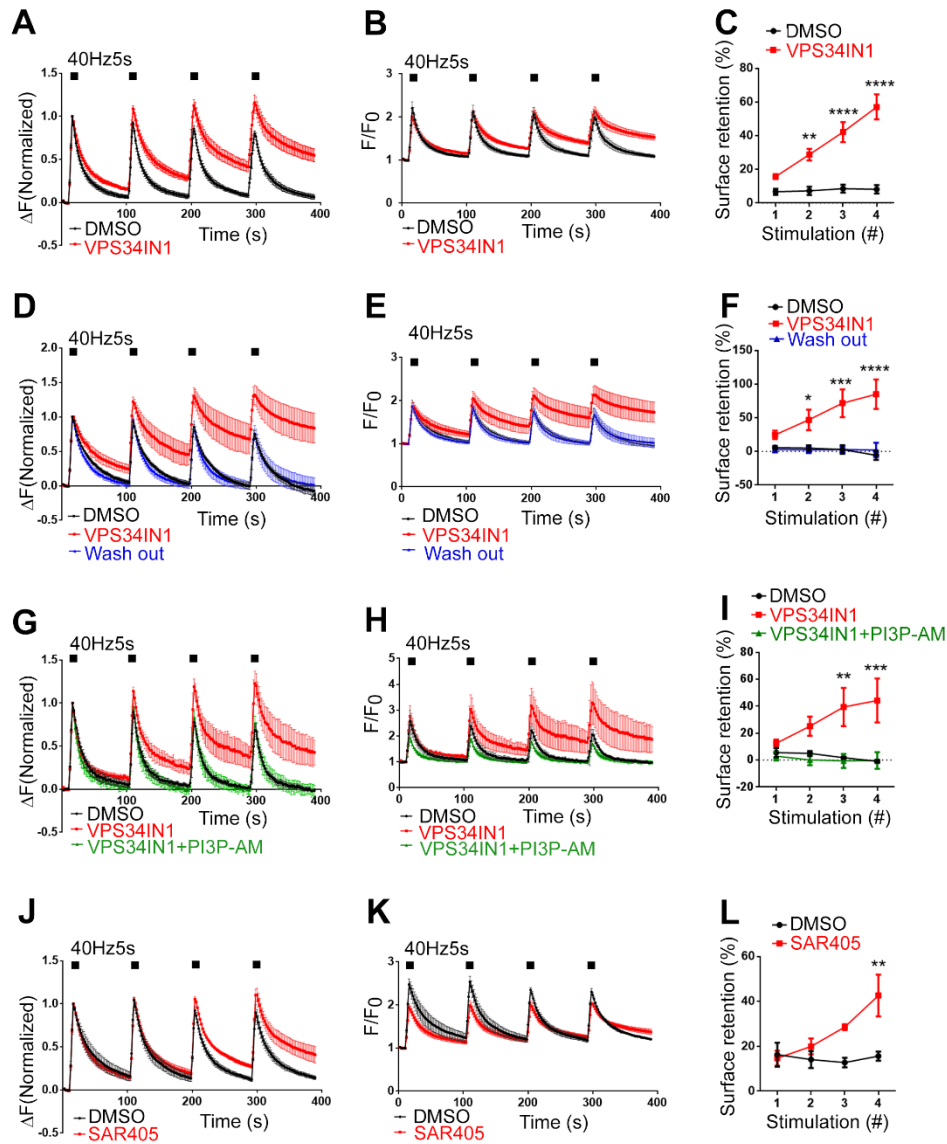
Figure 3.7. PI(3)P depletion blocks SV endocytosis.
Peak normalized **(A)** and surface normalized **(B)** Synaptophysin-pHluorin responses at synapses of mock (DMSO)- or VPS34IN1-treated hippocampal neurons stimulated with consecutive trains of 200 APs. **(C)** PI(3)P depletion in VPS34IN1-treated neurons causes the progressive accumulation of Synaptophysin-pHluorin on the neuronal surface. Surface retention of Synaptophysin-pHluorin 90s post-stimulus is plotted for each of the four successive stimulation trains. A total of ≥ 40 images per condition from 6 independent experiments. **(D-F)** Overnight removal of VPS34IN1 rescues the delayed SV endocytosis. Peak normalized **(D)** and surface normalized **(E)** Synaptophysin-pHluorin traces at synapses of DMSO- or VPS34IN1- treated hippocampal neurons or overnight wash out of VPS34IN1, and stimulated with trains of 200APs. **(F)** Surface retention of Synaptophysin-pHluorin 90s post-stimulus is plotted for each of four repetitive stimulation trains. A total of ≥ 20 images per condition from 3 independent experiments. **(G-I)** Exogenous supply of membrane-permeant PI(3)P acutely rescues defective Synaptophysin-pHluorin endocytosis

induced by VPS34 inhibition in hippocampal neurons. Peak normalized **(G)** and surface normalized **(H)** pHluorin traces at synapse of different treatments, including VPS34IN1 or co-incubation with PI(3)P-AM (20 µM) in hippocampal neurons. A total of 15 images per condition from 3 independent experiments. **(I)** Surface retention was plotted by the same method described in pervious experiments. **(J-L)** Another VPS34 inhibitor, SAR405, phenocopies delayed endocytosis induced by VPS34IN1. Peak Normalized **(J)** and surface normalized **(I)** Synaptophysin-pHluorin traces at synapse of DMSO- or SAR405 (30 µM)-treated synaptic terminals. **(L)** surface retention of each stimulus was calculated.
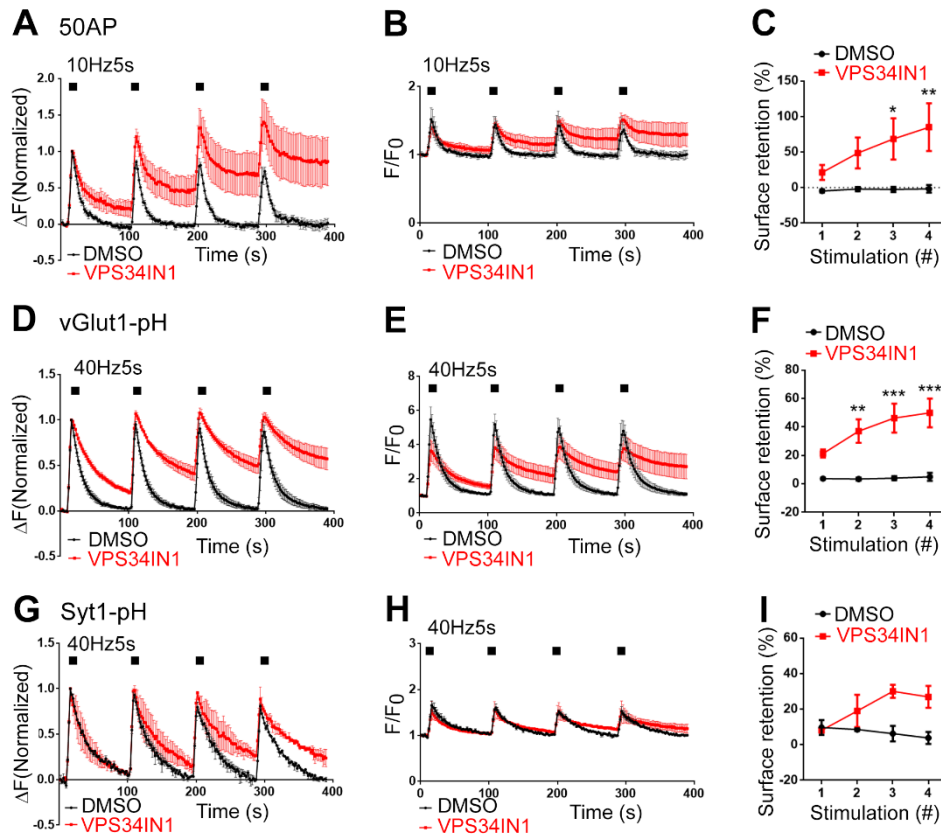

Figure 3.8. Defective endocytosis can be observed in other stimulation and pHluorin reporter

(A-C) Cultural hippocampal neurons were treated with VPS34IN1 (10 µM) for 1 h, and stimulated with four successive 50 APs (10 Hz, 5 s). Peak normalized (A) and surface normalized **(B)** Synaptophysin-pHluorin traces show the same delayed endocytosis as 200 APs (Fig.). **(C)** Surface retention of Synaptophysin-pHluorin 90s post-stimulus is plotted for each stimulation. A total of ≥ 11 images per condition from 3 independent experiments. **(D-F)** Cultural hippocampal neurons were transfected with vGlut1-pHluroin, treated with VPS34IN1 (10 µM), and stimulated with 4 x 200 APs. Peak normalized **(D)**, surface normalized **(E)** and Surface retention **(F)** of vGlut-1-pHluorin signals show the defective SV endocytosis. A total of ≥ 15 images per condition from 3 independent experiments. **(G-I)** Cultural hippocampal neurons were transfected with Synaptotagmin1-pHluroin, treated with VPS34IN1 (10 µM), and stimulated with 4 x 200 APs. Peak normalized **(D)**, surface normalized **(E)** and Surface retention **(F)** of Syt1-pHluorin signals show the delayed SV endocytosis. A total of ≥ 10 images per condition from 2 independent experiments

Delayed SV endocytosis monitored by pHluorin reporters may arise either due to incomplete endocytosis from the plasma membrane or downstream defects in endosomal fusion and vesicle reacidification. To test these two hypotheses, we repeated the Synaptophysin-pHluorin imaging where we stimulated neurons with several trains of 200 AP stimulations. This time we additionally applied acidic imaging buffer to quench the surface Synaptophysin-pHluorin fluorescence 10 s before the first and 90 s after the last stimulation. The drop in fluorescence levels upon acid quenching yields a measure of the surface levels of Synaptophysin-pHluorin. Using this approach, we found that the Synaptophysin-pHluorin reporter is accumulated on the surface of the plasma membrane after repetitive stimulation in PI(3)P depleted neurons (Figure 3.9A), and the ΔF2 is larger than ΔF1 (Figure 3.9B), meaning the accumulated fluorescence are quenchable. This data indicate that loss of PI(3)P results in incomplete endocytosis form the plasma membrane.
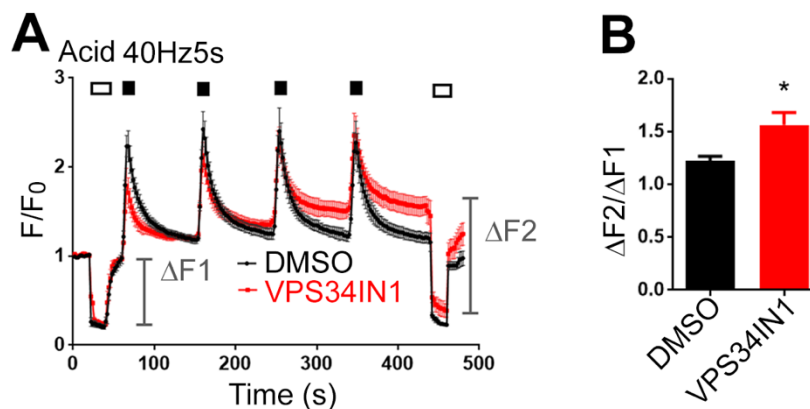

Figure 3.9. PI(3)P depletion cause surface accumulation of Synaptophysin-pHluorin signal.
(A) Normalized Synaptophysin-pHluorin responses in cultured hippocampal neurons stimulated with 4 x 200 APs with 90 s intervals after 1 h pre-treatment with DMSO or VPS34IN1 (10 μM) and subjected to low pH image buffer before and after the stimulation trains. (B) The ratio of surface fluorescence of Synaptophysin-pHluorin before and after 4 x 200 APs stimulation in DMSO- and VPS34IN1-treated neurons. A total of 15 images per condition from 4 independent experiments.

As an alternative approach, we used a knockdown strategy to monitor the effect of impaired PI(3)P synthesis on SV endocytosis. Endogenous VPS34 was depleted by specific shRNA (shVPS34) or treated with non-targeting control shRNA (shCtrl), and stimulated with trains of 200 APs (Figure 3.10A-C). Upon knockdown of VPS34, akin to VPS34 inhibitors, SV endocytosis was impaired and a higher fraction of Synaptophysin-pHluorin remained on the surface after SV fusion. This finding was further supported by the knockdown of VPS15, an essential subunit of the VPS34 complex, which also led to delayed kinetics of SV endocytosis upon repetitive stimulation (Figure 3.10D-F). To confirm that the knockdown approach successfully depletes PI(3)P in neurons we referred to PI(3)P labeling with GFP-2XFYVE. As expected, PI3P levels were significantly diminished in neurons transfected with shVPS34 or shVPS15, also indicating an efficient blockade of VPS34 or VPS15 activity (Figure 3.10G-H).
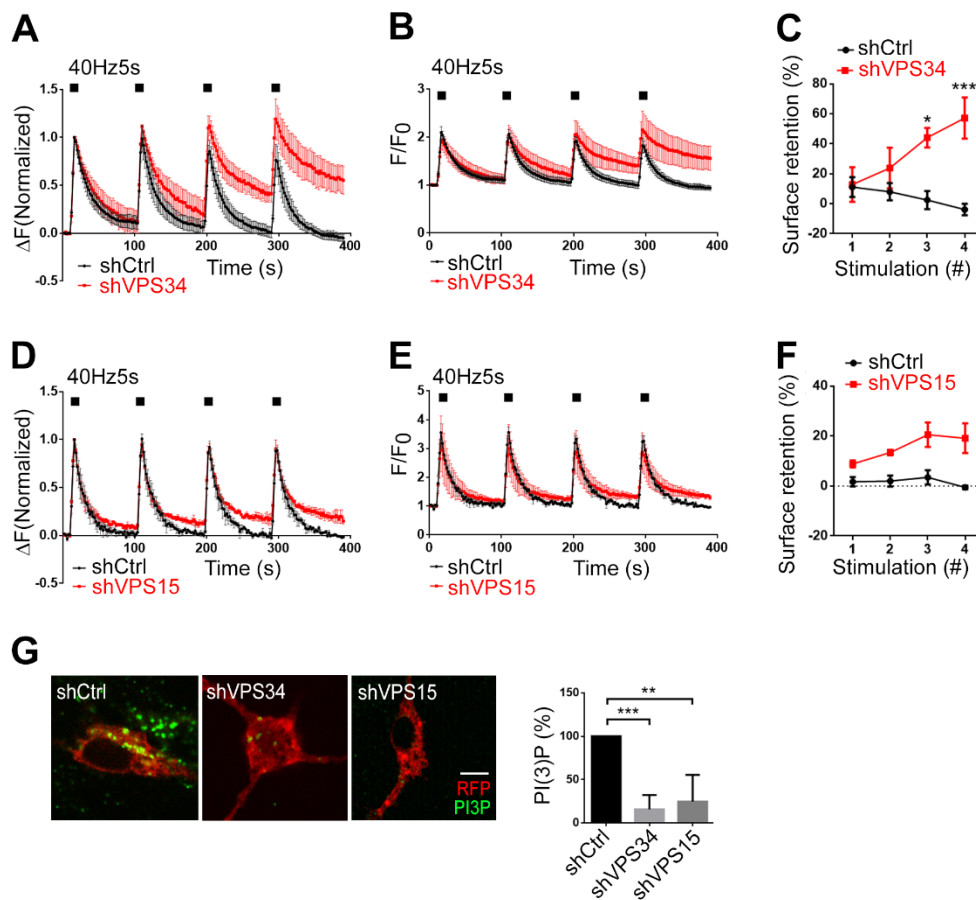
Figure 3.10. Knocking down of VPS34 subunits block synaptic vesicle endocytosis.
(A-C) Kinetic block of Synaptophysin-pHluorin endocytosis at hippocampal synapses depleted of VPS34. Hippocampal neurons depleted of endogenous VPS34 by specific shRNA (shVPS34) or treated with non-targeting control shRNA (shCtrl), and stimulated with trains of 200APs. Peak normalized **(A)** and Surface normalized **(B)** of pHluorin traces at synapses transfected with shCtrl or shVPS34. **(C)** Surface retention was plotted for each stimulus. A total of ≥10 images per condition from 3 independent experiments. **(D-F)** Blockage of Synaptophysin-pHluroin endocytosis at hippocampal synapses depleted of endogenous VPS15 (shVPS15), one of subunit of VPS34 complex, or treated with non-target control shRNA (shCtrl). Peak normalized **(D)** and surface normalized **(E)** of pHluorin traces at synapses transfected with shCtrl or shVPS15. **(F)** Surface retention was calculated for each stimulus at 90s after 200APs. **(G)** Using GFP-2XFYVE as a probe for PI3P labeling, PI3P level (in green) was depleted in neurons. RFP (in red) was the indicator for successful transfection. The PI3P intensity of each condition was plotted in right panel which indicates good knockdown efficiency.

To acutely manipulate PI3P levels in synaptic endosomes by another approach, an inducible chemically dimerization system was used together with Synaptophysin-pHluorin assay. The FRB-FKBP-Rapamycin heterodimer formation system is one of the most useful dimerization systems. Rapalog, a Rapamycin analog, binds to the 12-kDa FK506 binding protein (FKBP) and the FKBP-Rapamycin binding (FRB) domain, and triggers a tight heterodimer formation (Inobe and Nukina, 2016). The endosome-targeted FRB*-iRFP-Rab5 construct recruits mRFP-FKBP-hMTM1 in the vicinity of the same endosome upon Rapalog treatment. In our experiment, hippocampal neurons were transfected with mRFP-FKBP-hMTM1 and FRB*-iRFP-Rab5, and treated with Rapalog or ethanol as a solvent control. Rapalog-induced recruitment of PI(3)-phosphatase MTM1, an enzyme responsible for PI(3)P dephosphorylation into PI, led to kinetic block of SV endocytosis (Figure 3.11A-C). Using GFP-2XFYVE as a probe for PI(3)P labeling, mRFP-FKBP-hMTM1 and FRB*-iRFP-Rab5 co-expressing neurons showed a great depletion of PI(3)P in Rapalog-treated condition (Figure 3.11D).
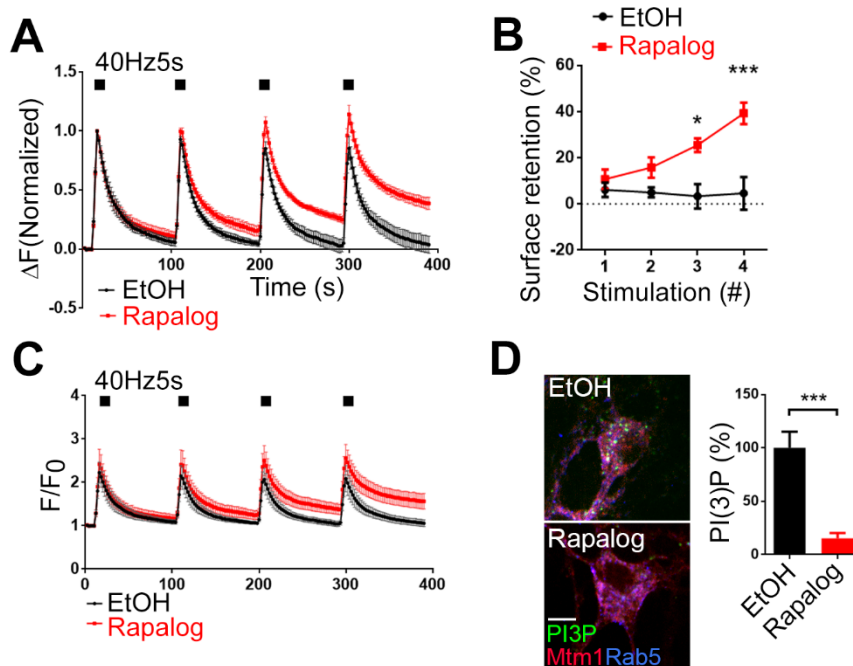
Figure 3.11. Locally depletion of endosomal PI(3)P affect synaptic vesicle endocytosis.
Cultured hippocampal neurons were transfected with mRFP-FKBP-hMTM1 and FRB*-iRFP-Rab5, treated with EtOH or Rapalog, and analyzed kinetics of synaptic vesicle endocytosis by Synaptophysin-pHluorin. Peak normalized **(A)** and surface normalized **(B)** of pHluorin traces show delayed endocytosis in endosomal PI(3)P depletion boutons at trains of 200APs. **(C)** Surface retention of Synaptophysin-pHluorin 90 s post-stimulus is plotted for each of the four successive 200 AP stimulation trains in hippocampal neurons expressing mRFP-FKBP-hMTM1 and FRB*-iRFP-Rab5 and treated with EtOH or Rapalog A total of $\geq$ 13 images per condition from 3 independent experiments. **(D)** Confocal images of cultured hippocampal neurons transfected with mRFP-FKBP-hMTM1 and FRB*-iRFP-Rab5, treated with EtOH or Rapalog and stained for PI(3)P. A total of $\geq$ 18 images per condition from 2 independent experiments.

Given the strong impact of neuronal activity on PI(3)P levels at excitatory synapses, we wondered whether the effects of VPS34IN1-induced PI(3)P depletion on SV endocytosis can be reversed by prior silencing of excitatory network activity. Hippocampal neurons were pre-incubated with NMDA receptor blocker AP5, MK801 or Na^+-channel blocker tetrodotoxin (TTX), followed by drug washout and AP train stimulation. Pre-treatment with either AP5 (Figure 3.12A-C.), TTX (Figure. 3.12D-F) or MK801 (Figure 3.12G-I) prevented

the inhibitory effect of PI(3)P depletion by VPS34IN1 on SV endocytosis. These results thus reveal a critical physiological function for endosomal PI(3)P in the control of SV endocytosis in excitatory neurons through an activity-dependent mechanism.
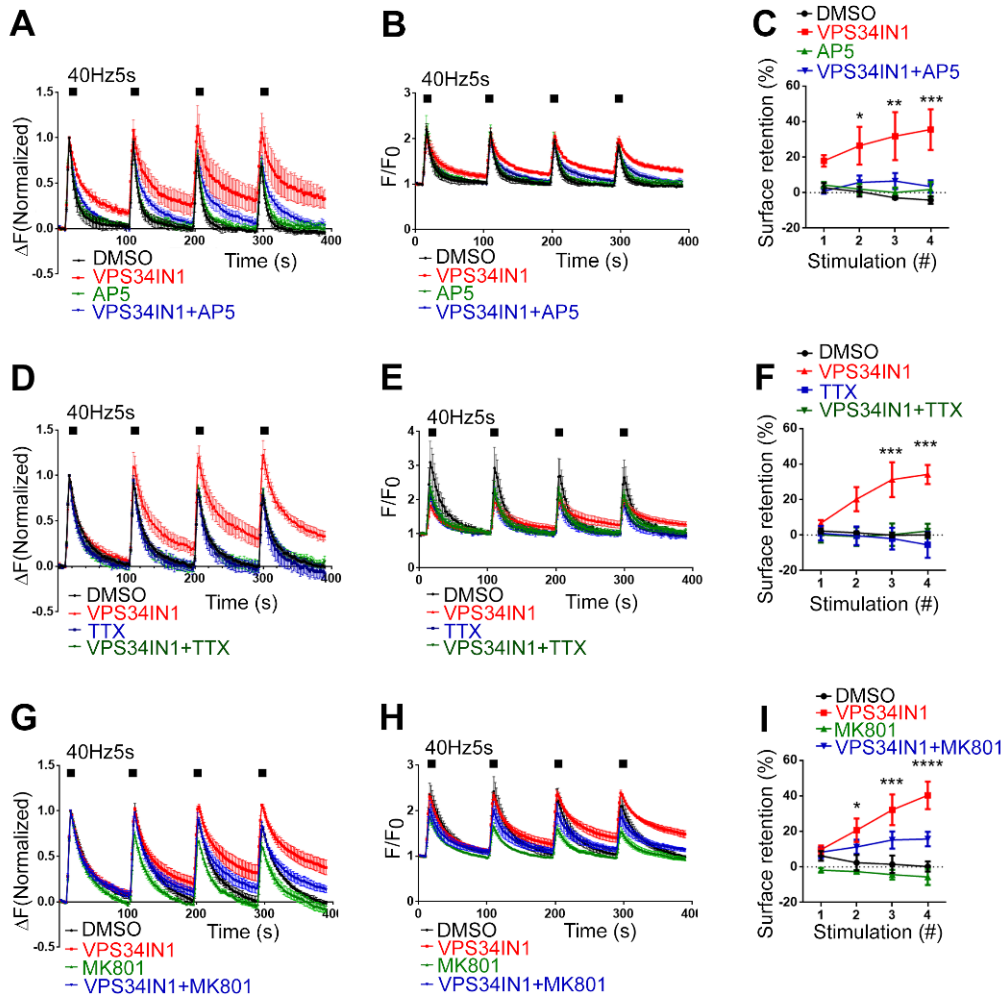

Figure 3.12. Impaired SV endocytosis upon VPS34IN1 treatment is activity-dependent.
(A-C) VPS34IN1-induced defects in SV endocytosis are reverted by parallel inhibition of NMDA receptors by AP5 (20 µM). Peak normalized **(A)** and surface normalized **(B)** of Synaptophysin-pHluorin traces show normal SV endocytosis by co-incubation with AP5 and VPS34IN1. **(C)** Surface retention was plotted for each stimulation. **(D-E)** Defective SV endocytosis induced by VPS34IN1 is recovered in parallel inhibition of neuronal activity by TTX (200nM). Peak normalized **(D)** and surface normalized **(E)** of pHluorin signals show no defect upon VPS34IN1 and TTX co-treatment. **(F)** Surface retention was plotted for each stimulation. **(G-I)** VPS3IN1-induced defective SV endocytosis are rescued by parallel inhibition by another NMDA blocker, MK801 (10 µM). Peak normalized **(G)**, surface normalized **(H)** and surface retention **(I)** were plotted and show the same results as (A-C). A total of ≥15 images per condition from 3 independent experiments.

3.3 Ultrastructural analysis of PI(3)P depleted synapses

To investigate the exact mechanism how PI(3)P depletion affects SV recycling, Dr. Dmytro Puchkov in our lab analyzed the ultrastructure of the synapses from VPS34IN1-treated hippocampal neurons at rest or stimulated with trains of 200 APs by electron microscopy, quantitative morphometry and tomographic 3D reconstructions (Figure 3.13). PI(3)P-depleted synapses showed a profound reduction in SV pool size and concomitant accumulation of endocytic invaginations which are generated from the plasma membrane. The number of endosome-like vacuoles (ELV), clathrin-coated pit (CCP) and clathrin-coated vesicles (CCV) were also increased in PI(3)P-depleted synapses compared to DMSO-treated control. (Figure 3.13) In the resting condition, no significant differences were observed in the number of SVs or other endocytic intermediates in VPS34IN1-treated neurons compared to control. A similar accumulation of endocytic pits and plasma membrane invaginations at synapses has been found in previous study using dynamin-1 or dynamin-1/3 knockout mice (Raimondi et al., 2011), indicating that loss of PI(3)P may interfere with a molecular mechanism that involves dynamin-mediated membrane fission at synapses.
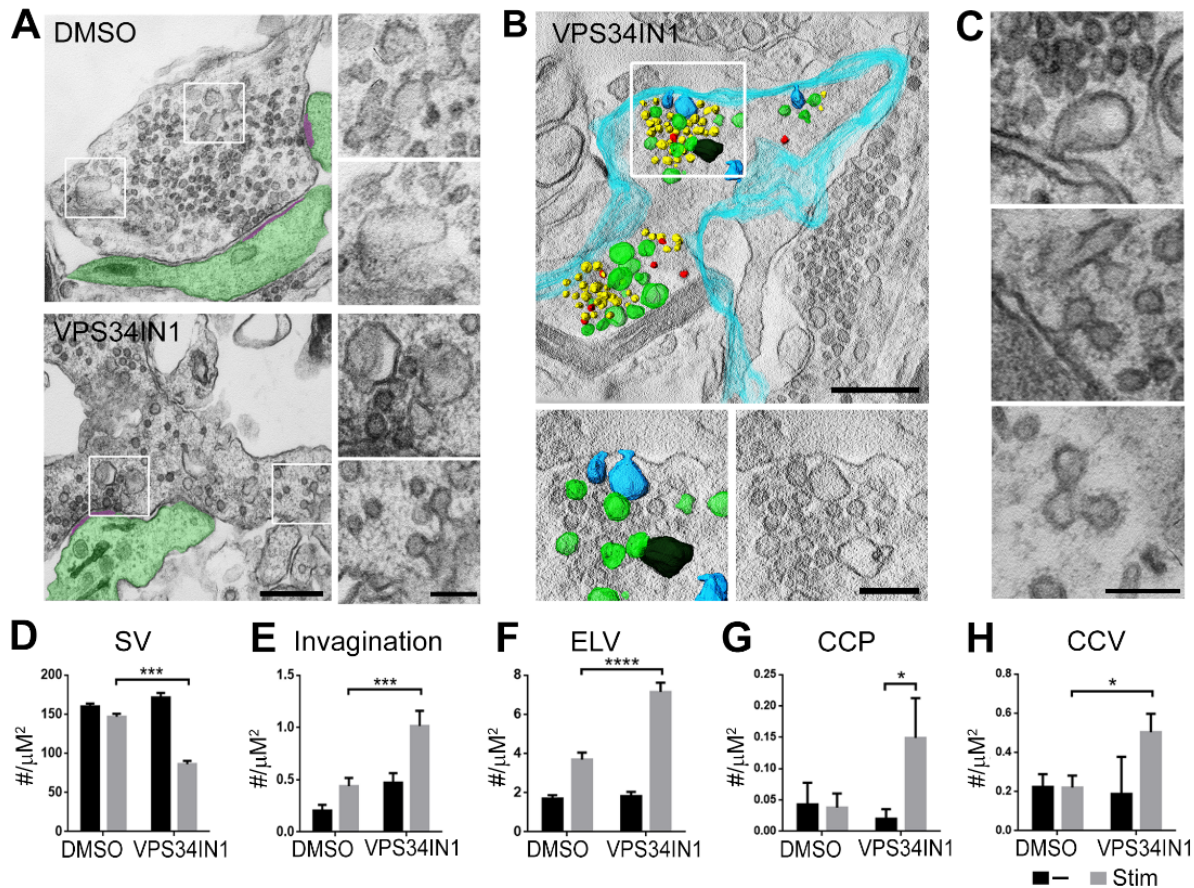
Figure 3.13. Ultrastructure of PI(3)P-depleted synapses.
(A) Examples of VPS34IN1- and DMSO-treated synapses following 4 x 200 AP stimulation. The postsynaptic compartment and the postsynaptic density are highlighted in green and purple, respectively. Note the reduced SV numbers and plasma membrane-derived endocytic intermediates in VPS34IN1-treated synapses. Scale bars, 500 nm (left) and 200 nm (right). **(B)** 3D-reconstruction of a synaptic terminal treated with VPS34IN1 and stimulated with 4 x 200 APs. The plasma membrane is colored in turquoise. Synaptic vesicles (yellow), plasma membrane-derived invaginations (blue), endosome-like vacuoles (green) and clathrin-coated vesicles (red) are highlighted. Scale bar, 500 nm (top) and 200 nm (bottom). **(C)** High magnification views of endocytic intermediates accumulated in stimulated hippocampal neurons treated with VPS34IN1. Scale bar, 200 nm. **(D-H)** Morphometric quantification of data shown in (A-C). Synapses of VPS34IN1-treated stimulated neurons display reduced numbers of SVs/ bouton area **(C),** and an accumulation of endocytic membrane invaginations **(D)**, endosome like vacuoles **(F)**, clathrin-coated pits, CCPs **(G)** and clathrin-coated vesicles, CCVs **(H)**. A total of 100 (SV) and 200 (invaginations, ELV, CCP and CCV) profiles per condition. Experiments shown here were performed by Dmytro Puchkov.

3.4 PI(3)P depletion blocks SV cycling by hyperactivation of Calpain2 downstream of Rab5

Since VPS34 and its product PI(3)P are mainly present on endosomes, and not directly involved in endocytic events from the plasma membrane, we hypothesized that the activity-dependent kinetic blockade of SV cycling when PI(3)P is depleted may result from a PI(3)P-dependent signaling cascade. To study its molecular mechanism, we checked the levels of SV proteins that may be altered upon VPS34 inhibition. Exocytic and endocytic SV proteins, like SNAP25, syntaxin 1A, clathrin heavy chain, heat shock protein 70 and dynamin, remain unchanged in VPS34IN1-treated cerebellar neuron lysates (Figure 3.14A). Caspase-3 levels were not changed in PI(3)P-depleted neurons, indicating that there is no caspase-3-dependent cell apoptosis occurred in VPS34IN1 treatment condition. Instead, we found a prominent change in the ratio of p35/p25 regulatory factor of the synaptic protein kinase Cdk5, an important enzyme for suppressing excitatory neurotransmission and release probability (Shah andLahiri, 2014; Tomizawa et al., 2002). p35/Cdk5 appeared to be proteolytically converted into hyperactive p25/Cdk5 form in PI(3)P-depleted neurons, this reaction is known to be catalyzed by the calcium-dependent cysteine protease Calpain (Wu and Lynch, 2006). Consistent with this finding, pharmacological inhibition of Calpain by ALLN prevented p35-to-p25 conversion (Figure 3.14B). To test if Calpain-dependent p35/p25 conversion is responsible for the defects in SV cycling in PI(3)P-depleted neurons, hippocampal neurons were treated with ALLN together with VPS34IN1. We found that SV endocytosis was unperturbed in PI(3)P-depleted neurons when Calpains is inactivated (Figure 3.14C-E). A similar rescue of VPS34IN1-induced SV endocytosis defect was observed when Calpains were inhibited by another calpain inhibitor Calpeptin (Figure 3.14F-H).
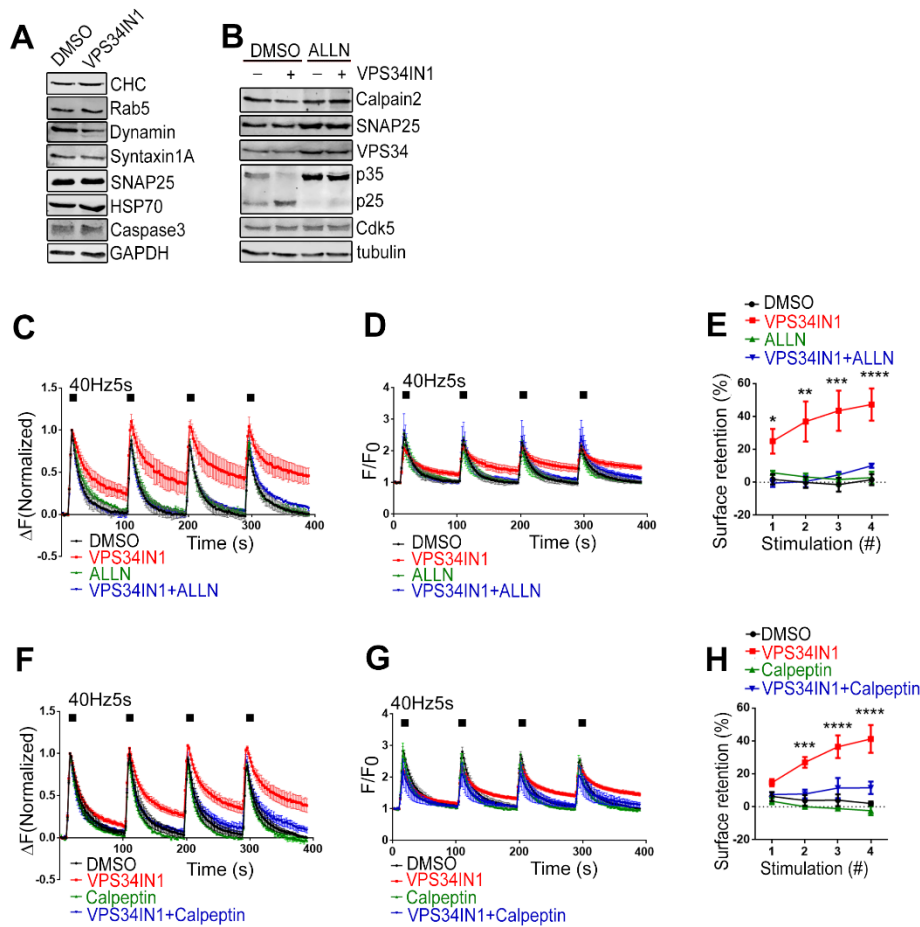
Figure 3.14. PI(3)P depletion kinetically blocks SV endocytosis by Calpain activation.
(A) Levels of various synaptic proteins in DMSO and VPS34IN1-treated cultured cerebellar granule neurons in culture. **(B)** Levels of synaptic proteins in DMSO- (0.1%) and VPS34IN1-(10 μM) treated cultured cerebellar granule neurons. VPS34 inhibition results in p35 processing to hyperactive p25, a reaction blocked by Calpain inhibitor ALLN (100 μM). N = 3. **(C-E)** Calpain inhibition by ALLN (100 μM) rescues the progressive accumulation of Synaptophysin-pHluorin on the neuronal surface induced by VPS34IN1. Peak normalized **(C)**, surface normalized **(D)** of Synaptophysin-pHluorin traces, and surface retention **(E)** of each stimulus was plotted, showing the rescue phenotype. **(F-H)** Calpain inhibition by another inhibitor, Calpeptin (10 μM) reduces the accumulation of Synaptophysin-pHluorin on the surface induced by VPS34IN1. Peak normalized **(F)**, surface normalized **(G)** of Synaptophysin-pHluorin traces, and surface retention **(H)** of each stimulus was plotted, showing the rescue phenotype. A total of ≥ 11 images per condition from 3 independent experiments.

There are two major Calpain isoforms expressed in the brain, Calpain1 and Calpain2, which play different roles in regulation of neuronal function (Huo et al., 2017). To test which isoform is important for PI(3)P-dependent regulation of SV endocytosis we used shRNAs that target either Calpain1 (Figure 3.15A-C) or Calpain2 (Figure 3.15D-F) in hippocampal neurons. We found that knockdown of Calpain2, but not Calpain1, prevents the VPS34IN1-induced inhibition of SV endocytosis, indicating that Calpain2 is the Calpain isoform that specifically acts downstream of PI(3)P signaling.
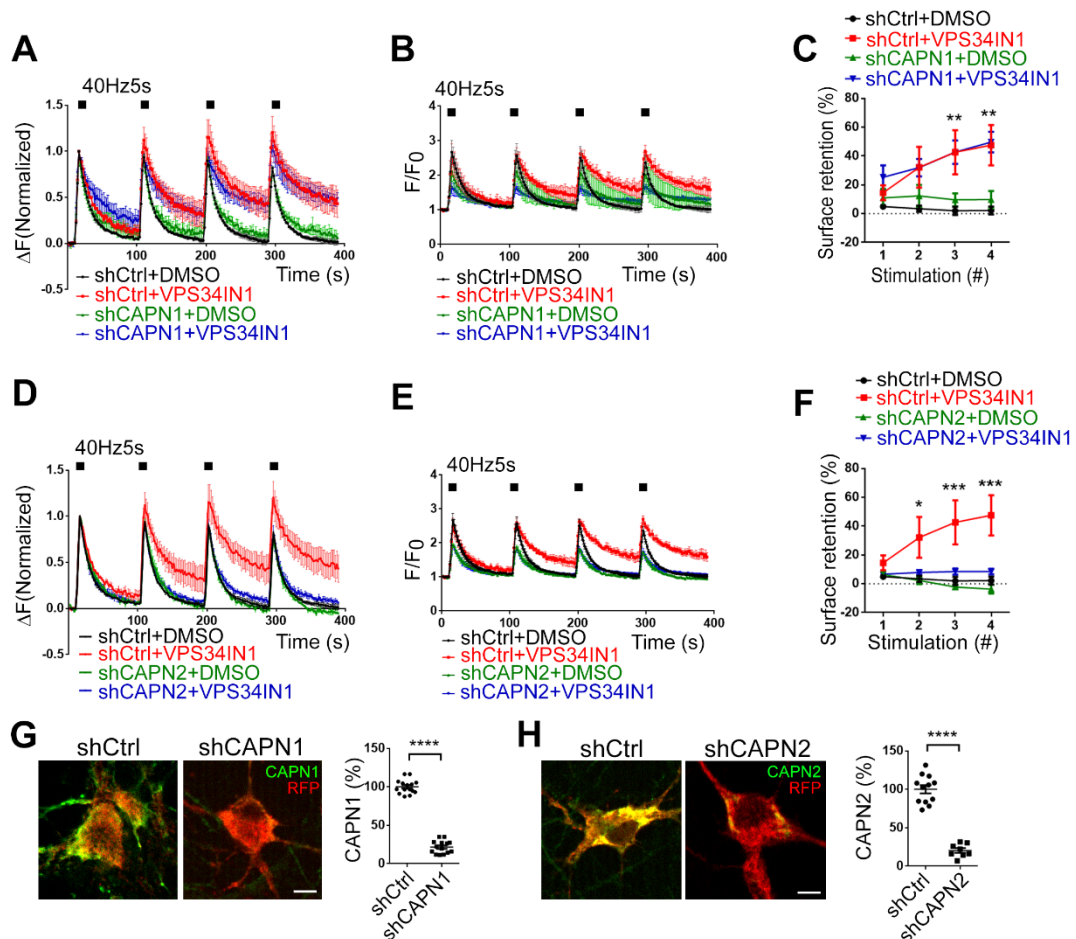

Figure 3.15. Calpain-2 is involved in delayed SV endocytosis induced by VPS34IN1.
(A-C) Cultured hippocampal neuron were transfected with control shRNA (shCtrl) or shRNA against calpain-1 (shCAPN1) and treated with DMSO or VPS34IN1. Peak normalized **(A)** and surface normalized **(B)** of Synaptophysin-pHluorin traces show that knockdown of Calpain doesn't rescue defective SV endocytosis induced by VPS34IN1. **(C)** Surface retention of Synaptophysin-pHluorin 90 s post-stimulus is plotted for each of the

four successive stimulation trains in shCtrl or shCAPN1 transfected neurons treated with DMSO or VPS34IN1 (10 µM). A total of ≥ 10 images per condition from 3 independent experiments. **(D-F)** Cultured hippocampal neuron were transfected with control shRNA (shCtrl) or shRNA against calpain-2 (shCAPN2) and treated with DMSO or VPS34IN1. Peak normalized **(D)** and surface normalized **(E)** of Synaptophysin-pHluorin traces show that knockdown of Calpain rescues defective SV endocytosis induced by VPS34IN1. **(F)** Surface retention of Synaptophysin-pHluorin 90 s post-stimulus is plotted for each of the four successive stimulation trains in shCtrl or shCAPN2 transfected neurons treated with DMSO or VPS34IN1 (10 µM). A total of ≥ 11 images per condition from 3 independent experiments. **(G-H)** immunostaining of Calapin-1 or -2 show successful knockdown in neurons.

Calpain activation is triggered by calcium influx. Therefore, we tested whether calcium was elevated in neurons treated with VPS34IN1. Hippocampal neurons were treated with VPS34IN1 and stained with the basal calcium indicator Fluo-4 (Figure 3.16A). PI(3)P depleted neurons displayed 40% elevation of basal calcium in their somata. To measure the calcium level at synapses, we used a recombinant plasmid that bears an additional red-shifted calcium sensor, RGECO, fused to the cytoplasmic domain of Synaptophysin-pHluorin (Jackson and Burrone, 2016). The basal RGECO signal at synapses was 30% higher in VPS34IN1-treated synapses (Figure 3.16B), indicating that calcium levels were also elevated at synapses after PI(3)P depletion. To determine the source of calcium, we used membrane-impermeable and permeable calcium chelators EGTA and EGTA-AM, as well as Xestospongin C, a blocker for IP_3-dependent calcium efflux from the endoplasmic reticulum (ER). We found that EGTA, the extracellular calcium chelator, can rescue impaired SV endocytosis induced by PI(3)P depletion (Figure 3.16C-E). Using a cell-permeable version of EGTA, EGTA-AM, to chelate the intracellular calcium, the increased surface retention of Synaptophysin-pHluorin induced by VPS34 inhibition was also rescued (Figure 3.16F-H). In contrast, blocking calcium efflux from the ER by Xestospongin C did not rescue defective SV endocytosis induced by VPS34IN1 (Figure 3.16I-K.). These data suggest that elevation in the concentration of intracellular calcium in PI(3)P-depleted neurons is mainly caused by calcium influx from the cell exterior.

Furthermore, we wondered if we can mimic the defective SV endocytosis by creating a high intracellular calcium environment by using Ionomycin to permeabilize the plasma membrane to allow for excessive calcium influx. Even though ionomycin treatment, similar to PI(3)P-depletion, caused an elevation in the intracellular calcium concentration, these neurons did not display a similar SV endocytosis defect (Figure 3.17). Taken together, these data indicated that even though elevated intracellular calcium plays a role in the SV endocytosis defect induced by PI(3)P depletion, it may not be the sole trigger for Calpain activation.
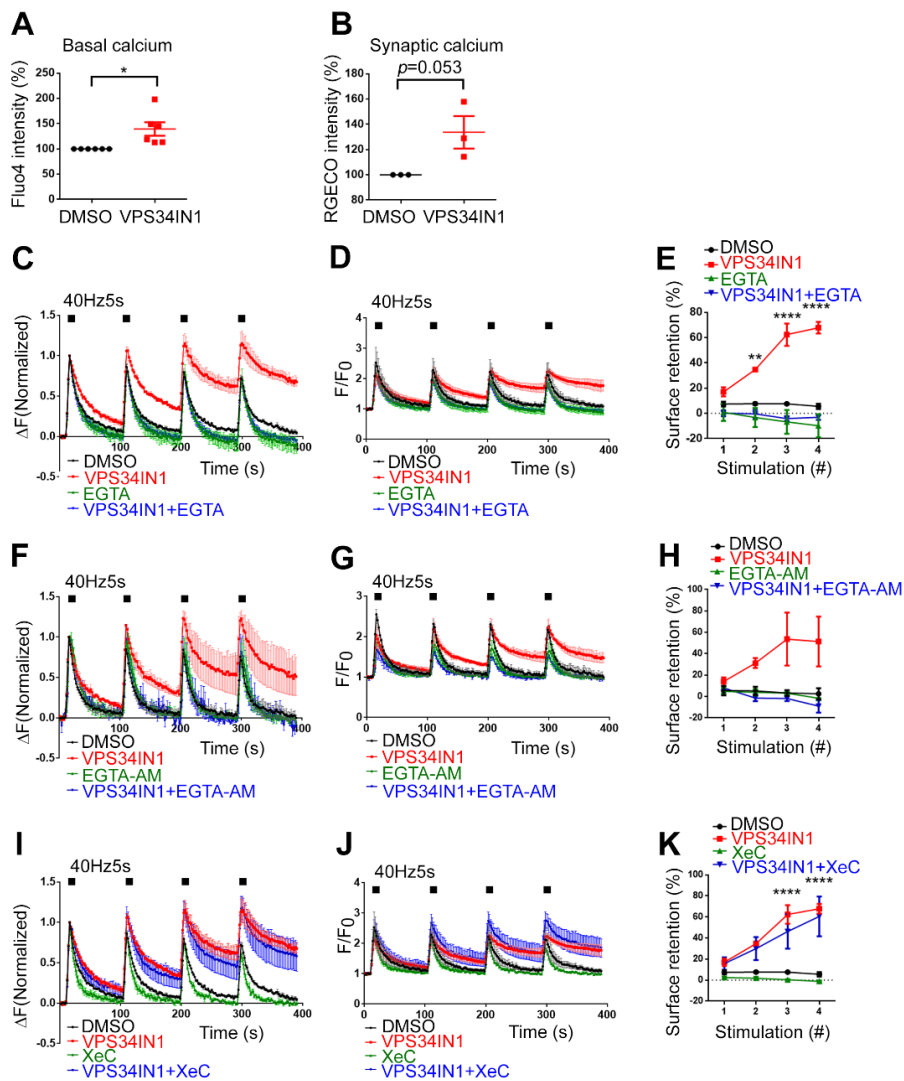

Figure 3.16. Calcium is required for calpain activation and contributes to the SV endocytosis defect.
(A) Cultured hippocampal neurons were treated by DMSO or VPS34IN1 (10 μM), and

moved to the medium containing calcium indicator, Fluo-4 (3 µM) and Pluronic F-127. Basal calcium level is detected by Fluo-4, and show 40% increase upon VPS34 inhibition. **(B)** Cultured hippocampal neurons were transfected with SypHy-RGECO and treated with DMSO or VPS34IN1 (10 µM). Synaptic calcium level is measured by RGECO signal. **(C-E)** Extracellular calcium chelation by EGTA (2mM) reverts the defective SV endocytosis. Peak normalized **(C)** and surface normalized of Synaptophysin-pHluorin traces reveal the normal SV endocytosis upon co-incubation of VPS34IN1 and EGTA. **(E)** Surface retention of Synaptophysin-pHluorin 90 s post-stimulus is plotted for each of the four successive stimulation trains. A total of ≥ 15 images per condition from 3 independent experiments. **(F-H)** Intracellular calcium chelation by cell permeable EGTA-AM (50 µM) revert the defective SV endocytosis. Peak normalized **(F)** and surface normalized **(G)** of Synaptophysin-pHluorin traces reveal the normal SV endocytosis upon co-incubation of VPS34IN1 and EGTA-AM. **(H)** Surface retention of Synaptophysin-pHluorin 90 s post-stimulus is plotted for each of the four successive stimulation trains. A total of ≥ 10 images per condition from 3 independent experiments. **(I-K)** Hippocampal neurons were treated with DMSO or VPS34IN1 (10 µM) together with or without Xestospongin C (XeC, 1 µM) to block calcium release from ER. Peak normalized **(I)** and surface normalized **(J)** of Synaptophysin-pHluorin traces show defective SV endocytosis upon co-incubation of VPS34IN1 and XeC. **(H)** Surface retention of Synaptophysin-pHluorin 90 s post-stimulus is plotted for each of the four successive stimulation trains. A total of ≥ 12 images per condition from 3 independent experiments.
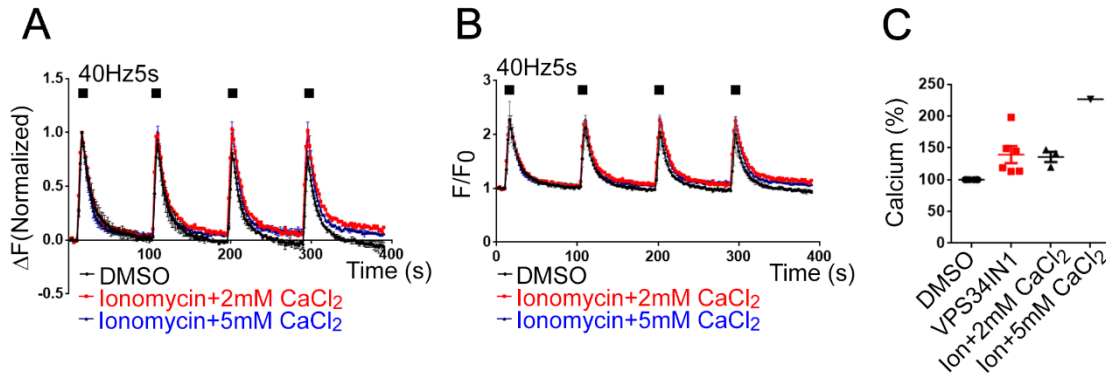

Figure 3.17. Increasing intracellular calcium is not the key factor for delayed SV endocytosis induced by VPS34IN1.

(A-B) Cultured hippocampal neurons were treated with Ionomysin (4 µM) and CaCl2 (2 mM or 5 mM) for 3 h. Peak normalized **(A)** and surface normalized **(B)** of Synaptophysin-pHluorin traces do not show any obvious defective SV endocytosis. A total of ≥ 12 images per condition from 2 independent experiments. **(C)** Cultured hippocampal neurons were treated by DMSO, VPS34IN1 (10 µM), Ionomycin (4 µM) and $CaCl_2$, and moved to the medium containing calcium indicator, Fluo-4 (3 µM) and Pluronic F-127. Basal calcium level is detected by Fluo-4, and show 40% increase upon VPS34IN1 or Ionomysin combined with 2 mM $CaCl_2$ treatment.

A previous study in non-neuronal cells has established that Calpain2 activity requires its recruitment to early endosomes by interacting with endosomal protein EEA1 and the small GTPase Rab5 (Mendoza et al., 2018). In parallel, loss of VPS34 has been found to cause Rab5 accumulation and hyperactivation (Bechtel et al., 2013). Therefore, we hypothesized that VPS34IN1-induced PI(3)P depletion may cause Calpain2 activation due to the accumulation of hyperactive Rab5 on endosomes. First, we confirmed the previous findings by Rab5 and Calpain2 coimmunostaining. We found that PI(3)P depletion led to enhanced accumulation of Rab5 in somatic and synaptic structures. These Rab5 accumulations most probably highlight enlarged endosomes, which are often positive for Calpain2 (Figure 3.18A-C), suggesting a correlation between PI(3)P, Rab5 and Calpain2. We propose that PI(3)P depletion upon VPS34 inhibition causes Calpain2 activation via its recruitment to enlarged endosomes. The precise mechanism of this recruitment process remains to be identified.

Next, we tested whether blockade of Rab5 activity can rescue VPS34IN1-induced SV endocytosis defect. Hippocampal neurons were transfected with either the dominant negative (DN) and constitutively active (CA) mutants of Rab5-mCherry (Figure 3.18D-I), and treated with VPS34IN1. Rab5 DN overexpression occluded the inhibition of SV endocytosis by VPS34 inhibition, while Rab5 CA had no impact. These findings thus indicate that PI(3)P depleted neurons may initiate a signaling pathway that enhances Rab5 activation, which then leads to elevated Calpain2 activity and, finally, resulting in Cdk5 hyperactivation (Figure 3.19).
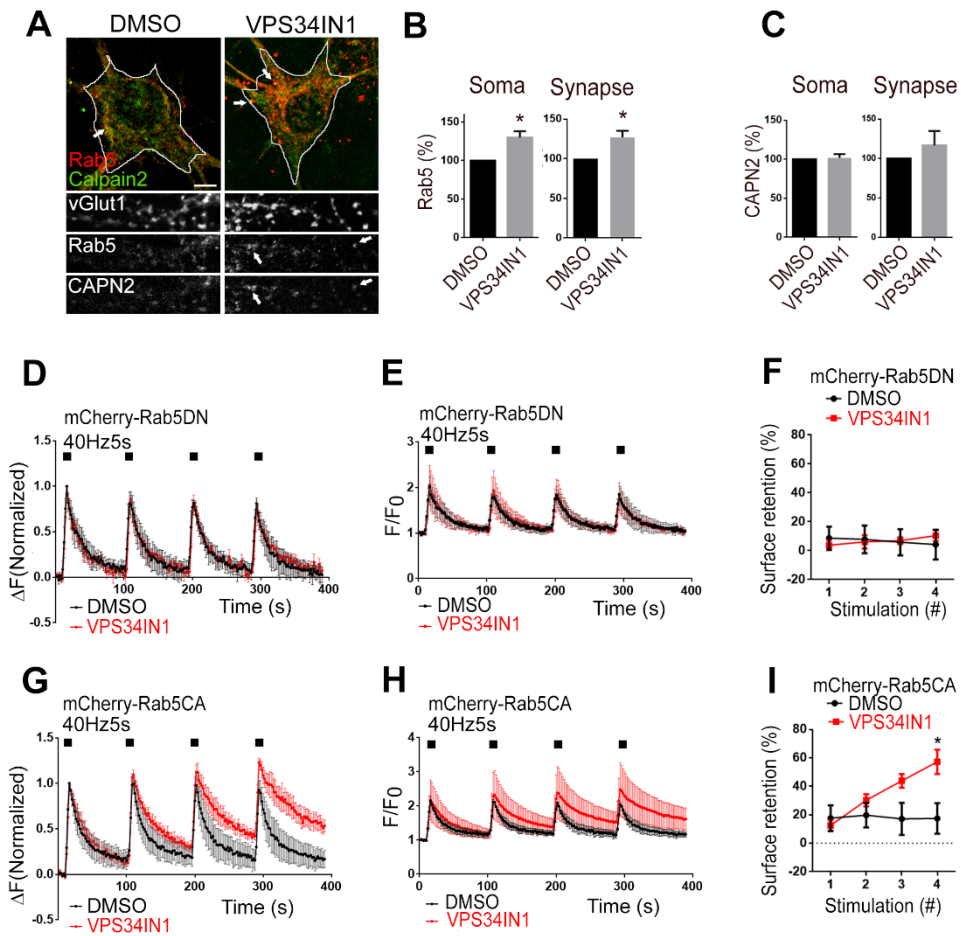
Figure 3.18. Rab5 is upstream of calpain-2 activation induced by PI(3)P depletion.
(A-B) VPS34IN1 treatment leads to increased levels of distinctive Rab5 puncta in neuronal somata and in vGLUT1-positive excitatory synapses. **(C)** Calpain-2 is localized to these Rab5-containing puncta, but there is no obvious accumulation of calpain-2. A total of 50 images per condition from 3 independent experiments. **(D-F)** Overexpression of dominant negative Rab5 (Rab5-DN) rescues the progressive accumulation of Synaptophysin-pHluorin on the surface in VPS34IN1-treated hippocampal. Peak normalized **(D)** and surface normalized **(E)** of Synaptophysin-pHluorin signals show delayed SV endocytosis upon VPS34 inhibition. **(F)** Surface retention is plotted for each stimulus and is slightly increased at the fourth stimulus in VPS34IN1- treated neurons. **(G-I)** Overexpression of constitutively active Rab5 (Rab5-CA) do not rescue progressive accumulation of Synaptophysin-pHluorin on the surface of VPS34IN1-treated hippocampal neurons is analyzed. A total of ≥ 10 images per condition from 3 independent experiments.
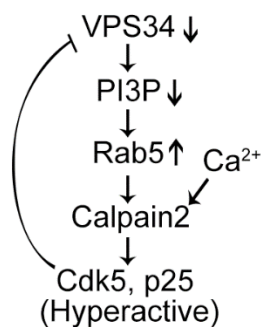
VPS34 ↓
↓
PI3P ↓
↓
Rab5 ↑   Ca²⁺
↓   ↙
Calpain2
↓
Cdk5, p25
(Hyperactive)

Figure 3.19. Signaling pathway for Cdk5 hyperactivation.
Hypothetical signaling pathway for the induction of hyperactive Cdk5 induced by repression of VPS34 downstream of neuronal activity.

Previous studies have shown that Cdk5 hyperactivation reduces presynaptic release probability (Kim and Ryan, 2010). If hyperactivation of Cdk5 underlies the defective excitatory synaptic transmission in VPS34IN1-treated neurons, repression of its activity should rescue impaired SV endocytosis and glutamatergic neurotransmitter release. To further understand the role of Cdk5 in neurotransmission and SV cycling, we treated hippocampal neurons with the Cdk5 inhibitor Roscovitine together with VPS34IN1 (Figure 3.20A-C). Cdk5 inhibition perfectly rescued the VP34IN1-induced SV endocytosis defect in response to repetitive stimulation. These results show that neuronal activity-induced PI(3)P depletion leads to Cdk5 hyperactivation which may control SV exo-/endocytosis in excitatory neurotransmission. Dr. Gaga Kochlamazashvili tested this hypothesis in acute slice preparation of hippocampal neurons, we found that Cdk5 inhibition also completely occluded the adverse effects of pharmacological inhibition of VPS34-mediated PI(3)P synthesis on excitatory neurotransmission (Figure 3.20D). Besides, Roscovitine reverted the increased paired pulse ratio induced by VPS34IN1, and instead led to a lower paired pulse ratio, an indication of elevated release probability (Figure 3.20E). Based on these findings, we conclude that PI(3)P depletion leads to Calpain2-mediated Cdk5 hyperactivation, which in turn reduces SV exo-/endocytosis, and thereby, downscales excitatory synaptic transmission.
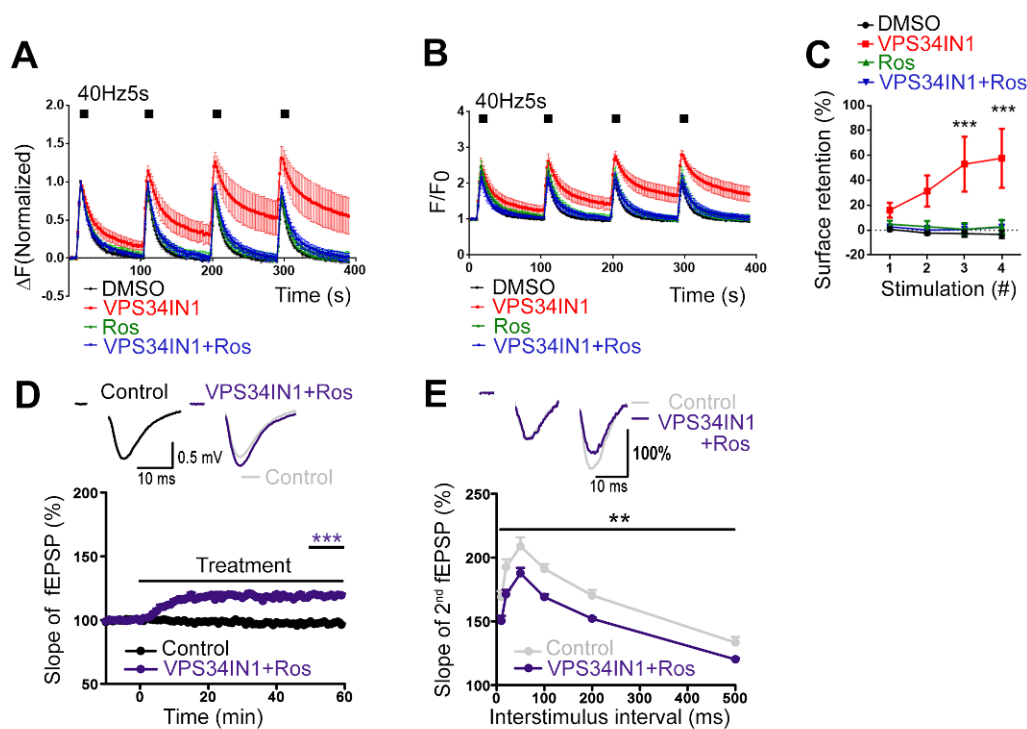
Figure 3.20. Cdk5 inhibition rescues defective SV endocytosis and neurotransmission induced by PI(3)P depletion.

(A-C) Cdk5 inhibition by Roscovitine (10 µM) rescues the progressive accumulation of Synaptophysin-pHluorin on the neuronal surface induced by VPS34IN1. Peak normalized **(A)** and surface normalized **(B)** of Synaptophysin-pHluorin traces show normal SV endocytosis in Roscovitine and VPS34IN1 co-treated neurons. **(C)**Surface retention of Synaptophysin-pHluorin 90 s post-stimulus is plotted for each of the four successive stimulation trains. A total of 20 images per condition from 4 independent experiments.

(D) Basal excitatory synaptic transmission of CA3-CA1 connections in acute hippocampal slices treated with DMSO (0.03%) or VPS34IN1 plus Roscovitine. Representative fEPSP traces (above) and the relative slope of fEPSPs (below) are shown. Concomitant application of VPS34IN1 and Roscovitine facilitates excitatory synaptic transmission, akin to Roscovitine alone(E). **(E)** Decreased paired paired-pulse facilitation (PPF) at hippocampal CA3-CA1 synapses treated with VPS34IN1 plus Roscovitine. Representative traces of fEPSPs PPF at a 20-ms interpulse interval and quantification over a range of interpulse intervals (10–500 ms) given as ratio of the second to the first response. The data show decreased facilitation of the second response in VPS34IN1- plus Roscovitine-treated acute hippocampal slices. Electrophysiology experiments were done by Dr. Gaga Kochlamazashvili **(D-G)**.

The balanced activity of the phosphatase Calcineurin and the kinase Cdk5 is known to set the release probability in neurons, and Calcineurin is known to counteract Cdk5 by dephosphorylating Cdk5 substrates (Kumashiro et al., 2005; Shah andLahiri, 2014). Given

that Cdk5 inhibition fully rescues PI(3)P depletion-indued SV endocytosis impairment, we wondered whether application of Calcineurin inhibitor Cyclosporin A would phenocopy VPS34IN1-induced defective SV endocytosis. Synaptophysin-pHluroin-expressing hippocampal neurons were treated with Cyclosporin A and stimulated with 200 AP trains (Figure 3.21). Effects of VPS34IN1 on the kinetics of SV endocytosis in response to trains stimulation were mimicked by Cyclosporin A treatment. These results confirm that neuronal PI(3)P is capable of regulating SV recycling and neurotransmission via modulating the Cdk5/Calcineurin balance through Calpain2 activity.
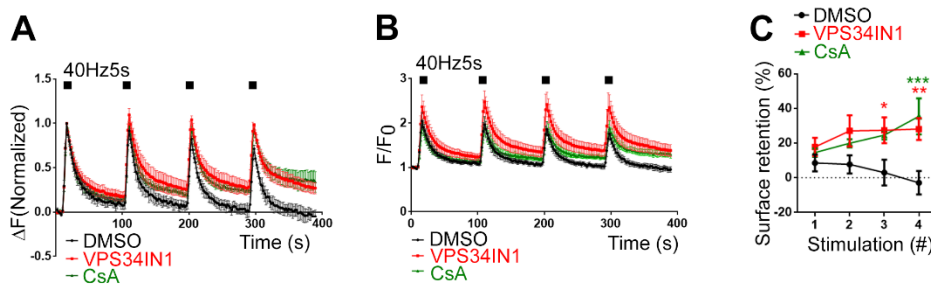

Figure 3.21. Calcineurin inhibition induced defective SV endocytosis.
(A-C) Calcineurin inhibition by Cyclosporin A (10 µM) phenocopies VPS34IN1-induced loss of PI(3)P with respect to the accumulation of Synaptophysin-pHluorin on the neuronal surface. Peak normalized **(A)** and surface normalized **(B)** of pHluorin signals were analyzed. **(C)** Surface retention of Synaptophysin-pHluorin 90 s post-stimulus is plotted for each of the four successive stimulation trains. A total of ≥ 15 images per condition from 3 independent experiments

3.5 The regulatory role of PI(3)P in neuronal network activity

Depressed excitatory neurotransmission induced by activity-dependent PI(3)P reduction may be important for controlling and restricting neuronal network activity (Marder and Goaillard, 2006; Nelson and Valakh, 2015). To investigate whether loss of PI(3)P restricts excitatory neurotransmission when inhibitory network is impaired, we disinhibited hippocampal neurons and measured polyspiking as an indication for neuronal excitability.

We found that activity-dependent disinhibition induced by 1 Hz stimulation within the hippocampal network resulted facilitation of PSs and a profound repression of polyspiking activity in VPS34IN1-treated slices, while Roscovitine caused the opposite phenotype (Figure 3.22A-B), suggesting that PI(3)P depletion restricts neuronal network activity by repressing excitatory transmission. To further confirm our findings, we applied GABA$_A$ receptor antagonist Picrotoxin to block inhibitory transmission, and then induce polyspike waves. PI(3)P depletion potently repressed the Picrotoxin-induced strong polyspilking activity, suggesting endosomal PI(3)P depletion restricts neuronal activity (Figure 3.22C-D). These results thus elucidate a crucial unknown function for endosomal phospholipid PI(3)P in the control of excitatory neurotransmission and neuronal network activity.
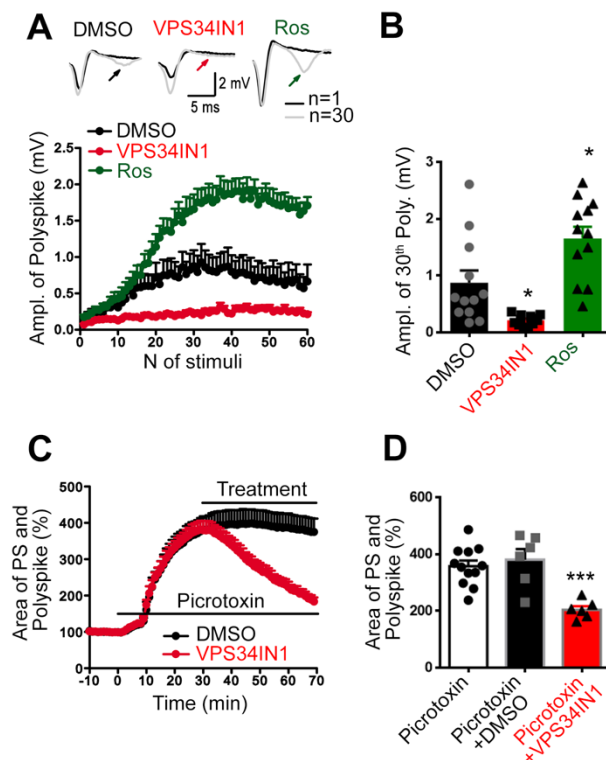

Figure 3.22. PI(3)P regulates neuronal network activity.
(A-B) Activity-dependent polyspiking of population spikes (PS) during 1 Hz stimulation is reduced by VPS34IN1 and facilitated by Roscovitine compared to DMSO-treated control slices. Top, representative traces of the 1st and 30th stimulus responses with polyspikes indicated by arrows. **(C-D)** PS and polyspike areas in the presence of picrotoxin (50 µM) and treated with DMSO or VPS34IN1 (10 µM). The experiments were done by Dr. Gaga Kochlamazashvili.

In addition to being a target of a signaling cascade that starts by PI(3)P depletion, Cdk5 also negatively regulates VPS34-mediated PI(3)P synthesis (Furuya et al., 2010). To investigate the role of Cdk5 and Calapin in activity-dependent PI(3)P loss, we measured PI(3)P levels in Cdk5 or Calpain inhibitor-treated neurons upon repetitive stimulation. We found that loss of Cdk5 and Calpain activity prevented the activity-induced PI(3)P depletion on endosomes in hippocampal neurons (Figure 3.23). Thus, we propose that the endosomal VPS34, Calpain and Cdk5 are part of the same autoregulated signaling cascade that scales excitatory neurotransmission in neuronal network.
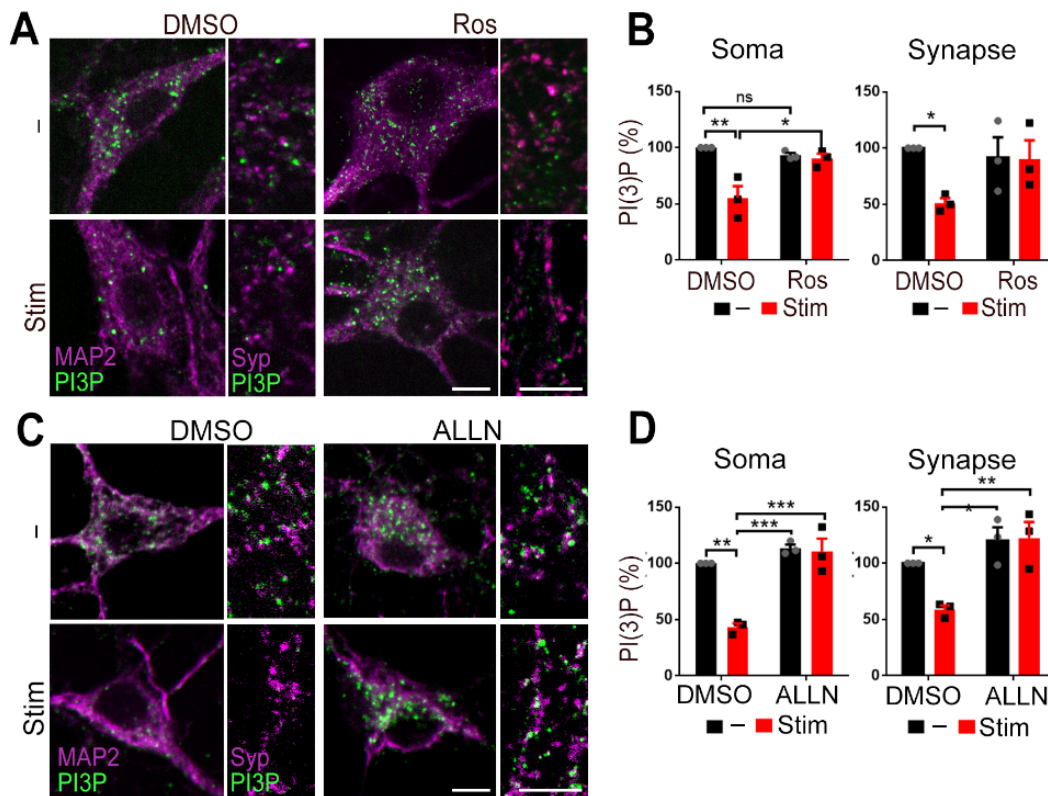

Figure 3.23. Cdk5 and Calpain inhibition restore the activity-induced PI(3)P depletion. **(A, C)** Cultured hippocampal neurons treated with Roscovitine (10 μM) or ALLN (100 μM), stimulated with 4 x 200 APs, fixed and stained for MAP2, Synaptophysin and PI(3)P. Scale bar, 10 μm. **(B, D)** Treatment with Roscovitine and ALLN prevents the stimulation-induced depletion of PI(3)P in MAP2-positive somata and Synaptophysin-positive synaptic regions. A total of ≥ 40 images per condition from 3 independent experiments.

Our findings identify a novel autoregulatory pathway for the cell-intrinsic control of excitatory neurotransmission and vesicle cycling by the endosomal PI(3)P that acts independently and in parallel to inhibitory synaptic input. Activity-induced repression of VPS34-mediated PI(3)P synthesis on endosome is shown to trigger the calcium- and Calpain2-mediated Cdk5 activation, resulting in impaired SV exo-/ endocytosis and reduced SV release to repress excitatory neurotransmission (Figure 3.24).
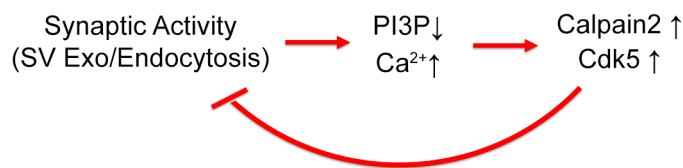

Figure 3.24. A working-model for the feedback regulation of excitatory synaptic activity. Neuronal activity downregulates VSP34-mediated synthesis of endosomal PI(3)P. PI(3)P depletion causes the activation of Calpain-2 and Cdk5 resulting in the repression of excitatory neurotransmission and kinetically impaired SV endocytosis.

4. Discussion

In this thesis, I have identified a novel feedback regulation mechanism that cell-intrinsically controls excitatory neurotransmission and vesicle recycling that operates through endosomal PI(3)P. Neuronal activity-induced activation of Cdk5 reduces PI(3)P synthesis by VPS34, and thereby triggers Rab5 and Calpain2 activation. p35-p25 conversion induced by elevated intracellular calcium and Calpain2-mediated cleavage leads to Cdk5 activation. The activity-dependent depletion of PI(3)P synthesized by VPS34 and depression of excitatory neurotransmission were occluded by pharmacological blockade of Cdk5 activity. These results unravel an unexpected and novel function for endosomal PI(3)P at synapses in SV cycling, scaling excitatory neurotransmission and stabilizing network activity, and this mechanism may explain the involvement of VPS34 in neurodevelopmental disease and neurodegeneration.

4.1 The role of phosphoinositides in synaptic function

Phosphoinositides are specifically localized to organelle membranes and regulate neuronal function by recruiting several phosphoinositide-binding proteins. The most well-studied phosphoinositide at the synapses is $PI(4,5)P_2$ that is mainly produced on the plasma membrane (Fon andEdwards, 2001). $PI(4,5)P_2$ is an important lipid component for SV priming, Ca^{2+}-triggered SV exocytosis and SV endocytosis by recruitung different SV proteins which contain $PI(4,5)P_2$-binding domain (Okamoto and Südhof, 1997; Saheki and DeCamilli, 2012; Südhof, 2012). One the other hand, the endosomal PI(3)P is considered to be involved in endosomal protein or membrane trafficking. Surprisingly, we found that the delayed SV endocytosis upon PI(3)P-depletion is due to incomplete endocytic uptake of SVs from the plasma membrane (Figure 3.9), suggesting that the endosomal PI(3)P has a novel function in SV recycling.

Additionally, phosphoinositides have been implicated in regulating synaptic plasticity. $PI(3,4,5)P_3$ synthesis by class I PI3K in crucial for maintaining AMPA receptor clustering (Arendt et al., 2010), and consequently modulates the synaptic plasticity. $PI(3,5)P_2$ is also involved in the trafficking of AMPA receptor to the plasma membrane on the postsynaptic site (Seebohm et al., 2012). In our study, we focused on the potential role of endosomal PI(3)P in SV recycling and neurotransmission, primarily focusing on the presynaptic terminal.

4.2 The PI(3)P/Calpain2/Cdk5 pathway

Calpains are intracellular Ca^{2+}-dependent proteases that play roles in diverse biological mechanism through limited proteolysis of their substrates. Calpain1 and Calpain2 are two major calpains expressed in the central nervous system and they are both localized at synapses. Calpains have many synaptic substrates such as NMDA receptor, AMPA receptor, postsynaptic density proteins, Dynamin, kinases and phosphatases, which are all involved in various steps of synaptic function. *In vitro* studies have shown that excess glutamate and Aβ-induced cleavage of NR2A and NR2B subunits of NMDA receptors happens via Calpain activation, which in turn downregulates NMDA receptor levels and prevents pathological process. Also, synaptic architecture proteins spectrin and MAP2 are substrates of Calpain for regulation of synaptic integrity and stability (Wu and Lynch, 2006). In our study, we have shown that PI3P depletion leads to Calpain activation at the synapse. Dynamin, which is one of the targets of Calpain, is also partially cleaved in VPS34IN1-treated cerebellar granule neurons (Figure 3.14A). This observation has raised the possibility that the impairments in SV recycling after PI(3)P depletion is due to dynamin cleavage. However, we have also made a number of observations that has invalidated this possibility: 1) Dynamin cleavage has not been observed in hippocampal cultures, which has been the major experimental model throughout this study. This may be due to differences of the culture conditions

between hippocampal and cerebellar cultures. The cerebellar neurons are cultured in the KCl-containing medium with high levels of baseline activity, whereas hippocampal neurons are maintained in conditions with limited network activity. 2) Inhibition of Cdk5, which is activated downstream of Calpains, did not rescue Dynamin cleavage in cerebellar neurons, even though it fully rescued VPS34IN1-induced SV endocytosis defect in hippocampal neurons. 3) Elevation of intracellular Ca^{2+} via ionomycin treatment had no effect on SV endocytosis, suggesting that elevated intracellular calcium concentration and Calpain are not the sole trigger for delayed endocytosis. Thus, we propose that Calpain activation does not directly target synaptic proteins involved in SV recycling, but rather utilizes an indirect feedback regulation through Cdk5 to modulate SV recycling and neurotransmission.

Interestingly, Cdk5 has been proposed to negatively regulate VPS34 activity via phosphorylation of VPS34 which leads to instability of the VPS34 complex (Furuya et al., 2010). Consistent with our hypothesis, pharmacological inhibition of Cdk5 and Calpain restore the activity-dependent PI(3)P depletion in hippocampal neurons (Figure 3.23), suggesting the presence of an autoregulatory signaling pathway between Cdk5, VPS34-mediated PI(3)P synthesis and Calpain2 (Figure 3.19) that scales excitatory neurotransmission. The phosphorylation site of VPS34 by Cdk5 has been identified. By generating phosphomimetic or phosphodeficient mutants of VPS34 it will be possible to directly study the physiological relevance of activity-dependent regulation of VPS34 via Cdk5 on neurotransmission and synaptic scaling.

4.3 The role of endosomal PI(3)P in neurotransmission

The VPS34 complex and its product PI(3)P play crucial roles in several cellular mechanisms. Even though the role of VPS34 in autophagy or intracellular protein trafficking in non-neuronal cells has been well studied, the role of PI(3)P in neurotransmission is poorly understood. During SV recycling, the endocytic vesicles are usually delivered to

endosome-like structures that have been proposed to be the major sorting platform for SV protein recycling or degradation. In our study, we have identified the presence of VPS34 in crude SV fraction, and proposed a novel function of endosomal PI(3)P in scaling excitatory neurotransmission by regulating SV cycling. SV exo- and endocytosis were severely impaired in the absence of VPS34 activity. The defects in SV exocytosis is not a direct consequence of dysfunctional SV endocytosis. Interestingly, the defects in SV exocytosis is severe only when neurons were stimulated by few AP stimulation, and no longer detectable under sustained stimulation condition. It is possible that the responded synaptic boutons we have detected upon 2 AP stimulation may differ to the one responded to strong and sustained stimulation. All the SVs at synapse are accessible upon 200APs stimulation and this strong saturation may bring SV release close to saturation, which may have concealed the effect of PI(3)P loss on SV release.

Acute inhibition of Cdk5 completely rescues defects in SV endocytosis during trains of APs in the near absence of PI(3)P, indicating that PI(3)P-containing endosomes are largely dispensable for SV cycling, contrary to the prior proposal (Hoopmann et al., 2010), where SVs were proposed to pass through an early endosomal compartment. In this study, we propose an alternative role for PI(3)P-positive endosomes. Instead of actively participating in the direct path that SVs use during their recycling, PI(3)P-positive endosomes respond to neuronal excitation and lose their PI(3)P, which eventually leads to Cdk5 activation for scaling down of neurotransmission. In the absence of neuronal activity, PI(3)P levels rise, maintaining Cdk5 in an inactive state which increases SV release probability and thus neuronal excitability through neurotransmitter release (Figure 4.1). Thus, we hypothesize that PI(3)P-containing neuronal endosome acts as a master checkpoint for cell-intrinsic control of excitatory neurotransmission and preventing hyperexcitation and epileptiform activity.
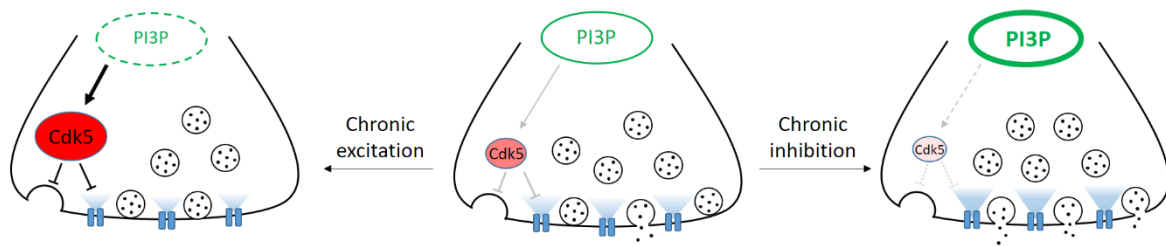
Figure 4.1. Hypothical model of PI(3)P serve as a checkpoint for neurotransmission. PI(3)P downregulation by chronic excitation and upregulation by chronic inhibition affect Cdk5 activity and its function in synaptic vesicle recycling and transmitter release. (Drew by Dr. Tolga Soykan)

4.4 The role of VPS34 complexes in other neuronal function

VPS34 complex II is important for various intracellular trafficking routes and it is the major enzyme to produce PI(3)P on endosomes. Here we blocked PI(3)P synthesis with different approaches, including pharmacological inhibition, Rapalog-induced dimerization system as well as gene knockdown. Direct inhibition of VPS34 complex activity via VPS34 knockdown or indirect inhibition via VPS15 knockdown showed successful depletion of P(3)P at somata and synapses. However, we cannot distinguish the contribution of VPS34 complex I and complex II using these approaches. To study which of the two complexes is primarily involved in the neurotransmission, a specific targeting method is required. We tried to knockdown UVRAG, a subunit of VPS34 complex II, but the commercially available UVRAG shRNA is not sufficient to deplete VPS34 activity (data not shown). Thus another approach for efficiently targeting UVRAG or ATG14 are required. Interestingly, UVRAG and ATG14 have VPS34-independent functions in endocytic trafficking. UVRAG binds to homotypic fusion and vacuole protein sorting (HOPS) complex, and acts as a Rab7 effector to trigger endosomal membrane fusion events (Balderhaar and Ungermann, 2013). Also, ATG14 interacts with SNAREs and associated proteins to mediate endosomal fusion (Diao

et al., 2015). The endocytic fusion defects affect the protein homeostasis and endosomal-lysosomal system in the cells. The VPS34 inhibition-induced complex instability may release more subunits form the complex, and affect other cellular functions.

Furthermore, the activity of VPS34 complex is tightly regulated. The posttranslational modification of VPS34 complex I and II subunits has been studied in various systems For example, phosphorylation of VPS34 subunit by Cdk5 inhibits the kinase activity and PI(3)P synthesis (Tsai et al., 2010), and mTOR phosphorylates Beclin1 or UVRAG to inhibit the complex activity and prevent induction of autophagy (Gulati et al., 2008). All these modifications of VPS34 complexes contribute to the regulation of their functions, and consequently play different roles in several cellular mechanisms. Besides, VPS34 is a positive regulator of Phosphatase and tensin homolog (PTEN) (Naguib et al., 2015), and hence a negative regulator of class I PI3K signaling. It is suggested that there is a potential crosstalk between VPS34 and other signaling pathways. In my thesis, I manipulated the PI(3)P synthesis through different approaches, including pharmacological treatment or knockdown of VPS34/VPS15, to validate the essential role of PI(3)P synthesis by VPS34 in SV recycling. However, we cannot exclude that inhibition of VPS34 may interfere with the function of other subunits, contribute to imbalanced signaling cascade, and finally cause defects in neuronal function. In this study, we also concluded that PI(3)P synthesis by VPS34 is required for SV endocytosis. The role of VPS34 in endocytosis is supported by a study based on Beclin1-deficient mice. It reported that loss of Beclin1 leads to PI(3)P mislocalization, abnormal endosome formation and severe neurodegeneration in cerebellar Purkinje cells and hippocampal neurons. Beclin1-deficient mammalian cells display reduced PI(3)P level and impaired EGFR endocytosis. The endocytic defects is due to disruption of Rab5-dependent endosome formation, suggesting that Beclin1 is required for VPS34 complex-mediated endocytosis (McKnight et al., 2014). Therefore, VPS34-mediated PI(3)P synthesis is a key regulator for endocytic events and endosome formation.

In addition to its role in endocytosis, a PI(3)P-binding protein Ankyrin is required for synaptic vesicles trafficking along microtubules. The dynactin complex, an adaptor for dynein-mediated retrograde transport, is crucial for vesicle transport through PI(3)P binding Ankyrin adaptor, and the axonal transport is disrupted in VPS34 depleted hippocampal neurons (Lorenzo et al., 2014). It is likely that the VPS34 inactivation-induced PI(3)P depletion not only impairs the SV cycling at the synapses, but also affects the retrograde transport along the axon. However, the detailed mechanism of how VPS34 complex regulates axonal retrograde transport requires further investigation.

4.5 The role of VPS34 and autophagy in neurons

Inhibition of VPS34 not only impairs the endosomal trafficking, but also reduces autophagy. However, the autophagy pathway is complex, and it is triggered by multiple steps and numerous regulators. The roles of autophagy in neuron has been addressed in several studies. For example, Beclin1-deficient murine embryonic fibroblasts showed decreased autophagy and endosomal trafficking, and loss of Beclin1 results in severe neurodegeneration (McKnight et al., 2014). The defective protein clearance induced by block of autophagy is implicated in several neurodegenerative diseases. In addition to the its role in pathological conditions, autophagy is required for synaptic function and neurotransmission (Figure 1.6) (Lieberman andSulzer, 2020). Intriguingly, using KCl to depolarize rat hippocampal neurons, transiently increased number of autophagosomes and enhanced autophagic degradation of AMPA receptors were observed, while these phenotypes were partially restored by AP5 or NMDA receptor blocker. suggesting that autophagy contributes to NMDA receptor- dependent synaptic plasticity (Shehata et al., 2012).

The role of VPS34 complexes in endosomal and autphagosomal pathways are deeply interconnected. It is crucial to understand the relationship between these pathways system in neurons. The experimental perturbations of VPS34 activity that impair SV endocytosis may

either arise from disruptions in either the endosomal trafficking or autophagy (Itakura et al., 2009). Thus, more comprehensive experiments based on specific targeting of individual VPS34 complexes are needed for elucidating the precise role of each VPS34 complex in neurotransmission.

4.6 The link between PI(3)P and Calpain

A previous study has shown that Calpains are recruited to early endosomes in a Rab5-dependent manner in non-neuronal cells (Mendoza et al., 2018). We also had a similar observation in our study showing that PI(3)P depletion-induced accumulation of Rab5 in the neuronal cell body and synapses where Calpain2 is recruited to (Figure 3.18). Interestingly, the Calpain activation is not merely dependent on Rab5 activity, given that the constitutively active Rab5-overexpressing neurons, did not exhibit similar levels of SV endocytosis defects as in VPS34IN1-treated neurons (Figure 3.18G-I). This suggests that Rab5 accumulation is necessary but not sufficient for triggering Calpain activation. Due to the complex function of VPS34, it is possible that other factors are involved in this pathway and it requires for further investigation.

Besides, we did not detect significantly increased Calpain2 signal at the soma and synapse (Figure 3.18C). The possible explanations may be due to the change of Calpain activity itself instead of its protein level. Alternatively the association between endogenous inhibitor Calpastatin and Calpain may change with PI(3)P reduction. A study have shown that viral transduction of Calpastatin in cortical neurons resulted in localization of Calpastatin to endosomal structures (Sengoku et al., 2004) which is then crucial for regulating the Calpain activity. VPS34 inhibition which causes abnormal endocytic function may also be responsible for changing the distribution of Calpastatin and thus affecting the Calpain activity.

4.7 Dysregulation of PI(3)P and Cdk5 in diseases

Dysfunctional intracellular protein trafficking and autophagy by VPS34 inactivation has been implicated in several neurodevelopmental diseases, neurodegenerative diseases, or mood disorders. In patients or mice with Alzheimer's disease (AD), PI(3)P is the only phosphoinositide which is selectively decreased in the brain tissue, and inhibition of VPS34 causes an enlargement of neuronal endosomes which then enhances the amyloidogenic processing of APP (Morel et al., 2013b). Multiple studied suggested that the Calpain activation-induced Cdk5 hyperactivation is a key pathological pathway for forming neurofibrillary tangles which is a feature for AD diagnosis. Here we propose that the Calpain/p25/Cdk5 pathway is directly linked to the VPS34 activity and PI(3)P levels and these two pathways can reciprocally control each other to modulate neurotransmission.

Additionally, VPS34 was proposed to be involved in pathogenesis of schizophrenia and bipolar disorder, and mutations in VPS34 are linked to increase the susceptibility to both mood disorders (Stopkova et al., 2004). Lithium is a widely used treatment for mood disorders, and it has effects on phosphoinositide pathway and synaptic scaling, suggesting the phosphoinositide metabolism and impaired synaptic plasticity could underlie the susceptibility of schizophrenia (Kavalali and Monteggia, 2020; Stopkova et al., 2004). We proposed that the endosomal VPS34-Cdk5 pathway plays a complementary role to homeostatic scaling, a mechanism for up- or downregulating synaptic weights under certain conditions. While we focus on the excitatory neurotransmission in hippocampus, we speculate that the basic principles of autoregulatory PI(3)P-Cdk5 pathway are conserved in other networks, such as cortex or cerebellum. To summarize, our findings are consistent with the possible involvement of PI(3)P in different neurological diseases, for instance, neurodevelopmental disease characterized by imbalance of excitatory/ inhibitory transmission (Nelson and Valakh, 2015), and in neurodegenerative disease. Therefore, pharmacological targeting of endosomal PI(3)P synthesis and turnover may become a

potential treatment of these diseases and other neurological disorders associated with epileptic forms of activity or excitatory/ inhibitory imbalance.

5. Bibliography

Abrahamsen, H., Stenmark, H., and Platta, H.W. (2012). Ubiquitination and phosphorylation of Beclin 1 and its binding partners: Tuning class III phosphatidylinositol 3-kinase activity and tumor suppression. FEBS Lett. *586*, 1584–1591.

Alers, S., Loffler, A.S., Wesselborg, S., and Stork, B. (2012). Role of AMPK-mTOR-Ulk1/2 in the Regulation of Autophagy: Cross Talk, Shortcuts, and Feedbacks. Mol. Cell. Biol. *32*, 2–11.

Arendt, K.L., Royo, M., Fernández-Monreal, M., Knafo, S., Petrok, C.N., Martens, J.R., and Esteban, J.A. (2010). PIP 3 controls synaptic function by maintaining AMPA receptor clustering at the postsynaptic membrane. Nat. Neurosci. *13*, 36–44.

Backer, J.M. (2008). The regulation and function of Class III PI3Ks: novel roles for Vps34. Biochem. J.

Backer, J.M. (2016). The intricate regulation and complex functions of the Class III phosphoinositide 3-kinase Vps34. Biochem. J *473*, 2251–2271.

Bago, R., Malik, N., Munson, M.J., Prescott, A.R., Davies, P., Sommer, E., Shpiro, N., Ward, R., Cross, D., Ganley, I.G., et al. (2014). Characterization of VPS34-IN1, a selective inhibitor of Vps34, reveals that the phosphatidylinositol 3-phosphate-binding SGK3 protein kinase is a downstream target of class III phosphoinositide 3-kinase. Biochem. J.

Balderhaar, H.J. klein., and Ungermann, C. (2013). CORVET and HOPS tethering complexes - coordinators of endosome and lysosome fusion. J. Cell Sci. *126*, 1307–1316.

Bechtel, W., Helmstädter, M., Balica, J., Hartleben, B., Kiefer, B., Hrnjic, F., Schell, C., Kretz, O., Liu, S., Geist, F., et al. (2013). Vps34 Deficiency Reveals the Importance of Endocytosis for Podocyte Homeostasis. 727–743.

Bianchetta, M.J., Lam, T.K.T., Jones, S.N., andMorabito, M.A. (2011). Cyclin-dependent kinase 5 regulates PSD-95 ubiquitination in neurons. J. Neurosci. *31*, 12029–12035.

Bickler, P.E., and Fahlman, C.S. (2004). Moderate increases in intracellular calcium activate neuroprotective signals in hippocampal neurons. Neuroscience *127*, 673–683.

Burman, C., and Ktistakis, N.T. (2010). Regulation of autophagy by phosphatidylinositol 3-phosphate. FEBS Lett. *584*, 1302–1312.

Cousin, M.A. (2015). Synaptic Vesicle Endocytosis and Endosomal Recycling in Central Nerve Terminals. Neurosci. Davis, G.W., and Müller, M. (2015). Homeostatic Control of Presynaptic Neurotransmitter Release. Annu. Rev. Physiol. *77*, 251–270.

Dhuriya, Y.K., and Sharma, D. (2020). Neuronal Plasticity: Neuronal Organization is Associated with Neurological Disorders. J. Mol. Neurosci.

Diao, J., Liu, R., Rong, Y., Zhao, M., Zhang, J., Lai, Y., Zhou, Q., Wilz, L.M., Li, J., Vivona, S., et al. (2015). ATG14 promotes membrane tethering and fusion of autophagosomes to endolysosomes. Nature *520*, 563–566.

DiPaolo, G., and DeCamilli, P. (2006). Phosphoinositides in cell regulation and membrane dynamics. Nature.

Fletcher, A.I., Shuang, R., Giovannucci, D.R., Zhang, L., Bittner, M.A., and Stuenkel, E.L. (1999). Regulation of exocytosis by cyclin-dependent kinase 5 via phosphorylation of Munc18. J. Biol. Chem. *274*, 4027–4035.

Fon, E.A., and Edwards, R.H. (2001). Molecular mechanisms of neurotransmitter release. Muscle and Nerve *24*, 581–601.

Frere, S., and Slutsky, I. (2018). Alzheimer's Disease: From Firing Instability to Homeostasis Network Collapse. Neuron *97*, 32–58.

Fu, A.K.Y., Ip, F.C.F., Fu, W.Y., Cheung, J., Wang, J.H., Yung, W.H., and Ip, N.Y. (2005). Aberrant motor axon projection, acetylcholine receptor clustering, and neurotransmission in cyclin-dependent kinase 5 null mice. Proc. Natl. Acad. Sci. U. S. A. *102*, 15224–15229.

Furuya, T., Kim, M., Lipinski, M., Li, J., Kim, D., Lu, T., Shen, Y., Rameh, L., Yankner, B., Tsai, L.H., et al. (2010). Negative Regulation of Vps34 by Cdk Mediated Phosphorylation. Mol. Cell *38*, 500–511.

Gautreau, A., Oguievetskaia, K., and Ungermann, C. (2014). Function and regulation of the endosomal fusion and fission machineries. Cold Spring Harb. Perspect. Biol.

Goto, K., Iwamoto, T., and Kondo, H. (1994). Localization of mRNAs for calpain and calpastatin in the adult rat brain by in situ hybridization histochemistry. Mol. Brain Res. *23*, 40–46.

Granseth, B., Odermatt, B., Royle, S.J.J., and Lagnado, L. (2006). Clathrin-Mediated Endocytosis Is the Dominant Mechanism of Vesicle Retrieval at Hippocampal Synapses. Neuron *51*, 773–786.

Gstrein, T., Edwards, A., Přistoupilová, A., Leca, I., Breuss, M., Pilat-Carotta, S., Hansen, A.H., Tripathy, R., Traunbauer, A.K., Hochstoeger, T., et al. (2018). Mutations in Vps15 perturb neuronal migration in mice and are associated with neurodevelopmental disease in humans. Nat. Neurosci. *21*, 207–217.

Gulati, P., Gaspers, L.D., Dann, S.G., Joaquin, M., Nobukuni, T., Natt, F., Kozma, S.C., Thomas, A.P., and Thomas, G. (2008). Amino Acids Activate mTOR Complex 1 via Ca2+/CaM Signaling to hVps34. Cell Metab. *7*, 456–465.

Henne, W.M., Buchkovich, N.J., and Emr, S.D. (2011). The ESCRT Pathway. Dev. Cell *21*, 77–91.

Hernandez, D., Torres, C.A., Setlik, W., Cebrián, C., Mosharov, E.V., Tang, G., Cheng, H.C., Kholodilov, N., Yarygina, O., Burke, R.E., et al. (2012). Regulation of Presynaptic Neurotransmission by Macroautophagy. Neuron *74*, 277–284.

Heuser, J.E., and Reese, T.S. (1973). Evidence for recycling of synaptic vesicle membrane during transmitter release at the frog neuromuscular junction. J. Cell Biol. *57*, 315–344.

Hoffmann, S., Orlando, M., Andrzejak, E., Bruns, C., Trimbuch, T., Rosenmund, C., Garner, C.C., and Ackermann, F. (2019). Light-activated ROS production induces synaptic autophagy. J. Neurosci. *39*, 2163–2183.

Hood, J.L., Brooks, W.H., and Rossman, T.L. (2004). Differential compartmentalization of the calpain/calpastatin network with the endoplasmic reticulum and Golgi apparatus. J. Biol. Chem. *279*, 43126–43135.

Hoopmann, P., Buckers, J., Punge, A., Westphal, V., Opazo, F., Rizzoli, S.O., Hell, S.W., Lauterbach, M.A., Barysch, S.V., and Bethani, I. (2010). Endosomal sorting of readily releasable synaptic vesicles. Proc. Natl. Acad. Sci. *107*, 19055–19060.

Huo, Y., Aboud, K., Kang, H., Cutting, L.E., and Bennett, A. (2017). Calpain-1 and calpain-2: the yin and yang of synaptic plasticity and neurodegeneration. *39*, 1–13.

Huotari, J., and Helenius, A. (2011). Endosome maturation. EMBO J.

Inaguma, Y., Matsumoto, A., Noda, M., Tabata, H., Maeda, A., Goto, M., Usui, D., Jimbo, E.F., Kikkawa, K., Ohtsuki, M., et al. (2016). Role of Class III phosphoinositide 3-kinase in the brain development: possible involvement in specific learning disorders. J. Neurochem.

Inobe, T., and Nukina, N. (2016). Rapamycin-induced oligomer formation system of FRB-FKBP fusion proteins. J. Biosci. Bioeng. *122*, 40–46.

Itakura et al. (2009). Beclin 1 Forms Two Distinct Phosphatidylinositol 3-Kinase Complexes with Mammalian Atg14 and UVRAG. Mol. Biol. Cell *20*, 2673–2683.

Jackson, R.E., and Burrone, J. (2016). Visualizing presynaptic calcium dynamics and vesicle fusion with a single genetically encoded reporter at individual synapses. Front. Synaptic Neurosci. *8*, 1–12.

Jeans, A.F., vanHeusden, F.C., Al-Mubarak, B., Padamsey, Z., and Emptage, N.J. (2017). Homeostatic Presynaptic Plasticity Is Specifically Regulated by P/Q-type Ca2+ Channels at Mammalian Hippocampal Synapses. Cell Rep. *21*, 341–350.

Kamei, H., Saito, T., Ozawa, M., Fujita, Y., Asada, A., Bibb, J.A., Saido, T.C., Sorimachi, H., and Hisanaga, S.I. (2007). Suppression of calpain-dependent cleavage of the CDK5 activator p35 to p25 by site-specific phosphorylation. J. Biol. Chem. *282*, 1687–1694.

Kavalali, E.T., and Monteggia, L.M. (2020). Targeting Homeostatic Synaptic Plasticity for Treatment of Mood Disorders. Neuron *106*, 715–726.

Kehrl, John and Shi, C.-S. (2019). Traf6 and A20 Regulate Lysine 63-Linked Ubiquitination of Beclin 1 Controlling TLR4-Induced Autophagy Chong-Shan. Physiol. Behav. *176*, 139–148.

Kelly, B.L., and Ferreira, A. (2006). β-amyloid-induced dynamin 1 degradation is mediated by N-methyl-D-aspartate receptors in hippocampal neurons. J. Biol. Chem. *281*, 28079–28089.

Kim, J., Kim, Y.C., Fang, C., Russell, R.C., Kim, J.H., Fan, W., Liu, R., Zhong, Q., and Guan, K.L. (2013). Differential regulation of distinct Vps34 complexes by AMPK in nutrient stress and autophagy. Cell *152*, 290–303.

Kim, S.H., and Ryan, T.A. (2010). CDK5 Serves as a Major Control Point in Neurotransmitter Release. Neuron *67*, 797–809.

Kimura, T., Ishiguro, K., and Hisanaga, S.I. (2014). Physiological and pathological phosphorylation of tau by Cdk5. Front. Mol. Neurosci. *7*, 1–10.

Kokotos, A.C., and Cousin, M.A. (2015). Synaptic vesicle generation from central nerve terminal endosomes. Traffic.

Kononenko, N.L., Puchkov, D., Classen, G.A., Walter, A.M., Pechstein, A., Sawade, L., Kaempf, N., Trimbuch, T., Lorenz, D., Rosenmund, C., et al. (2014). Clathrin/AP-2 mediate

synaptic vesicle reformation from endosome-like vacuoles but are not essential for membrane retrieval at central synapses. Neuron *82*, 981–988.

Kristina A. McLinden, S.T. and E.G. (2012). At the Fulcrum in Health and Disease: Cdk5 and the Balancing Acts of Neuronal Structure and Physiology Kristina. *2012*, 1–26.

Kulkarni, A., Chen, J., and Maday, S. (2018). Neuronal autophagy and intercellular regulation of homeostasis in the brain. Curr. Opin. Neurobiol. *51*, 29–36.

Kumashiro, S., Lu, Y.F., Tomizawa, K., Matsushita, M., Wei, F.Y., and Matsui, H. (2005). Regulation of synaptic vesicle recycling by calcineurin in different vesicle pools. Neurosci. Res. *51*, 435–443.

Lamb, C.A., Yoshimori, T., and Tooze, S.A. (2013). The autophagosome: Origins unknown, biogenesis complex. Nat. Rev. Mol. Cell Biol. *14*, 759–774.

Lieberman, O.J., and Sulzer, D. (2020). The Synaptic Autophagy Cycle. J. Mol. Biol. *432*, 2589–2604.

Lorenzo, D.N., Badea, A., Davis, J., Hostettler, J., He, J., Zhong, G., Zhuang, X., and Bennett, V. (2014). A PIK3C3-Ankyrin-B-Dynactin pathway promotes axonal growth and multiorganelle transport. J. Cell Biol. *207*, 735–752.

Marat, A.L., and Haucke, V. (2016). Phosphatidylinositol 3-phosphates—at the interface between cell signalling and membrane traffic. EMBO J. *35*, 561–579.

Marder, E., and Goaillard, J.M. (2006). Variability, compensation and homeostasis in neuron and network function. Nat. Rev. Neurosci. *7*, 563–574.

McBride, H.M., Rybin, V., Murphy, C., Giner, A., Teasdale, R., and Zerial, M. (1999). Oligomeric complexes link Rab5 effectors with NSF and drive membrane fusion via interactions between EEA1 and syntaxin 13. Cell *98*, 377–386.

McKnight, N.C., Zhong, Y., Wold, M.S., Gong, S., Phillips, G.R., Dou, Z., Zhao, Y., Heintz, N., Zong, W.X., and Yue, Z. (2014). Beclin 1 Is Required for Neuron Viability and Regulates Endosome Pathways via the UVRAG-VPS34 Complex. PLoS Genet. *10*, 1–18.

Mendoza, P.A., Silva, P., Díaz, J., Arriagada, C., Canales, J., Cerda, O., and Torres, V.A. (2018). Calpain2 mediates Rab5-driven focal adhesion disassembly and cell migration. Cell Adhes. Migr. *12*, 185–194.

Michetti, M., Salamino, F., Tedesco, I., Averna, M., Minafra, R., Melloni, E., and Pontremoli, S. (1996). Autolysis of human erythrocyte calpain produces two active enzyme forms with different cell localization. FEBS Lett. *392*, 11–15.

Milosevic, I. (2018). Revisiting the Role of Clathrin-Mediated Endoytosis in Synaptic Vesicle Recycling. Front. Cell. Neurosci. *12*, 1–13.

Miranda, A.M., Lasiecka, Z.M., Xu, Y., Neufeld, J., Shahriar, S., Simoes, S., Chan, R.B., Oliveira, T.G., Small, S.A., andDiPaolo, G. (2018). Neuronal lysosomal dysfunction releases exosomes harboring APP C-terminal fragments and unique lipid signatures. Nat. Commun. *9*.

Morel, E., Chamoun, Z., Lasiecka, Z.M., Chan, R.B., Williamson, R.L., Vetanovetz, C., Dall'Armi, C., Simoes, S., Point Du Jour, K.S., McCabe, B.D., et al. (2013). Phosphatidylinositol-3-phosphate regulates sorting and processing of amyloid precursor protein through the endosomal system. Nat. Commun. *4*, 1–13.

Moulder, K.L., Jiang, X., Taylor, A.A., Olney, J.W., and Mennerick, S. (2006). Physiological Activity Depresses Synaptic Function through an Effect on Vesicle Priming. *26*, 6618–6626.

Munson, M.J., Allen, G.F., Toth, R., Campbell, D.G., Lucocq, J.M., and Ganley, I.G. (2015). mTOR activates the VPS 34– UVRAG complex to regulate autolysosomal tubulation and cell survival . EMBO J. *34*, 2272–2290.

Murthy, V.N., Schikorski, T., Stevens, C.F., Zhu, Y., and Jolla, L. (2001). in Neurotransmitter Release and Synapse Size. *32*, 673–682.

Murray, J.T., Panaretou, C., Stenmark, H., Miaczynska, M., and Backer, J.M. (2002). Role of Rab5 in the recruitment of hVps34/p150 to the early endosome. Traffic *3*, 416–427.
.
Naguib, A., Bencze, G., Cho, H., Zheng, W., Tocilj, A., Elkayam, E., Faehnle, C.R., Jaber, N., Pratt, C.P., Chen, M., et al. (2015). PTEN functions by recruitment to cytoplasmic vesicles. Mol. Cell *58*, 255–268.

Nelson, S.B., and Valakh, V. (2015). Excitatory/Inhibitory balance and circuit homeostasis in Autism Spectrum Disorders A theory of excitatory/inhibitory imbalance in Autism HHS Public Access. Neuron *87*, 684–698.

Nicot, A.S., and Laporte, J. (2008). Endosomal phosphoinositides and human diseases. Traffic *9*, 1240–1249.

Ohashi, Y., Tremel, S., and Williams, R.L. (2019). VPS34 complexes from a structural perspective. J. Lipid Res. *60*, 229–241.

Okamoto, M., and Südhof, T.C. (1997). Mints, munc18-interacting proteins in synaptic vesicle exocytosis. J. Biol. Chem. *272*, 31459–31464.

Papadopoulos, T., Rhee, H.J., Subramanian, D., Paraskevopoulou, F., Mueller, R., Schultz, C., Brose, N., Rhee, J.S., and Betz, H. (2017). Endosomal phosphatidylinositol 3-phosphate promotes gephyrin clustering and GABAergic neurotransmission at inhibitory postsynapses. J. Biol. Chem. *292*, 1160–1177.

Pasquier, B. (2015). SAR405, a PIK3C3/VPS34 inhibitor that prevents autophagy and synergizes with MTOR inhibition in tumor cells. Autophagy.

Poteryaev, D., Datta, S., Ackema, K., Zerial, M., and Spang, A. (2010). Identification of the switch in early-to-late endosome transition. Cell *141*, 497–508.

Raimondi, A., Ferguson, S.M., Lou, X., Armbruster, M., Paradise, S., Giovedi, S., Messa, M., Kono, N., Takasaki, J., Cappello, V., et al. (2011). Overlapping Role of Dynamin Isoforms in Synaptic Vesicle Endocytosis. Neuron.

Rodal, A.A., Blunk, A.D., Akbergenova, Y., Jorquera, R.A., Buhl, L.K., and Littleton, J.T. (2011). A presynaptic endosomal trafficking pathway controls synaptic growth signaling. J. Cell Biol.

Russell, R.C., Tian, Y., Yuan, H., Park, H.W., Chang, Y., Kim, H., Neufeld, T.P., Dillin, A., and Guan, K. (2014). ULK1 induces autophagy by phosphorylating Beclin-1 and activating Vps34 lipid kinase. *15*, 741–750.

Rutherford, L.C., Nelson, S.B., and Turrigiano, G.G. (1998). BDNF has opposite effects on the quantal amplitude of pyramidal neuron and interneuron excitatory synapses. Neuron *21*, 521–530.

Sabatini, D.M. (2006). mTOR and cancer: Insights into a complex relationship. Nat. Rev. Cancer *6*, 729–734.

Saheki, Y., and DeCamilli, P. (2012). Synaptic vesicle endocytosis. Cold Spring Harb. Perspect. Biol. *4*.

Samuels, B.A., and Tsai, L.H. (2003). Cdk5 is a dynamo at the synapse. Nat. Cell Biol. *5*, 689–690.

Seaman, M.N.J., Marcusson, E.G., Cereghino, J.L., and Emr, S.D. (1997). Endosome to Golgi retrieval of the vacuolar protein sorting receptor, Vps10p, requires the function of the VPS29, VPS30, and VPS35 gene products. J. Cell Biol. *137*, 79–92

Seeburg, D.P., Feliu-mojer, M., Gaiottino, J., and Pak, D.T.S. (2008). Cdk5 and plk2 mediate homeostatic plastic Abeta. *58*, 571–583.

Seebohm, G., Neumann, S., Theiss, C., Novkovic, T., Hill, E.V., Tavaré, J.M., Lang, F., Hollmann, M., Manahan-Vaughan, D., and Strutz-Seebohm, N. (2012). Identification of a novel signaling pathway and its relevance for GluA1 recycling. PLoS One *7*.

Sengoku, T., Bondada, V., Hassane, D., Dubal, S., and Geddes, J.W. (2004). Tat-calpastatin fusion proteins transduce primary rat cortical neurons but do not inhibit cellular calpain activity. Exp. Neurol. *188*, 161–170.

Shah, K., and Lahiri, D.K. (2014). Cdk5 activity in the brain - multiple paths of regulation. J. Cell Sci. *127*, 2391–2400.

Shao, H., Chou, J., Baty, C.J., Burke, N.A., Watkins, S.C., Stolz, D.B., and Wells, A. (2006). Spatial Localization of m-Calpain to the Plasma Membrane by Phosphoinositide Biphosphate Binding during Epidermal Growth Factor Receptor-Mediated Activation. Mol. Cell. Biol. *26*, 5481–5496.

Shehata, M., Matsumura, H., Okubo-Suzuki, R., Ohkawa, N., and Inokuchi, K. (2012). Neuronal stimulation induces autophagy in hippocampal neurons that is involved in AMPA receptor degradation after chemical long-term depression. J. Neurosci. *32*, 10413–10422.

Shen, W., and Ganetzky, B. (2009). Autophagy promotes synapse development in Drosophila. J. Cell Biol. *187*, 71–79.

Simonsen, A., Gaullier, J.M., D'Arrigo, A., andStenmark, H. (1999). The Rab5 effector EEA1 interacts directly with syntaxin-6. J. Biol. Chem. *274*, 28857–28860.
Soykan, T., Maritzen, T., andHaucke, V. (2016). Modes and mechanisms of synaptic vesicle recycling. Curr. Opin. Neurobiol.

Soykan, T., Kaempf, N., Sakaba, T., Vollweiter, D., Goerdeler, F., Puchkov, D., Kononenko, N.L., and Haucke, V. (2017). Synaptic Vesicle Endocytosis Occurs on Multiple Timescales and Is Mediated by Formin-Dependent Actin Assembly. Neuron *93*, 854-866.e4.

Stopkova, P., Saito, T., Papolos, D.F., Vevera, J., Paclt, I., Zukov, I., Bersson, Y.B., Margolis, B.A., Strous, R.D., andLachman, H.M. (2004). Identification of PIK3C3 promoter variant associated with bipolar disorder and schizophrenia. Biol. Psychiatry *55*, 981–988.

Subramanian, D., Laketa, V., Müller, R., Tischer, C., Zarbakhsh, S., Pepperkok, R., and Schultz, C. (2010). Activation of membrane-permeant caged PtdIns(3)P induces endosomal fusion in cells. Nat. Chem. Biol. *6*, 324–326.

Südhof, T.C. (2012). The presynaptic active zone. Neuron *75*, 11–25.

Südhof, T.C., and Rizo, J. (2011). Synaptic Vesicle Exocytosis. 2011.

Takamori, S. (2016). Presynaptic Molecular Determinants of Quantal Size. Front. Synaptic Neurosci.

Takamori, S., Holt, M., Stenius, K., Lemke, E.A., Grønborg, M., Riedel, D., Urlaub, H., Schenck, S., Brügger, B., Ringler, P., et al. (2006). Molecular Anatomy of a Trafficking Organelle. Cell *127*, 831–846.

Tarricone, C., Dhavan, R., Peng, J., Areces, L.B., Tsai, L.H., and Musacchio, A. (2001). Structure and regulation of the CDK5-p25nck5a complex. Mol. Cell *8*, 657–669.

Thomas Biederer, Pascal S. Kaeser, and T.A.B. (2017). Trans-cellular nano-alignment of synaptic function. Physiol. Behav. *176*, 139–148.

Tomizawa, K., Ohta, J., Matsushita, M., Moriwaki, A., Li, S.-T., Takei, K., and Matsui, H. (2002). Cdk5/p35 Regulates Neurotransmitter Release through Phosphorylation and Downregulation of P/Q-Type Voltage-Dependent Calcium Channel Activity. J. Neurosci. *22*, 2590–2597.

Tsai, L.-H., Yuan, J., Furuya, T., Kim, M., Lipinski, M., Li, J., Kim, D., Lu, T., Shen, Y., Rameh, L., et al. (2010). Negative Regulation of Vps34 by Cdk Mediated Phosphorylation. Mol. Cell *38*, 500–511.

Turrigiano, G. (2012). Homeostatic synaptic plasticity: Local and global mechanisms for stabilizing neuronal function. Cold Spring Harb. Perspect. Biol. *4*, 1–17.

Turrigiano, G.G., and Nelson, S.B. (2004). Homeostatic plasticity in the developing nervous system. Nat. Rev. Neurosci. *5*, 97–107.

Turrigiano, G.G., Leslie, K.R., Desai, N.S., Rutherford, L.C., and Nelson, S.B. (1998). Activity-dependent scaling of quantal amplitude in neocortical neurons. Nature *391*, 892–896.

Vaisid, T., Kosower, N.S., Katzav, A., Chapman, J., andBarnoy, S. (2007). Calpastatin levels affect calpain activation and calpain proteolytic activity in APP transgenic mouse model of Alzheimer's disease. Neurochem. Int. *51*, 391–397.

Vilariño-Güell, C., Wider, C., Ross, O.A., Dachsel, J.C., Kachergus, J.M., Lincoln, S.J., Soto-Ortolaza, A.I., Cobb, S.A., Wilhoite, G.J., Bacon, J.A., et al. (2011). VPS35 mutations in parkinson disease. Am. J. Hum. Genet. *89*, 162–167.

Voglmaier, S.M., Kam, K., Yang, H., Fortin, D.L., Hua, Z., Nicoll, R.A., and Edwards, R.H. (2006). Distinct Endocytic Pathways Control the Rate and Extent of Synaptic Vesicle Protein Recycling. Neuron.

Wang, L., Budolfson, K., and Wang, F. (2011). Pik3c3 deletion in pyramidal neurons results in loss of synapses, extensive gliosis and progressive neurodegeneration. Neuroscience.

Wang, J., Fedoseienko, A., Chen, B., Burstein, E., Jia, D., and Billadeau, D.D. (2018). Endosomal receptor trafficking: Retromer and beyond. Traffic *19*, 578–590.

Watanabe, S., and Boucrot, E. (2017). Fast and ultrafast endocytosis. Curr. Opin. Cell Biol.

Watanabe, S., Liu, Q., Davis, M.W., Hollopeter, G., Thomas, N., Jorgensen, N.B., and Jorgensen, E.M. (2013a). Ultrafast endocytosis at Caenorhabditis elegans neuromuscular

junctions. Elife *2013*, 1–24.

Watanabe, S., Rost, B.R., Camacho-Pérez, M., Davis, M.W., Söhl-Kielczynski, B., Rosenmund, C., and Jorgensen, E.M. (2013b). Ultrafast endocytosis at mouse hippocampal synapses. Nature *504*, 242–247.

Watanabe, S., Trimbuch, T., Camacho-Pérez, M., Rost, B.R., Brokowski, B., Söhl-Kielczynski, B., Felies, A., Davis, M.W., Rosenmund, C., and Jorgensen, E.M. (2014). Clathrin regenerates synaptic vesicles from endosomes. Nature *515*, 228–233.

Watt, A.J., VanRossum, M.C.W., Macleod, K.M., Nelson, S.B., and Turrigiano, G.G. (2000). Activity Coregulates Quantal AMPA and NMDA Currents at Neocortical Synapses of NMDA currents. Neuron *26*, 659–670.

Wen, X., Saltzgaber, G.W., and Thoreson, W.B. (2017). Kiss-and-run is a significant contributor to synaptic exocytosis and endocytosis in photoreceptors. Front. Cell. Neurosci. *11*, 1–18.

Wienisch, M., and Klingauf, J. (2006). Vesicular proteins exocytosed and subsequently retrieved by compensatory endocytosis are nonidentical. Nat. Neurosci. *9*, 1019–1027.

Wollert, T., Yang, D., Ren, X., Lee, H.H., Im, Y.J., and Hurley, J.H. (2009). The ESCRT machinery at a glance. J. Cell Sci. *122*, 2163–2166.

Wu, H.Y., and Lynch, D.R. (2006). Calpain and synaptic function. Mol. Neurobiol. *33*, 215–236.

Wucherpfennig, T., Wilsch-Bräuninger, M., and González-Gaitán, M. (2003). Role of Drosophila Rab5 during endosomal trafficking at the synapse and evoked neurotransmitter release. J. Cell Biol.

Xu, D., Wang, Z., Wang, C., Zhang, D., Wan, H., Zhao, Z., Gu, J., Zhang, Y., Li, Z., Man, K., et al. (2016). PAQR 3 controls autophagy by integrating AMPK signaling to enhance ATG 14L-associated PI 3K activity . EMBO J. *35*, 496–514.

Xu, J., Kurup, P., Zhang, Y., Goebel-Goody, S.M., Wu, P.H., Hawasli, A.H., Baum, M.L., Bibb, J.A., andLombroso, P.J. (2009). Extrasynaptic NMDA receptors couple preferentially to excitotoxicity via calpain-mediated cleavage of STEP. J. Neurosci. *29*, 9330–9343.

Zatz, M., and Starling, A. (2005). Calpains and Disease. N. Engl. J. Med. *352*, 2413–2423.

Zheng, W.H., Bastianetto, S., Mennicken, F., Ma, W., and Kar, S. (2002). Amyloid β peptide induces tau phosphorylation and loss of cholinergic neurons in rat primary septal cultures. Neuroscience *115*, 201–211

Zhou, X., Wang, L., Hasegawa, H., Amin, P., Han, B.-X., Kaneko, S., He, Y., and Wang, F. (2010). Deletion of PIK3C3/Vps34 in sensory neurons causes rapid neurodegeneration by disrupting the endosomal but not the autophagic pathway. Proc. Natl. Acad. Sci. *107*, 9424–9429.

6. Appendix
6.1 Appendix A: Abbreviations

Ach	Acetylcholine
AD	Activity-dependent bulk endocytosis
ADBE	Alzheimer's disease
AMPA	α-amino-3-hydroxy-5- methyl-4-isoxazole-propionic acid
AMPK	AMP-activated protein kinase
AP	Action potential
APP	Amyloid precursor protein
ASCF	Artificial cerebrospinal fluid
ATG	Autophagy-related gene
AZ	Active zone
BAR	Bin/Amphiphysin/RVS (BAR) domain-containing protei
BARA	Beta-alpha repeated
BARKOR	Beclin 1-associated autophagy-related key regulator
BATS	Backor/ATG14L autophagosome targeting sequence
BECLIN	Bcl-2 interacting protein; C2, protein kinase C conserved region 2
CAPN1	Calpain1
CAPN2	Calpain2
C/C	Coiled coil
CCP	Clathrin-coated pit
CCV	Clathrin-coated vesicle
CHC	Clathrin heavy chain
CIE	Clathrin-independent endocytosis
CME	Clathrin-independent endocytosis
DIV	Day in vitro
ELV	Endosome-like structure/vacuole
EM	Electron microscopy
ER	Endoplasmic reticulum
ESCRT	Endosomal complex required for transport
EtOH	Ethanol
fEPSP	field excitatory postsynaptic potential
FV	Fiber volley
Hsc70	Heat shock cognate 70
LTD	Long-term depression
LTP	Long-term potentiation
MTM1	Myotubularin1

mTOR	mammalian target of rapamycin
mTORC1	mammalian target of rapamycin complex I
MVB	Multivesicular body
NMDA	N-methyl-D-aspartate receptor
NMJ	Neuromuscular junction
PH	Pleckstrin-homology
PI	Phosphoinositide
PI(3)P	Phosphatidylinositol-3-phosphate
PI(3,4)P2	Phosphatidylinositol-3,4-bisphosphate
PI(3,5)P2	Phosphatidylinositol-3,5-bisphosphate
PI(4,5)P2	Phosphatidylinositol-4,5-bisphosphate
PI3K	Phosphoinositide-3-kinase
Plk2	Polo-like kinase 2
PHLPP1	PH domain and Leucine rich repeat Protein Phosphatase1
PPF	Paired pulse facilitation
PS	Population spike
PSD	Postsynaptic density
shCtrl	Non-target control shRNA
SV	Synaptic vesicle
SNARE	Soluble NSF-attachment protein receptor
Syt	Synaptotagmin
Syp	Synaptophysin
TTX	Tetrodotoxin
Ros	Roscovitine
RRP	Readily releasable pool
UVRAG	UV radiation resistance-associated gene
vGlut1	Vesicular glutamate transporter 1
vGAT	Vesicular GABA transporter
VPS	Vacuolar protein sorting
WD40	40 amino acids that ends with tryptophan (W) and aspartic acid (D)

6.2 Appendix B: List of Figures

6.3 Appendix C: Curriculum vitae

Guan-Ting Liu

EDUACATION

Freie University Berlin
Leibniz-Institut für Molekulare Pharmakologie (FMP)　　Berlin, Germany
Department of Biology, Chemistry and Pharmacy　　　　　　　　　　06/2016-
National Taiwan University
Taipei, Taiwan

Master of Science: Graduate Institute of Microbiology　　　07/2012-07/2014
Chung Yuan Christian University
Chungli, Taiwan
Bachelor of Science: Bioscience of Technology　　　　　　　09/2008-06/2012

SCIENCE EXPERIENCES

Leibniz-Institut für Molekulare Pharmakologie (FMP)　　Berlin, Germany
PhD student, Department Molecular Pharmacology and Cell Biology　　06/2016-
- Working on 'Role of PI3P -based endosomal scaffolds in neurotransmission'

National Taipei University of Nursing and Health Sciences　　Taipei, Taiwan

Research Assistant, Center of General Education　　　　　　08/2014-03/2016

- Identified of the mechanism of EBV BFRF1 induced nuclear envelope-associated
  vesicle formation and its regulatory role on nucleocytoplasmic transport.

- Conducted experiments and Supervised graduate students

National Taiwan University　　　　　　　　　　　　　　Taipei, Taiwan

Lab Assistant, Department of Microbiology　　　　　　　　07/2013-08/2014

- Supervised undergraduate students conducting lab work

Mackay Memorial Hospital　　　　　　　　　　　　　　Taipei, Taiwan

Intern Student, Department of Medical Research　　　　　　07/2010-09/2011

- Studied on 'Target Therapeutic Agent AMN107 Modulates Differentiation and
  Polarization of Human Macrophages'

RESEARCH

1. **Guan-Ting Liu**, Gaga Kochlamazashvili, Dmytro Puchkov, Rainer Müller, Carsten Schultz, Albert I. Mackintosh, Dennis Vollweiter, Tolga Soykan1*, Volker Haucke* (2020) Endosomal phosphatidylinositol 3-phosphate levels scale excitatory neurotransmission and vesicle cycling. Manuscript submitted.

2. **Guan-Ting Liu**, Hsiu-Ni Kung, Chung-Kuan Chen, Cheng Huang, Yung-Li Wang, Cheng-Pu Yu, and Chung-Pei Lee. (2018) Improving nuclear envelope dynamics by EBV BFRF1 facilitates intranuclear component clearance through autophagy. FASEB J

3. Chung-Pei Lee, **Guan-Ting Liu**, Hsiu-Ni Kung, Po-Ting Liu, Lu-Ping Chow, Ling-Shih Chang, Annie Angers, Antonella Farina, Fadila Bouamr and Mei-Ru Chen*. (2016) The Ubiquitin Ligase Itch and Ubiquitination Regulate BFRF1-Mediated Nuclear Envelope Modification for Epstein-Barr Virus Maturation. Journal of Virology

4. **Guan-Ting, Liu** (2014) The mechanism of EBV BFRF1 induced nuclear envelope-associated vesicle formation and its regulatory role on nucleocytoplasmic transport, unpublished Master thesis, National Taiwan University

Oral presentation

- Epstein-Barr virus BFRF1 employs cellular ESCRT machinery to induce the alteration of nuclear envelope for virus maturation, 2015 ICGEB DNA Tumor Virus Meeting, Trieste, Italy

Poster presentation

- The role of PI 3-phosphate-based endosomal scaffolds in neurotransmission. 2018 SFB/TRR186 Internation Symposium, Germany
- The noncanonical late domain of BFRF1 is critical for modulating nuclear envelope and the nuclear egress of Epstein-Barr virus, 2014 International Herpesvirus Workshop, Kobe, Japan
- The molecular mechanism of EBV induced structural change of nuclear envelope, 2014 Biomedical Research Symposium of Nation Health Research Institutes, Taiwan